SUBSURFACE PHOSPHORUS TRANSPORT AND SCALE DEPENDENT PHOSPHORUS LEACHING IN ALLUVIAL FLOODPLAINS

By

DEREK MICHAEL HEEREN

Bachelor of Science in Agricultural and Biosystems Engineering
South Dakota State University
Brookings, S.D.
2004

Master of Science in Agricultural Engineering
South Dakota State University
Brookings, S.D.
2008

Submitted to the Faculty of the
Graduate College of the
Oklahoma State University
in partial fulfillment of
the requirements for
the Degree of
DOCTOR OF PHILOSOPHY
July, 2012

SUBSURFACE PHOSPHORUS TRANSPORT AND SCALE DEPENDENT PHOSPHORUS LEACHING IN ALLUVIAL FLOODPLAINS

Dissertation Approved:

Dr. Garey A. Fox

Dissertation Adviser

Dr. Daniel E. Storm

Dr. Glenn O. Brown

Dr. Chad J. Penn

Outside Committee Member

Dr. Sheryl A. Tucker

Dean of the Graduate College

TABLE OF CONTENTS

Chapter Page

Chapter Page

LIST OF TABLES

LIST OF FIGURES

Figure Page

Figure Page

Figure Page

Figure Page

Figure Page

Figure Page

Figure Page

CHAPTER I

INTRODUCTION

1.1. A LEGAL PERSPECTIVE ON EXCESS PHOSPHORUS IN OZARK WATERSHEDS

Increased nutrient loads have resulted in several adverse impacts on surface water quality, including excessive algal growth, and fish kills across the United States and especially in the Illinois River Watershed (IRW) (Andrews et al., 2009). Lake Eucha, a source of water for Tulsa, Okla., suffered from drinking water taste and odor issues that were attributed to algal production (Blackstock, 2003). Both Lake Eucha and the IRW are in the Ozark ecoregion of northeastern Oklahoma and northwestern Arkansas (Figure 1.1). Nitrogen is a concern, but phosphorus (P) is generally considered the limiting nutrient in most surface water systems (Daniel et al., 1998). All critical nutrient source areas and transport mechanisms within a watershed need to be quantified and managed in order to protect and enhance drinking water systems, recreation activities, and aquatic ecosystems.

Arkansas et al. v. Oklahoma et al., 503 U.S. 91 (1992), was the first lawsuit addressing this issue. This case reached the U.S. Supreme Court certiorari after the Court of Appeals for the Tenth Circuit. Justice Stephens delivered the opinion for the unanimous court. *Arkansas v. Oklahoma* focused on point source pollution of the Illinois River and the application of the 1972

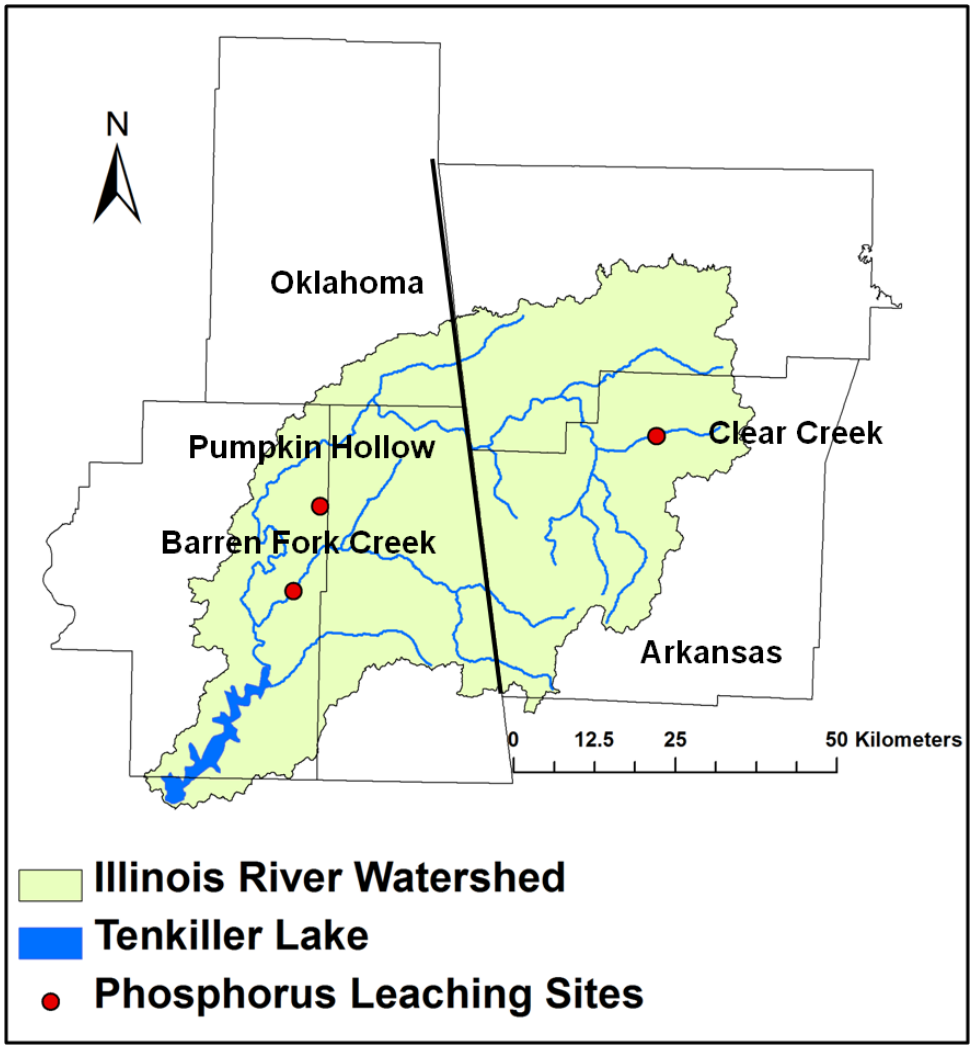

Figure 1.1. Selected floodplain sites in the Ozark ecoregion.

Clean Water Act (CWA). In particular, a Waste Water Treatment Plant (WWTP) in Fayetteville, Ark., had obtained an Environmental Protection Agency (EPA) issued permit to discharge into a tributary of the Illinois River, although Oklahoma water quality (WQ) standards allowed no degradation of the Illinois River. A significant finding was that the Supreme Court upheld the EPA in requiring an upstream state to meet downstream WQ standards, based on § 401(a)(2) of the CWA (33 U.S.C. §1341(a)(2)). Even if the CWA were silent on this, according to Justice Stephens, the EPA would be justified by the Chevron Doctrine (*Chevron U.S.A. Inc. v. Natural Resources Defense*

Council, Inc., 467 U.S. 837, 842-845 (1984)). The findings of *Arkansas v. Oklahoma* continues to have a bearing on WQ in the IRW today. Total Maximum Daily Load (TMDL) standards are being developed for the IRW and will have an impact on upstream sources in Arkansas (Pryor et al., 2011).

Progress has been made in cleaning the IRW, with the Illinois River being declared a scenic river by the state of Oklahoma. EPA recommended a P standard of 0.01 mg/L, but Arkansas was concerned about a very low P standard limiting opportunities for growth since the Fayetteville–Springdale–Rogers Metropolitan Area is one of the fastest growing areas in the nation (Soerens et al., 2003). Based on published data by Clark et al. (2000), the P standard was established at 0.037 mg/L, which is the standard set for Oklahoma Scenic Rivers (OWRB, 2010). Communities in Arkansas and Oklahoma have invested more than $225 million to improve WQ (Pryor et al., 2011). Flow adjusted total phosphorus (TP) concentrations in the Illinois River near the state line (Watts, Okla.) have been decreasing since about 2002 (Haggard, 2010), which matches a known change in WWTP effluent discharge. Engel (2008) also reported reductions in WWTP loads since 2003.

In *City of Tulsa v. Tyson Foods et al.* (2003, U.S. District Court for the Northern District of Oklahoma), the city of Tulsa, Okla., filed suit against the poultry industry and the city of Decatur, whose WWTP receives most of its waste from a poultry processing plant (Soerens et al., 2003). This dispute was over the Eucha watershed which is also in the Ozark ecoregion and provides roughly half of the water supply for the city of Tulsa. The WQ in Lake Eucha had deteriorated significantly, including taste and odor problems that were attributed to algal production (Blackstock, 2003). The poultry industry has grown tremendously in the last few decades in the Ozark ecoregion of northeastern Oklahoma and northwestern Arkansas and has been a great economic benefit to local communities (Soerens et al., 2003). The poultry waste, known as poultry litter, is a valuable fertilizer and is often land applied to pastures and hay fields. However, excess poultry litter application can result in high soil P levels, resulting in high P levels in rainfall runoff to streams. Storm et al. (2001) found that anthropogenic non-point sources, including poultry litter, were responsible for 73% of the

P load to Lake Eucha. Engle (2003) found that on a watershed scale mass balance of P, much more P is imported than exported. These imports are largely associated with feed for the poultry industry. *Tulsa v. Tyson* was also concerned with a WWTP for the city of Decatur, Okla., but was focused primarily on non-point sources. The lawsuit was settled in 2003 with agreements regarding the management of nutrients (including poultry litter) in the watershed, including a P index specific to the Eucha watershed mandated by the court (DeLaune et al., 2006).

At least two interesting things came out of this case. The first issue regarded the admissibility of models for expert witness (Blackstock, 2003). Storm et al. (2001) presented data from the Soil and Water Assessment Tool (SWAT) model, which was used to evaluate P sources and loads in the watershed. The court applied the *Daubert* test for admissibility of scientific evidence, which includes four factors: capable of empirical testing, publication in a peer-reviewed journal, error rate, and acceptance in the scientific community. The court found most of the SWAT results admissible, making it the first court case to use SWAT results as scientific evidence (Blackstock, 2003).

The second issue was the application of the 1980 Comprehensive Environmental Response, Compensation, and Liability Act (CERCLA) to agriculture (Warren, 2003). Poultry litter was considered a hazardous substance under CERCLA. This is significant because "CERCLA provides for strict liability for any person found responsible for depositing hazardous substances in such a way as to endager human health or safety." The court held that a watershed could be considered a "facility", but failed to hold poultry companies liable for "arranging" the disposal of poultry waster (Warren, 2003).

In the ongoing litigation of *Oklahoma ex rel. Edmondson v. Tyson Foods et al.* (filed June 13, 2005), Oklahoma Attorney General Drew Edmondson sued 11 poultry companies. Oklahoma sought both monetary damages and injunctive relief under CERCLA (McBride, 2011) in the Tulsa federal court. Storm et al. (2010) found that 13% of the total P load in the Illinois River was directly from

poultry litter, and 11% from elevated soil P levels. U.S. District Judge Gregory Frizzell found that the Cherokee Nation was a required party and dismissed the monetary claims of the suit for lack of standing. This was upheld by the Tenth Circuit (McBride, 2011), meaning that Tyson likely escaped paying damages and leaving Oklahoma limited to the pursuit of an injunction. Judge Frizzell later ruled that poultry litter is not a solid waste, but the Attorney General has appealed and the Tenth Circuit Court of Appeals (Denver, Colo.) will hear the case.

Finally, the viability of WQ trading should be addressed. There are several methods of pollution control, ranging from voluntary programs with cost sharing incentives to powerful regulation with strict liability. The Clean Air Act of 1970 provided a prototype for a strong command and control approach, while the Clean Air Act Amendments of 1990 pioneered a new approach of setting overall limits but allowing flexibility in how to achieve these. In response to acid rain caused largely by emissions from electrical utilities, emissions trading was established as a way to aid the reduction of atmospheric SO_2. With this market based approach, the target levels were achieved in 2007, three years before the deadline and at one-fourth of the expected cost. EPA believes that this success can be applied to water quality as well (EPA, 2003). The Final Water Quality Trading Policy (EPA, 2003) promotes and provides guidelines for WQ trading under the authority of the CWA. EPA has done 37 WQ trading pilot projects in 22 states (Pittman, 2011). While obstacles can be challenging, the benefits of a market based approach can be significant where WQ trading is feasible (Ribaudo, 2008; Yandle, 2008).

Seven success factors have been identified for evaluating the feasibility of WQ trading opportunities (Bastian, 2011), including a driver for action, understanding of water quality, alternative feasible solutions, greater cost-effectiveness, a large scale market that warrants investment, equal or better results, and a stakeholder-endorsed framework. Bastian (2011) concluded that at least five of the seven success factors exist in the IRW. A TMDL, which would provide the foundation for a WQ trading program, is being developed by the EPA as part of the Project for Water Quality Modeling

and TMDL Development for the Illinois River Watershed in Arkansas and Oklahoma (Pryor et al., 2011). The major hindrances for WQ trading is considered to be uncertainty of non-point source loads (Lee and Douglas-Mankin, 2011), resulting in inflated (conservative) trading ratios for point source to non-point source transactions. Lee and Douglas-Mankin (2011) quantified the environmental equivalence of point source and non-point source trades using the SWAT model in order to improve the accuracy of environmental trading ratios. This effectively lowered the trading ratios, increasing the likelihood of transactions by making them more competitive to those with point source loads.

1.2. OBJECTIVES AND OVERVIEW

Increased nutrient loads have resulted in several adverse impacts on surface water quality, including excessive algal growth, fish kills, and drinking water taste and odor issues across the United States and especially in the Ozark ecoregion of northeastern Oklahoma and northwestern Arkansas. Nitrogen is a concern, but phosphorus (P) is generally considered the limiting nutrient in most surface water systems (Daniel et al., 1998). Scientists and engineers need to identify critical nutrient source areas and transport mechanisms within a catchment in order to cost effectively protect and enhance drinking water systems, recreation activities, and aquatic ecosystems. While surface runoff is considered to be the primary transport mechanism for P (Gburek et al., 2005), subsurface transport through coarse subsoil to gravel bed streams may be significant and represents a source of P not alleviated by current conservation practices (e.g., riparian buffers). Therefore, the overarching objective of this research was to characterize subsurface phosphorus transport in the coarse gravel floodplains of the Ozark ecoregion. Specific objectives included identifying the influence of preferential flow paths, demonstrating P transport associated with stream-aquifer interaction, comparing subsurface P transport rates to surface runoff P transport rates, and quantifying P leaching through the topsoil.

Initially an injection test was performed which showed preferential flow and physical non-equilibrium in the coarse gravel vadose and phreatic zones (Chapter 2). Preferential flow paths were interpreted to be buried gravel bars. Then, long-term flow and transport monitoring was performed at two floodplain sites, showing aquifer heterogeneity and large scale bank storage of stream water (Chapter 3), as well as large scale, stage-dependent transient storage of P in the alluvial aquifer (Chapter 4). Subsurface P transport rates in the alluvial aquifers were quantified and found to be significant compared to surface runoff P transport rates (Chapter 5). In order to quantify P leaching through the vadose zone, a berm method was developed (Chapter 6) and utilized for plot scale infiltration experiments (Chapter 7). The surface soil type (ranging from silt loam to clean gravel) and macroporosity were found to have a significant impact on P leaching capacity, and the impact of experimental scale was considered. Several people have contributed significantly to this work, as noted in footnotes and the acknowledgements at the end of each chapter.

CHAPTER II

PREFERENTIAL FLOW EFFECTS ON SUBSURFACE CONTAMINANT TRANSPORT IN ALLUVIAL FLOODPLAINS[1]

2.1. ABSTRACT

For sorbing contaminants, transport from upland areas to surface water systems is typically considered to be due to surface runoff, with negligible input from subsurface transport assumed. However, certain conditions can lead to an environment where subsurface transport to streams may be significant. The Ozark region, including parts of Oklahoma, Arkansas, and Missouri, is one such environment, characterized by cherty, gravelly soils and gravel bed streams. Previous research identified a preferential flow path (PFP) at an Ozark floodplain along the Barren Fork Creek in northeastern Oklahoma and demonstrated that even a sorbing contaminant, i.e., phosphorus, can be transported in significant quantities through the subsurface. The objective of this research was to investigate the connectivity and floodplain-scale impact of subsurface physical heterogeneity (i.e., PFPs) on contaminant transport in alluvial floodplains in the Ozarks.

[1] Published in *Transactions of the ASABE*
Heeren, D. M., R. B. Miller, G. A. Fox, D. E. Storm, T. Halihan, and C. J. Penn. 2010. Preferential flow effects on subsurface contaminant transport in alluvial floodplains. *T. ASABE* 53(1): 127-136.

This research also evaluated a hypothesis that alluvial groundwater acts as a transient storage zone, providing a contaminant sink during high stream flow and a contaminant source during stream baseflow. The floodplain and PFP were mapped with two electrical resistivity imaging techniques. Low-resistivity features (i.e., less than 200 Ω-m) corresponded to topographical depressions on the floodplain surface, which were hypothesized to be relict stream channels with fine sediment (i.e., sand, silt, and clay) and gravel deposits. The mapped PFP, approximately 2 m in depth and 5 to 10 m wide, was a buried gravel bar with electrical resistivity in the range of 1000 to 5000 Ω-m. To investigate the PFP, stream, and groundwater dynamics, a constant-head trench test was installed with a conservative tracer (Rhodamine WT) injected into the PFP at approximately 85 mg/L for 1.5 h. Observation wells were installed along the PFP and throughout the floodplain. Water table elevations were recorded in real-time using water level loggers, and water samples were collected throughout the experiment. Results of the experiment demonstrated that stream/aquifer interaction was spatially non-uniform due to floodplain-scale heterogeneity. Transport mechanisms included preferential movement of Rhodamine WT along the PFP, infiltration of Rhodamine WT into the alluvial groundwater system, and then transport in the alluvial system as influenced by the floodplain-scale stream/aquifer dynamics. The electrical resistivity data assisted in predicting the movement of the tracer in the direction of the mapped preferential flow pathway. Spatially variable PFPs, even in the coarse gravel subsoils, affected water level gradients and the distribution of material into the shallow groundwater system.

2.2. INTRODUCTION

In order to protect water systems and aquatic ecosystems, a complete understanding is needed of the nutrient transport mechanisms within a catchment. Riparian buffer zones have been installed adjacent to stream systems across the U.S. and abroad to prevent sediment, nutrient, and pesticide transport to streams. Because buffers primarily address the commonly observed and more easily understood surface runoff transport mechanism (Lacas et al., 2005; Popov et al.,

2005; Reichenberger et al., 2007; Poletika et al., 2009; Sabbagh et al., 2009), effectiveness becomes an issue if a transport pathway through the subsurface circumvents the surface trapping objectives of the riparian buffer (Cooper et al., 1995; Lacas et al., 2005).

Spatial variability in hydraulic conductivity (Carlyle and Hill, 2001), preferential flow pathways (McCarty and Angier, 2001; Polyakov et al., 2005; Fuchs et al., 2009), and limited sorption capacity in riparian zone soils (Cooper et al., 1995; Carlyle and Hill, 2001; Polyakov et al., 2005) promote subsurface nutrient transport. It is well known that paleochannels, i.e., linear deposits of coarse-grained sediments, exist across floodplains and link modern channel flows to distal floodplain areas (Stanford and Ward, 1992; Poole et al., 1997, 2002; Amoros and Bornette, 2002; Naiman et al., 2005). Hydrologic pathways become complex with deposits of coarse alluvium (Naiman et al., 2005). Limited research has been performed on monitoring and understanding subsurface contaminant transport mechanisms in riparian floodplains (Lacas et al., 2005). Tellam and Lerner (2009) emphasize the impact of stream-aquifer interactions on stream chemistry and suggest electrical resistivity, piezometers with pressure loggers, and chemical tracers as potential methods for better characterizing sediment distributions and solute transport.

Local or regional conditions can lead to conditions where subsurface transport may be important (Turner and Haygarth, 2000; Lacas et al., 2005; Fuchs et al., 2009). For example, in northeastern Oklahoma and northwestern Arkansas, phosphorus sources from the Illinois River basin to Lake Tenkiller are estimated to be 35% from point sources, 15% from poultry litter application, and 50% from other nonpoint sources (Storm et al., 2006). In this basin, there is a statistically significant ($\alpha = 0.05$) correlation between baseflow phosphorus concentrations and poultry house density in nonpoint-source impacted streams, which are characterized by cherty soils and gravel bed streams (Storm et al., 2010). These baseflow data suggest that groundwater mechanisms may play an important role in phosphorus fate and transport in basins with gravelly subsoils. We hypothesize that these mechanisms include: (1) connectivity between phosphorus in

surface runoff and shallow groundwater, and phosphorus consequently moving with the groundwater to the stream, and (2) alluvial deposits providing a transient storage zone, i.e., acting as a sink during high flow events (with elevated phosphorus concentrations) and a source during baseflow.

A study by Fuchs et al. (2009) at one field site along the Barren Fork Creek in northeastern Oklahoma demonstrated that subsurface transport of injected phosphorus during three tracer tests was significant in localized preferential flow paths (PFPs). Using a trench to inject phosphorus into the subsurface flow system, these high-velocity pathways transported phosphorus at the same concentrations as were applied to the trench. Fine material less than 2 mm in diameter in the non-preferential flow pathways appeared to adsorb phosphorus from the water and retard phosphorus movement. In addition, background phosphorus concentrations in the PFP were higher than background phosphorus concentrations in non-preferential flow paths, suggesting that a phosphorus transport connection exists between the PFPs and the stream and/or upland areas. However, this research was limited to monitoring flow and transport pathways of less than 3 m from the trench for the PFP and 5 to 7 m from the trench for non-preferential flow paths.

The objectives of this research were to investigate the presence and impact of subsurface physical heterogeneity (i.e., PFPs) on contaminant transport in alluvial floodplains. Specific tasks included determining the location and connectivity of the PFP to a stream using subsurface mapping techniques and documenting the movement of a conservative tracer (i.e., Rhodamine WT) along a mapped PFP and areas surrounding the PFP. This research also evaluated a hypothesis that the alluvial groundwater acts as a transient storage zone, providing a contaminant sink during high stream flow and a contaminant source during stream baseflow. It should be emphasized that this research does not address the fate and transport of contaminants in the

vadose zone between the soil surface and the alluvial gravel. It is hypothesized that separate preferential paths occur in that zone, but such pathways were not explored in this research.

2.3. MATERIALS AND METHODS

2.3.1. Barren Fork Creek Floodplain Site

The riparian floodplain site (Figure 2.1) along the Barren Fork Creek (Figure 1.1) is located immediately downstream of the Eldon Bridge U.S. Geological Survey (USGS) gauge station (07197000) in the Ozark region of northeastern Oklahoma (35.90° N, -94.85° W). The southern border of the floodplain is a bedrock bluff that rises approximately 5 to 10 m above the floodplain elevation and limits channel migration to the south. The Barren Fork Creek, a tributary of the Illinois River, flows in the vicinity of the bluff near the western boundary of the study region. Historical aerial photographs demonstrate the recent geomorphic activity of the site. An abandoned stream channel is present just upstream of the studied floodplain and shows that the stream historically flowed in a more western direction than its current southwestern flow path. In this watershed, in-stream phosphorus concentrations increase with flow (Tortorelli and Pickup, 2006).

Fuchs et al. (2009) described some of the soil and hydraulic characteristics of the Barren Fork Creek floodplain site. The floodplain consists of alluvial gravel deposits underlying 0.5 to 1.0 m of topsoil (Razort gravelly loam). Soil hydraulic studies on these soil types have shown that subtle morphological features can lead to considerable differences in soil water flow rates (Sauer and Logsdon, 2002). Topsoil infiltration rates are reported to range between 1 and 4 m/d based on USDA soil surveys (USDA, 1970). The gravel subsoil, classified as coarse gravel based on the Wentworth (1922) scale, consists of approximately 80% (by mass) of particle diameters greater than 2.0 mm, with an average particle size (d_{50}) of 13 mm. Estimates of hydraulic conductivity for the gravel subsoil range between 140 and 230 m/d based on falling-head trench tests (Fuchs et al.,

2009). Soil particles less than 2.0 mm in the gravelly subsoil consist of secondary minerals, such as kaolinte and noncrystalline Al and Fe oxyhydroxides. Ammonium oxalate extractions on this finer material estimated initial phosphorus saturation levels of 4.2% to 8.4% (Fuchs et al., 2009).

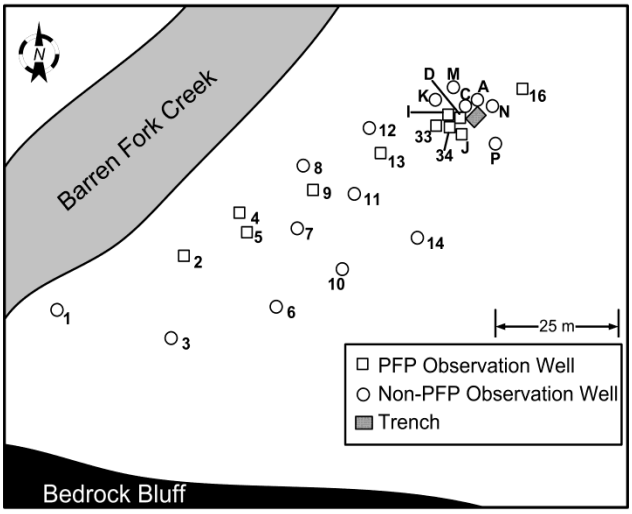

Figure 2.1. Barren Fork Creek field site with installed observation wells used for tracer injection studies. Observation wells were installed along the mapped preferential flow pathway (PFP) and outside the pathway (non-PFP). Lettered observation wells were originally used by Fuchs et al. (2009); numbered observation wells were installed to monitor tracer movement from the trench system over larger distances. The Barren Fork Creek illustration represents the width of the bankfull channel, not the actual width of the stream at the time of the test. Streamflow is from the northeast to the southwest. The bedrock bluff is at the south boundary of the image.

2.3.2. Riparian Floodplain Subsurface Mapping

Resistivity mapping is based on measuring the electrical properties of near-surface earth materials (McNeill, 1980), which vary with grain size, pore-space saturation, pore water solute content, and electrical properties of the minerals. The electrical behavior of earth materials is controlled by Ohm's law, in which current is directly proportional to voltage and inversely proportional to resistance. Generally, electrical current travels readily in solute-rich pore water and very poorly in air. In addition, cations adsorbed to soil particle surfaces reduce resistivity. Clay particles have a large surface area per volume and thus have generally lower resistivity (1 to 100 Ω-m) compared to sands or gravels (10 to 800 Ω-m), which are lower than limestone bedrock (McNeill, 1980). The potential voltage measured when a known current is injected into the

ground will vary with the resistance of the subsurface material. The resistance, when normalized for length and area, becomes resistivity, a material property (McNeill, 1980). Varying the separation between paired current and potential electrodes produces resistivity values for different depths.

The subsurface of the alluvial floodplain at the Barren Fork Creek site was mapped using two methods of electrical resistivity and a high-precision base station global positioning system (GPS). General wide-scale mapping was accomplished with the Geometrics OhmMapper, a capacitively coupled, A-C dipole-dipole system, and more detailed imaging was performed with a SuperSting DC resistivity meter (Advanced Geosciences, Inc., Austin, Tex.) (Poole et al., 1997, 2002; Pellerin, 2002; McCorley et al., 2003; Robinson et al., 2008). The OhmMapper system consisted of a transmitter dipole and five receiver dipoles, each 5 m long with a transmitter-receiver offset (rope length) of 10 m. This produced an array 40 m long towed by an all-terrain vehicle mounted with a high-precision GPS receiver, providing data for a 5 m maximum depth into the soil profile. The smaller-scale, high-precision electrical resistivity mapping was planned based on results from the OhmMapper. The SuperSting used 56 electrodes placed in the ground at a spacing ranging from 1 to 2.5 m, producing data to a depth of 13 to 20 m, respectively (Halihan et al., 2005), to generate two-dimensional resistivity profiles (lines). The GPS (TOPCON HiperLite Plus) was configured with a base station and three rover units. The OhmMapper produced a grid of 21 resistivity sections, including 16 oriented east-west and five oriented north-south. The SuperSting was used to collect seven sections including three north-south, one east-west, and three angled from northwest-southeast. One of the SuperSting lines overlapped with an OhmMapper line, allowing the measured resistivity of the two methods to be compared. The magnitudes of the resistivity results were different, which was expected for different methods of measurement. However, the patterns in these data were the same for both the SuperSting and the OhmMapper.

Although the wide range of resistivity for materials generally prevents determination of the actual subsurface material from resistivity alone, the patterns and positions of resistivity can be used to make an initial prediction about subsurface structures, which can be tested later with additional ground truth data. Soil samples served as one source of ground truth data; however, undisturbed core samples were difficult to collect from the unconsolidated gravel at the study site. Therefore, disturbed soil samples were collected from layers on the Barren Fork Creek banks both within and below the mapped PFP. Sampling of the PFP was assisted through subsequent streambank erosion at the site during several rainfall/flow events following the injection test. Gravel was separated from the sample using a 2 mm sieve (No. 10), and the percentage of particles less than 2.0 mm by mass was calculated. An additional ground truth data set was also utilized in this research: electrical resistivity imaging of a gravel bar exposed during baseflow conditions in the Barren Fork Creek. Disturbed soil samples were also collected from the upper layers (i.e., 10 to 20 cm) of the gravel bar and sieved to determine the percentage by mass of particles less than 2.0 mm.

2.3.3. Installation of Observation Well Field

In the study by Fuchs et al. (2009), 15 observation wells were installed at various locations around a constant-head trench, with the majority of the observation wells located between the trench and the stream. Several of these observation wells (A, C, D, I, J, K, M, N, and P in Figure 2.1) were utilized for this tracer injection study. In order to monitor potential tracer movement over much larger distances, additional observation wells were installed in the riparian floodplain (Figure 2.1). The observation wells installed to a depth of approximately 5 m were constructed of schedule 40 PVC and had a 3 m screened section at the base. The observation wells were installed using a Geoprobe (Kejr, Inc., Salina, Kansas) drilling machine. Observation wells 2, 4, 5, 9, 13, 33, and 34 in Figure 2.1 were located along the mapped PFP. Twenty-four of the observation wells (i.e., observation wells 1-14, 16, 33-34, A, C, D, I, J, and N) and the trench

were instrumented with automated water level loggers (HoboWare, Onset Computer Corp., Cape Cod, Mass.) to monitor water pressure and temperature at 1 min intervals. One logger was placed above the water table to account for changes in atmospheric pressure. Observation wells were surveyed so that the actual water table elevations could be calculated from water depth data. Stream stage data from a nearby USGS gauge station (07197000) was used in the analysis. Two stream sampling points were also utilized to collect water quality samples from the Barren Fork Creek.

2.3.4. Injection Experiment

The trench constructed by Fuchs et al. (2009) was utilized in this research to induce a constant water head and a tracer source to the subsurface alluvial gravel, with subsequent monitoring of flow and tracer transport in the observation well field. The dimensions of the trench were approximately 0.5 m wide by 2.5 m long by 1.2 m deep. The bottom of the trench was located approximately 25 to 50 cm below the interface between the topsoil and gravel layers. A bracing system consisted of a frame constructed with 5 cm by 13 cm wood studs covered with 2 cm plywood. The top and bottom were left open to allow water to infiltrate directly into the gravel layer.

Prior to the injection, each observation well and the Barren Fork Creek were sampled and analyzed for background Rhodamine WT levels. In addition, a water level indicator (Solinst Canada, Ltd., Georgetown, Ontario, Canada) was used to determine the depth to the water table in each observation well prior to injection. This provided a representation of the hydraulic gradient in the subsurface and a correlation between the water level and the pressure reading from the water level loggers. Next, water was pumped from the Barren Fork Creek into the trench using two pumps with a combined pumping rate of approximately 0.010 m3/s (160 gpm) to induce water movement. Pumping started at 11:36 a.m. on 3 April 2009. The steady-state water level in

the trench was held as constant as possible between 148 to 152 cm above the bottom of the trench.

Pumping continued for approximately 2.8 h prior to Rhodamine WT injection in order to reach pseudo-steady-state flow conditions. Rhodamine WT was injected into the trench in the pumped inflow water for 1.5 h at a constant rate using a variable-rate chemical pump to obtain a constant trench solution of 85 mg/L. This peak, constant concentration was achieved within approximately 15 min of injection initiation due to the storage volume of the trench. After the injection began, a total of approximately 260 samples were taken from the observation wells, trench, and creek for the duration of the experiment in order to monitor the movement of the Rhodamine WT tracer. A peristaltic pump sampled the observation wells at approximately 10 cm below the steady-state water level. Pumping ended 6.9 h from the beginning of Rhodamine WT injection for the first pump and 7.4 h from beginning of Rhodamine WT injection for the second pump. Rhodamine WT concentrations were measured with a Trilogy laboratory fluorometer (Turner Designs, Inc., Sunnyvale, Cal.), which had a minimum detection limit of 10 μg/L.

2.4. RESULTS AND DISCUSSION

2.4.1. Riparian Floodplain Subsurface Mapping

The grid of OhmMapper resistivity sections showed a series of low-resistivity structures that were roughly parallel to the existing stream channel and separated by higher-resistivity features (Figure 2.2). These were interpreted as relict cut-off stream channels, which were subsequently filled with fine sediments (i.e., sand, silt, and clay) and gravel having low resistivity. The higher-resistance areas may have represented gravel-dominated lateral or mid-channel bars. The Barren Fork Creek, adjacent to the site, is a gravel-bed Ozark stream with prominent mid-channel and lateral gravel bars. The topography of the site is generally level, but several similar linear depressions coincided with the mapped low-resistance areas.

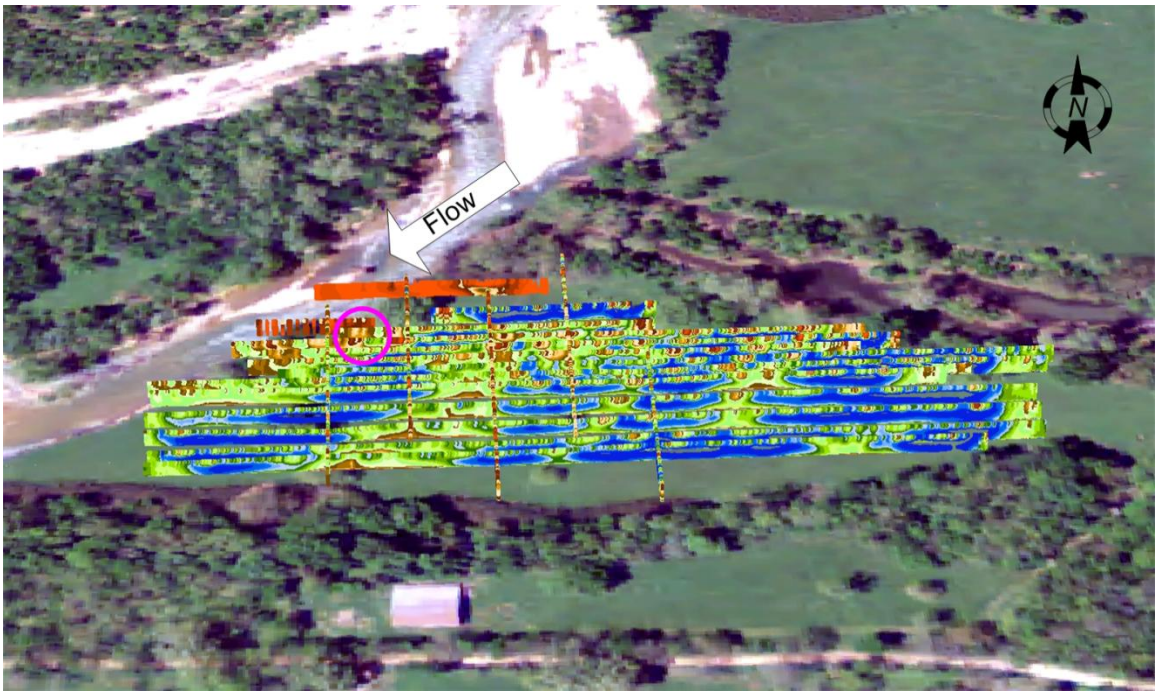

Figure 2.2. Three-dimensional rendering of OhmMapper resistivity showing low-resistivity (blue) structures. View is to the north; Barren Fork Creek is to the northwest of the image, with the arrow indicating the general streamflow direction. The location of the trench is identified with a pink circle. Underlying image is 2008 aerial photograph from USDA (2008).

The SuperSting two-dimensional resistivity profiles (lines) could be placed within the well field, and those profiles were used to attempt to locate the PFP. The wells affected by the PFP discovered in the original pumping test (Fuchs et al., 2009) were near a zone of high resistivity (i.e., 1000 to 5000 Ω-m) from the trench to the southwest (Figure 2.3). This trend in high resistivity was parallel to the trench shown by the low-resistivity features revealed by the OhmMapper lines, suggesting a common origin of formation.

The high-resistivity feature at the trench indicated that the structure was likely dominated by coarse gravel and may create a direct hydraulic connection with the adjacent Barren Fork Creek. An interesting feature from the imaging was the vertical position of the PFP above the shallow groundwater system, especially with increasing distance from the Barren Fork Creek (Figure 2.3). The SuperSting image of an exposed gravel bar verified the hypothesis of the PFP consisting of similar subsoils as the gravel bar. Resistivity of the coarse gravel layers within the

gravel bar fell within the same range as the PFP (i.e., 1000 to 5000 Ω-m), as shown in Figure 2.4. Furthermore, sieve analysis of disturbed soil samples confirmed the similarity of the PFP to the gravel bar. Percent of soil material less than 2.0 mm in the PFP, gravel bar, and in streambank samples not within the PFP were approximately 6%, 13%, and 20% by mass, respectively.

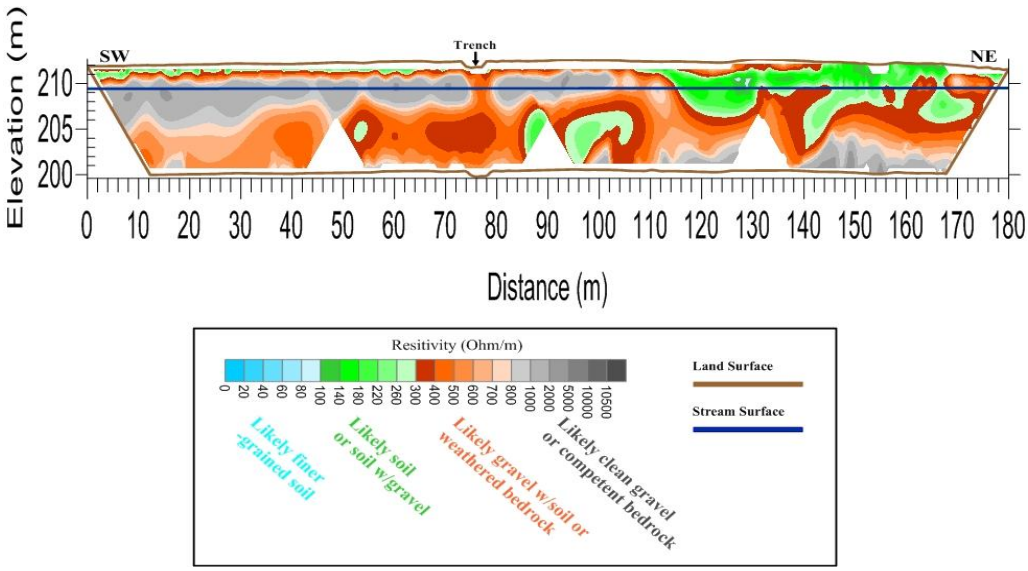

Figure 2.3. Composite SuperSting image, showing mapped electrical resistance (Ω-m), running southwest to northeast along the hypothesized preferential flow pathway. The x-axis represents the horizontal distance along the ground; the y-axis is elevation above mean sea level. The line, which is approximately parallel to the stream, begins only 5 m from the stream (near observation well 2 in Figure 2.1) and continues through the trench (at approximately 75 m).

2.4.2. Injection Experiment

Since the injection experiment was conducted when the stage in the Barren Fork Creek corresponded to a recession limb of the streamflow hydrograph, the direction of the groundwater flow gradients was expected to be downstream and toward the stream. Surprisingly, the flow gradient direction prior to injection was directed into the alluvial groundwater and downstream along the Barren Fork Creek (Figure 2.5a). The water table profile during steady-state injection showed a mound in the shallow aquifer near the trench (Figure 2.5b, Table 2.1). The mounding was limited in lateral extent because of the permeable nature of the shallow gravel subsoils. Therefore, artificially induced radial flow occurred near the trench; however, the water table rise

moving away from the trench became negligible, so that tracer movement mimicked natural, groundwater flow conditions.

(a)

SE NW

(b)

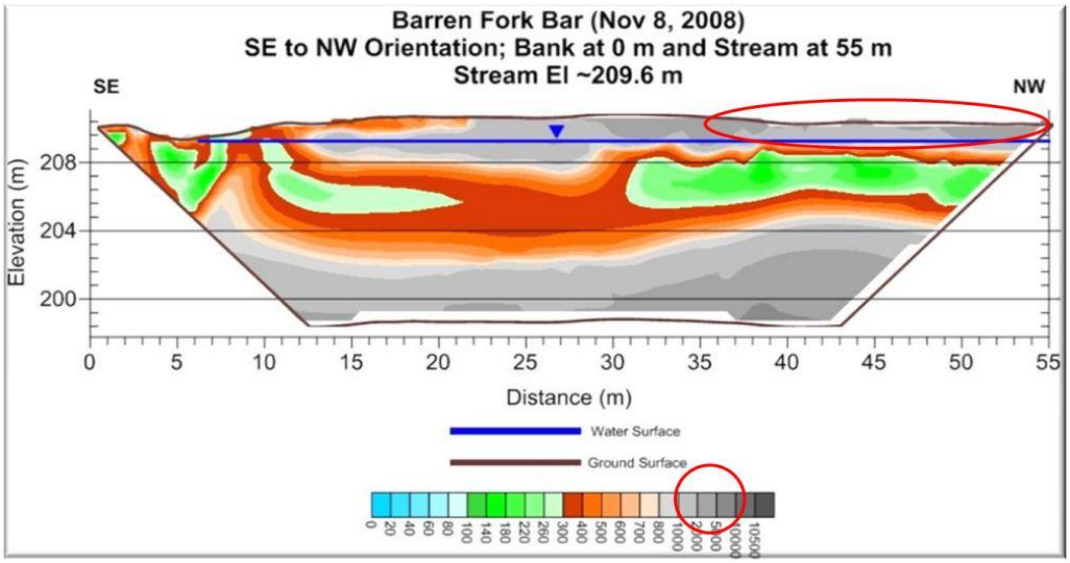

Figure 2.4. (a) Exposed gravel bar in the streambed of the main channel of the Barren Fork Creek and (b) electrical resistivity imaging of the gravel bar from the SuperSting meter. Color bar in (b) refers to electrical resistance in Ω-m. Red circle focuses on recent gravel bar deposits of coarse gravel.

Table 2.1. Water level change (Δh) between the initiation of pumping and the start of Rhodamine injection, the maximum observed Rhodamine WT concentration (c_{max}), and the time after Rhodamine injection at which the peak concentration (t_{peak}) was measured.

Sampling Point	Δh (cm)	c_{max} (µg/L)	t_{peak} (h)
Trench	151.5	86,000	0.3
1	-0.2[a]	<10	--[b]
2	-0.1[a]	<10	--
3	0.0	<10	--
4	0.3	<10	--
5	0.3	<10	--
6	0.1	83	8.2
7	0.4	<10	--
8	0.2	<10	--
9	0.3	<10	6
10	0.4	3,800	8.9
11	0.5	2,600	5.9
12	0.9	15	5.9
13	1.8	2,600	4.6
14	0.6	13,000	6.1
16	1.0	13	8.5
33	1.9	37,000	2.4
34	2.4	69,000	1.6
A	1.4	7,200	3.7
C	1.8	36,000	0.6
D	2.5	64,000	0.4
I	--	74,000	1.1
J	2.4	70,000	0.4
M	0.9	<10	--
N	1.3	4,000	3.7
P	2.1	16,000	4.5

[a] Stream stage was decreasing during the injection experiment (i.e., -0.9 cm between pumping and Rhodamine injection).

[b] No peak concentration due to the lack of observations above the limit of detection.

While groundwater flow was generally directed away from the stream and into the riparian floodplain at this location (i.e., a losing stream), some spatial heterogeneity was observed based on the groundwater level measurements. The primary source of this spatial heterogeneity occurred near the mapped PFP adjacent to the stream. Groundwater levels were higher along this linear feature, suggesting that the PFP was a spatially discrete hyporheic flow pathway (Figure 2.5). Such results suggested that equations for predicting hyporheic flux area and stream/aquifer interactions that neglect subsurface physical heterogeneity (e.g., Cardenas, 2009) were not appropriate at this scale or for these hydraulic conditions. This indicates that more research needs

to be performed to better characterize stream-aquifer interactions at sites with highly conductive alluvial aquifers and that these highly conductive aquifers can possess significant spatial heterogeneity.

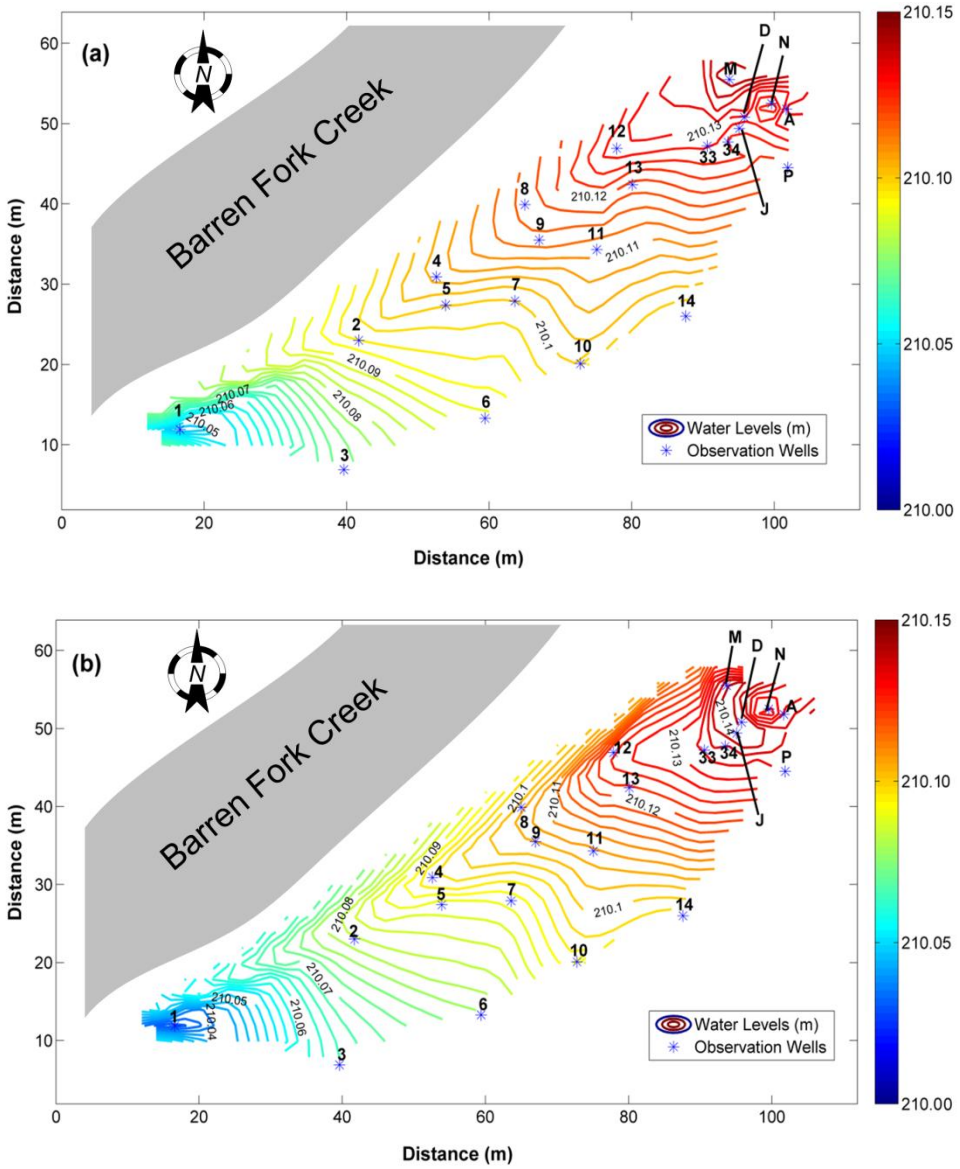

Figure 2.5. Water table elevations at (a) 11:15 a.m., before water injection into the trench, and (b) after 8 h of water injection. The scale on each graph is the water level contour level (above mean sea level in m). The Barren Fork Creek illustration represents the width of the bankfull channel, not the actual width of the stream at the time of the test.

All background Rhodamine WT samples, including the Barren Fork Creek and the observation wells, were below the detection limit except two, which were both approximately 20

µg/L. Rhodamine WT concentrations induced in the trench were approximately 85 mg/L for approximately 1.5 h (Figure 2.6). Concentrations in observation well 34, located in the PFP and within 5 m of the trench, mimicked concentrations in the trench, except for the concentration tail. Peak concentration in observation wells further downstream along the PFP (i.e., observation wells 34, 33, and 11) decreased with distance from the trench (Table 2.1, Figure 2.6).

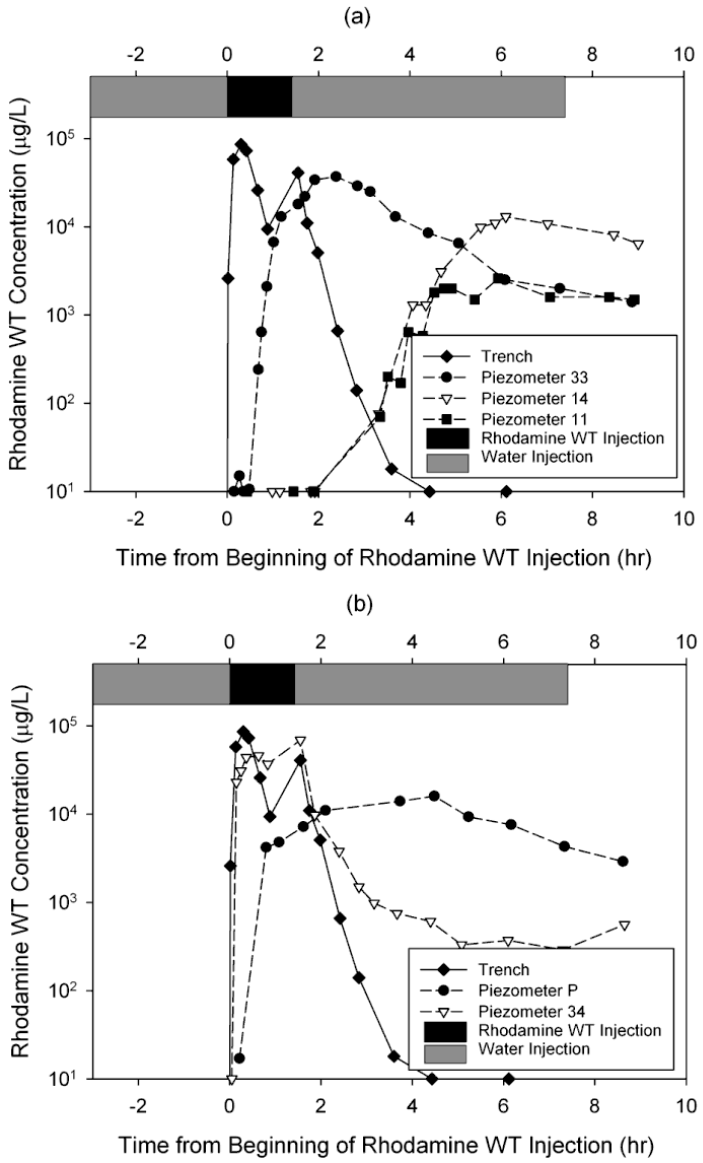

Figure 2.6. Rhodamine WT concentrations measured in the trench and observation wells during the injection experiments.

In the larger study area, Rhodamine WT was transported according to local gradients in the groundwater system. In fact, Rhodamine WT was detected in observation wells outside of the PFP at relatively large concentrations (i.e., 1000 to 10,000 µg/L), but only on the side of the PFP away from the Barren Fork Creek (Table 2.1, Figure 2.7). The Barren Fork Creek, which never had Rhodamine WT concentrations above the detection limit, was recharging the alluvial groundwater (Figure 2.5), thereby transporting Rhodamine WT farther away from the stream. It should be noted that no Rhodamine WT concentrations above the detection limit were observed in several observation wells, including those located immediately adjacent to the Barren Fork Creek (i.e., 1-5, 7-9, K, and M) and several within 5 to 10 m of the trench.

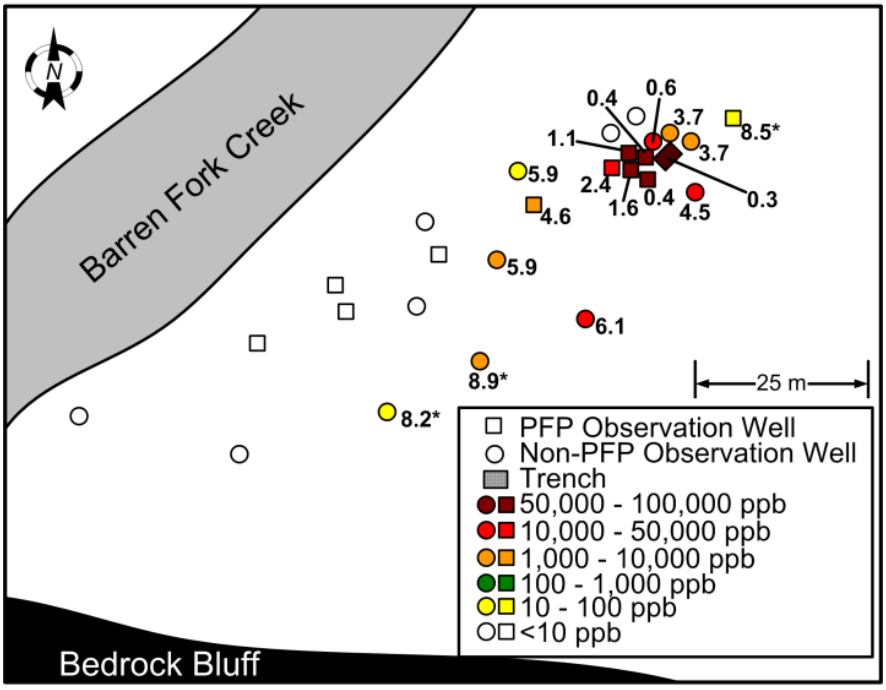

Figure 2.7. Peak Rhodamine WT concentrations in each observation well. Observation wells are labeled with the time (h) to the peak of the curve from the beginning of the injection. An asterisk indicates that there were not enough samples to characterize a complete curve for that observation well; the concentration and time correlate to the sample with the maximum concentration. The Barren Fork Creek illustration represents the width of the bankfull channel, not the actual width of the stream at the time of the test.

An interesting result from the trench test was the observation of asymmetrical breakthrough curves for the Rhodamine WT concentrations in many of the observation wells

(Figure 2.6). This asymmetrical breakthrough, with the tail of the curve remaining high, suggested that the system was largely influenced by physical heterogeneity at the macroscopic scale (i.e., 10^{-1} to 10^{1} m), a result that was not surprising based on the electrical resistivity mapping. As discussed by Brusseau (1998), the presence of smaller hydraulic conductivity zones most likely created locations in the flow field with little advective transport. Of course, similar asymmetrical breakthrough curves can also be caused by chemical nonequilibrium (Wilson et al., 2004), but sorption-desorption processes were not expected to be primary transport mechanisms due to the use of the minimally sorbing Rhodamine WT in the low organic carbon content, gravel soils.

For example, consider observation well P in figure 2.6b. Rhodamine WT concentrations in this observation well increased to approximately 10,000 μg/L and remained elevated for most of the experiment, including after Rhodamine WT injection into the constant-head trench. However, observation wells along the PFP with a similar distance from the trench (i.e., observation well 34 in Figure 2.6b) more closely resembled the expected rising and falling breakthrough curve due to injection and cessation of Rhodamine WT into the trench. Concentrations in observation well P began to slowly decrease 4.5 h after initiation of Rhodamine injection or 3 h after the last Rhodamine WT injection into the trench, and concentrations remained above 1000 μg/L for 8 h after initiation of injection.

Therefore, it appeared that gravel subsoils surrounding observation well P acted as source/sink areas and contributed mass to the higher advective domains (i.e., PFP) over time. These results, combined with the influence of the PFP and the stream recharging the groundwater, confirmed the hypothesis of the alluvial groundwater acting as a transient storage zone, at both medium (i.e., 10^{1} m) and larger scales (i.e., 10^{2} m), as shown in the concentration plume map of Figure 2.7.

Since the PFP was above the water table, it was not active before pumping began. During the injection, it was hypothesized that water from the trench flowed through the PFP (vertically positioned above the base flow groundwater table) and infiltrated into the alluvial groundwater system (Figure 2.8). In fact, manual water level sensors were not able to read a specific water table elevation in observation wells D and J, hypothesized to be the result of perched water flowing laterally along the PFP and then entering and dropping down the observation well shaft. While perching did occur, it should be noted that the PFP was not separated from the underlying subsoils by an impermeable layer. The potential for infiltration into the shallow groundwater as water flowed laterally along the PFP was relatively high.

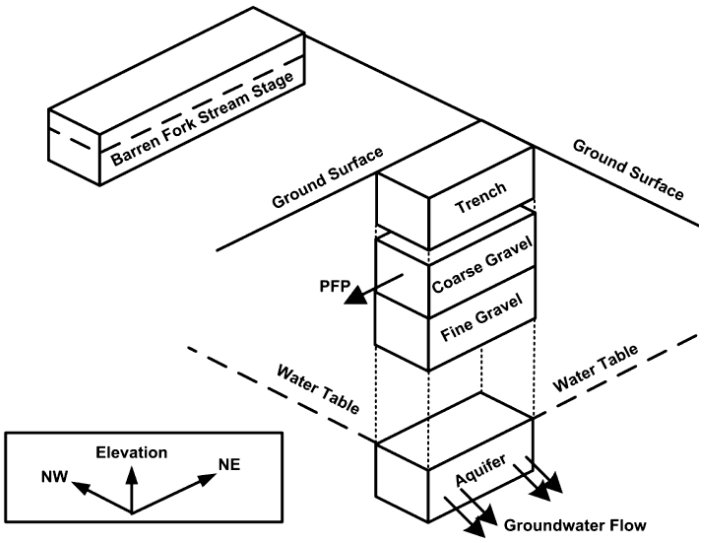

Figure 2.8. Conceptual model of the alluvial floodplain system. Rhodamine WT from the trench flowed through the preferential flow path (PFP) to the west before infiltrating through a fine gravel layer to the groundwater. The PFP essentially distributed the tracer across a wide extent of the aquifer.

A comparison between observation wells 33 and P supported the hypothesis that the PFP, when active, distributed tracer to the alluvial groundwater along the length of the PFP, after which movement was driven by the interaction between the stream and alluvial groundwater. While both observation wells were similar distances from the trench, only observation well 33 was located along the PFP (Figure 2.1). At the start of Rhodamine WT injection, the groundwater

gradient from the trench to observation well P (i.e., approximately 0.4 m/m) was higher than it was from the trench to observation well 33 (i.e., approximately 0.3 m/m). If transport was only driven by groundwater gradients, then observation well P would be expected to have a higher peak concentration and a shorter time to the peak. However, due to the impact of the PFP, Rhodamine WT concentrations in observation well 33 peaked at 37 μg/L (compared to 16 μg/L for observation well P) at 2.4 h after initiation of the Rhodamine WT injection (compared to 4.5 h for observation well P). The PFP appears to account for the large spread of the plume to the west (e.g., observation wells 11-13 in Figure 2.7) when the general direction of the groundwater gradient was to the south.

2.5. SUMMARY AND CONCLUSIONS

This research identified the presence and demonstrated the impact of subsurface physical heterogeneity (i.e., a preferential flow pathway) on water and conservative tracer transport in a riparian floodplain system. The preferential flow pathway was successfully identified and mapped using electrical resistivity imaging and appeared to create a direct hydraulic connection between the Barren Fork Creek and the subsurface of the riparian floodplain. The preferential flow pathway also appeared to influence water level gradients in the riparian floodplain. The tracer injection further demonstrated that the preferential flow pathway influenced the movement and the distribution of tracer into the shallow groundwater system. The electrical resistivity data assisted in predicting the southwestern movement of the tracer in the direction of the mapped preferential flow pathway. The resistivity mapping demonstrated the presence of vertical layering, which resulted in a lateral distribution of water and tracer before entering the groundwater system. The interaction between the Barren Fork Creek and the alluvial groundwater then controlled the movement of the tracer in the shallow groundwater. This enhanced lateral distribution resulted in a greater westward migration of the tracer plume than would have been predicted based only on the water table gradient.

The results verified the hypothesis of the alluvial groundwater acting as a transient storage zone, as contaminants in the stream can be stored in the alluvial groundwater. The preferential flow pathway, vertically positioned above the shallow groundwater system, may not become hydrologically active except under high flow events. This is important, however, as high flow events usually contribute significantly to total contaminant loads to downstream water reservoirs. Additionally, the preferential flow pathways may become active during recharge between the surface and subsurface, affecting the distribution of material into the shallow groundwater system. Future research is needed to understand the connectivity between nutrient (i.e., phosphorus) concentrations on the surface with the PFP and the underlying alluvial aquifer, as well as to better characterize stream-aquifer interactions at sites with highly conductive alluvial aquifers.

2.6. ACKNOLWEDGEMENTS

This material is based on work supported by the Oklahoma Conservation Commission with a U.S. Environmental Protection Agency Region VI 319 grant, and an Oklahoma State University Team Initiative Proposal (TIP) grant through the College of Agricultural Sciences and Natural Resources. The author acknowledges Dan Butler of the Oklahoma Conservation Commission for providing access to the riparian floodplain property along the Barren Fork Creek. The author acknowledges Amanda K. Fox, Stillwater, Oklahoma, for assisting with figure development and reviewing an earlier version of the manuscript; Glenn V. Wilson, USDA-ARS, Oxford, Mississippi, for reviewing an earlier version of the manuscript; and Maria L. Chu-Agor and Jorge A. Guzman, Department of Biosystems and Agricultural Engineering, Oklahoma State University, for assisting with data collection.

CHAPTER III

DIVERGENCE AND FLOW DIRECTION AS INDICATORS OF SUBSURFACE HETEROGENEITY AND STAGE-DEPENDENT TRANSIENT STORAGE IN ALLUVIAL FLOODPLAINS

3.1. ABSTRACT

A better understanding of stream-aquifer interactions is needed for both estimating contaminant transport in alluvial stream systems and water policy. Assuming homogeneity in alluvial aquifers is convenient, but limits our ability to accurately predict stream-aquifer interactions in alluvial floodplains. Research is needed on focused, as opposed to diffuse, groundwater discharge/recharge to streams and the magnitude and role of transient storage in alluvial aquifers, especially relative to changes in stream stage. The objective of this research was to document and quantify the effect of flow heterogeneity (i.e., focused or preferential flow pathways, PFPs) and transient storage on groundwater flow patterns relative to changes in stream stage using flow divergence and direction. Monitoring was performed adjacent to the Barren Fork Creek and Honey Creek in northeastern Oklahoma. Based on results from subsurface electrical resistivity mapping, observation wells were installed in PFPs and non-PFP subsoils. Water levels in the wells were recorded real-time using pressure transducers for a period of six weeks, which included multiple high flow events. A cubic interpolation was utilized to determine the head for

points in a two-dimensional well field grid, and the gradient, divergence, and direction were calculated for each point in space on 30 minute intervals. Divergence was used to quantify heterogeneity in hydraulic conductivity and flow direction was used to assess the potential for large-scale transient storage. The PFPs appeared to act as divergence zones allowing stream water to quickly enter the groundwater system, or as flow convergence zones draining a large groundwater area. Maximum divergence or convergence occurred with maximum rates of change in stream stage. Flow directions in the groundwater changed considerably between base and high flows, suggesting that the floodplains acted as a transient storage zone, rapidly storing and releasing water during passage of a storm hydrograph. During storm events at both sites, the average groundwater direction changed by at least 90° from the average groundwater direction during baseflow. The procedures in this research provide methodologies for quantifying subsurface heterogeneity, focused recharge/discharge, and transient storage in groundwater for alluvial floodplains. This research has important implications relative to the impact of large scale (i.e., beyond near-streambed) and stage-dependent storage on contaminant movement through alluvial stream systems and management activities in floodplains. Groundwater models of these alluvial floodplains should account for the non-random nature of heterogeneity in hydraulic conductivity, as well as the fact that some PFPs may only become activated after a minimum stream stage is reached.

3.2. INTRODUCTION

Simplifying assumptions are a necessity in describing the natural environment. For example, Cardenas (2009) modeled stream-aquifer interactions within meander bands assuming homogenous hydraulic conductivity in the alluvial aquifer. However, assuming homogeneity limits our ability to accurately predict stream-aquifer interactions in alluvial floodplains. In fact, the Committee on Hydrologic Sciences of the National Research Council (NRC, 2004) identified several research needs in regard to groundwater fluxes across interfaces. The NRC committee

specifically identified the need to determine the relative importance of diffuse versus focused recharge/discharge in hydro-geologic settings. Additional research is needed to document the occurrence of focused recharge and discharge relative to changes in stream stage.

It is well known that deposits of coarse alluvium in floodplains result in complex hydrologic pathways (Naiman et al., 2005). Distal floodplain areas can be linked to modern channel flows by paleochannels, i.e. linear deposits of coarse-grained sediments (Stanford and Ward, 1992; Poole et al., 1997, 2002; Amoros and Bornette, 2002; Naiman et al., 2005). Local or regional conditions can lead to circumstances where subsurface transport may be important (Turner and Haygarth, 2000; Lacas et al., 2005; Fuchs et al., 2009). Subsurface nutrient transport is promoted by spatial variability in hydraulic conductivity (Carlyle and Hill, 2001), preferential flow pathways (McCarty and Angier, 2001; Polyakov et al., 2005; Fuchs et al., 2009), and limited sorption capacity in riparian zone soils (Cooper et al., 1995; Carlyle and Hill, 2001; Polyakov et al., 2005). Tellam and Lerner (2009) suggest electrical resistivity and piezometers with pressure loggers as potential methods for better characterizing sediment distributions and solute transport in these systems.

For example, phosphorus transport to streams has been assumed to primarily take place in surface runoff, resulting in a high emphasis on riparian buffer zones as a conservation practice. Because buffers adjacent to streams primarily address the commonly observed and more easily understood surface runoff transport mechanism (Reichenberger et al., 2007; Sabbagh et al., 2009), their effectiveness may be limited if a transport pathway through the subsurface circumvents the surface trapping objectives of the riparian buffer (Cooper et al., 1995; Lacas et al., 2005). Previous research (Fuchs et al., 2009) on the Barren Fork Creek in northeastern Oklahoma demonstrated that subsurface transport of phosphorus was significant in localized preferential flow paths (PFPs). Subsequent research (Heeren et al., 2010) mapped the extent of the subsurface PFPs with electrical resistivity equipment. A series of low resistivity structures

that were roughly parallel to the current stream channel were separated by higher resistivity features. Low resistivity areas were interpreted as relict cut-off stream channels which had been filled with fine sediments (i.e., sand, silt and clay) and gravel having low electrical resistivity. The higher resistance areas, including the PFP, were interpreted to be buried gravel-dominated lateral or mid-channel bars, which were highly resistant to electrical current but highly conductive to water flow.

The importance of spatial heterogeneity in soils has been recognized, but quantifying parameter heterogeneity, such as hydraulic conductivity, has proven difficult. Rooij and Stagnitti (2000) performed solute leaching experiments on laboratory soil columns and collected drainage from 300 discrete compartments. The variable amounts of solute collected indicated convergence and divergence of flow lines in the vadose zone, which was used to "…quantify the nature and severity of flow heterogeneity and preferential flow." Divergence of pore flow velocity has been incorporated into groundwater contaminant transport modeling (Kavvas and Karakas, 1995), and divergence has been observed in subsurface flow models due to heterogeneity in anisotropy (Kumar et al., 2009). However, the divergence of the water table gradient using field data has not been used to characterize heterogeneity of hydraulic conductivity in unconfined aquifers.

It is also hypothesized that highly conductive alluvial systems are transient storage zones for nutrients, acting as a sink during high flow and a source during base flow. However, limited data have been presented that documents and quantifies the transient nature of groundwater in alluvial floodplains, other than near streambed hyporheic flow. Limited research has been performed to investigate transient storage relative to shifts in surface and subsurface flow conditions (Zarnetske et al., 2007).

Therefore, the objective of this research was to document and quantify the impact of flow heterogeneity (i.e., PFPs) on groundwater flow patterns relative to changes in stream stage using

flow divergence and direction. This research strengthens our current understanding of flow and contaminant interaction between streams and alluvial aquifers and can be used to help quantify the efficiency of conservation practices in alluvial floodplains. This research utilized data sets of two instrumented floodplain sites in the Ozark ecoregion of Oklahoma, but such results may be applicable for gravel bed systems worldwide.

3.3. MATERIALS AND METHODS

3.3.1. Barren Fork Creek and Honey Creek Floodplain Sites

The alluvial floodplain sites were located in the Ozark region of northeastern Oklahoma (Figure 3.1). The Barren Fork Creek site (Figure 3.2a, latitude: 35.90°, longitude: -94.85°) was immediately downstream of the Eldon Bridge U.S. Geological Survey (USGS) gage station 07197000. With a watershed size of 845 km^2, the Barren Fork Creek site had a median daily flow of 3.6 $m^3 s^{-1}$. The Honey Creek site (Figure 3.2b, latitude: 36.54°, longitude: -94.70°) was also located immediately downstream of a USGS gage station 07189542. As a smaller order stream, Honey Creek site had a 0.54 $m^3 s^{-1}$ median daily flow and a 150 km^2 watershed.

Both floodplain sites consisted of alluvial gravel deposits underlying a mantle of topsoil (Razort gravelly loam). Topsoil thickness ranged from 0.5 to 1.0 m at the Barren Fork Creek site and from 0.1 to 0.5 m at the Honey Creek site. Soil hydraulic studies on these soil types have shown that subtle morphological features can lead to considerable differences in hydraulic conductivity (Sauer and Logsdon, 2002). The riparian area on Honey Creek was located on the inside of a meander bend, an area likely to be aggradational. Located on the outside of a meander bend, the stream is actively eroding away the study area along the Barren Fork Creek. Fuchs

Figure 3.1. Location of riparian floodplain sites in the Ozark ecoregion of Oklahoma.

et al. (2009) described some of the soil and hydraulic characteristics of the Barren Fork Creek floodplain site, including estimates of hydraulic conductivity for the gravel subsoil between 140 and 230 m d^{-1} based on falling head trench tests.

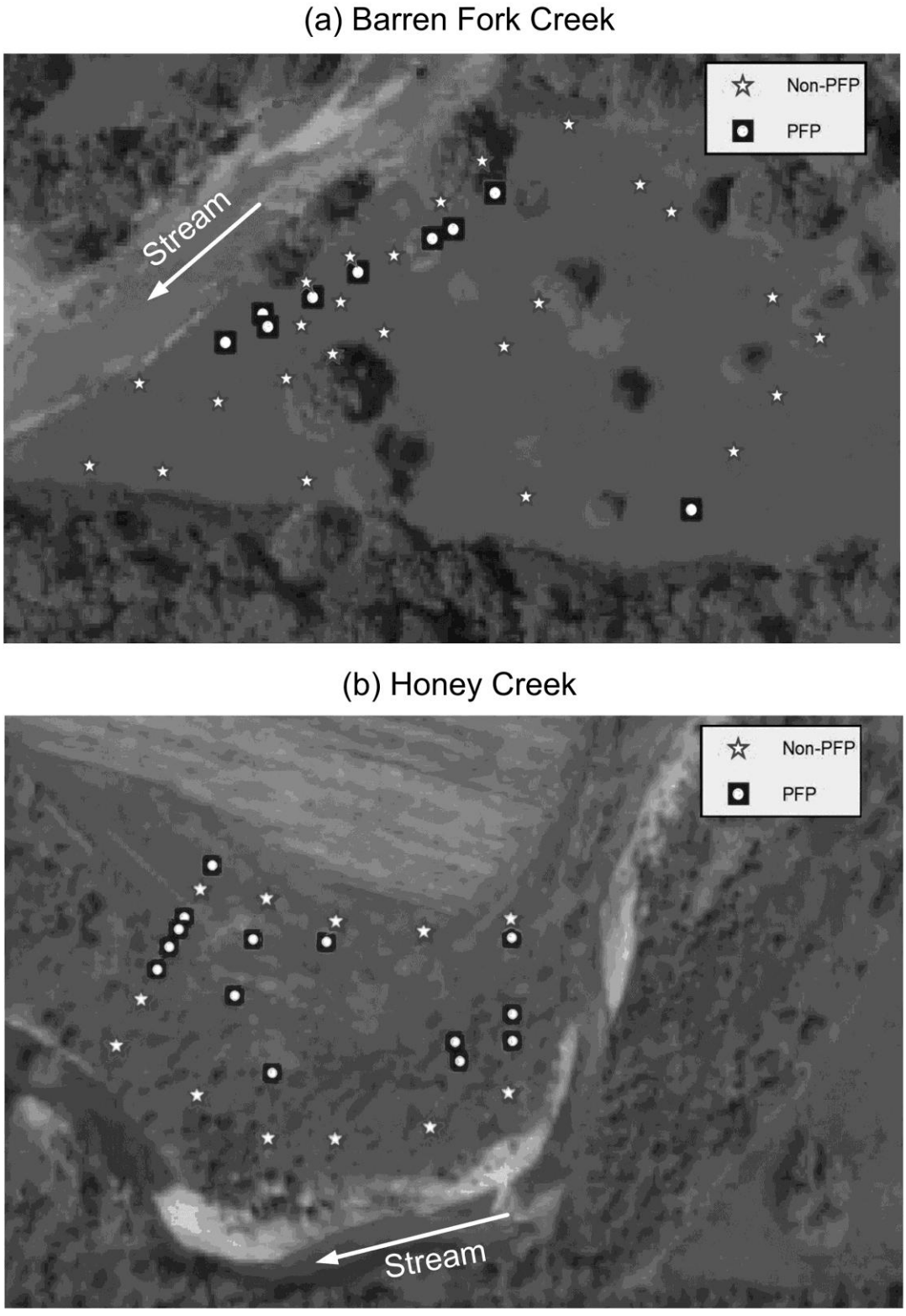

Figure 3.2. (a) Barren Fork Creek site, located near Tahlequah, OK, and (b) Honey Creek site, located near Grove, OK, showing preferential flow path (PFP) and non-PFP observation well locations. The white arrows indicate stream flow direction.

3.3.2. Observation Well Installation and Long Term Monitoring

Assuming a positive correlation between electrical resistivity and hydraulic conductivity, observation well locations were selected both in PFPs and in non-PFP subsoils (Figure 3.2), based on previous electrical resistivity results (Heeren et al., 2010; Miller et al., 2010; Miller, 2012). Using a Geoprobe Systems drilling machine (6200 TMP, Kejr, Inc., Salina, KS), observation wells were installed in the alluvial floodplains to a depth of approximately 3 to 5 m with a 2 to 3 m screened section at the base. Well locations were surveyed using a TOPCON HiperLite Plus global positioning system configured with a base station and rover unit (4 cm accuracy). These data were corrected for positional errors using the National Geodetic Survey Online Positioning User Service (OPUS). Since the water table elevation data were more sensitive to measurement error than horizontal position, a laser level was used to determine the elevation at the top of each well (1 cm accuracy).

At each site, twenty-four observation wells were instrumented with automated water level loggers (HoboWare, Onset Computer Corp., Cape Cod, MA) to monitor water pressure and temperature at five minute intervals from April 3 to May 14, 2009. One logger was placed above the water table at each site to account for changes in atmospheric pressure. Reference water table elevations, obtained with a water level indicator, were then calculated. The logger data were processed with HoboWare Pro software, which accounted for changes in atmospheric pressure as well as changes in water density due to temperature. The local USGS gage stations were used to analyze stream stage.

3.3.3. Divergence as an Indicator of Subsurface Heterogeneity

Water table elevation data were analyzed with Matlab (The Mathworks, Natick, MA). Using 30-minute intervals, a cubic interpolation was performed to determine the head for points in a two-dimensional well field grid. Contour maps were plotted with equipotential lines using 2-cm spacing. The gradient (L L^{-1}) of the scalar head field was calculated for each point in space using the following equation (Hunt, 1995):

$$\vec{i} = \nabla h = \frac{\partial h}{\partial x}\hat{x} + \frac{\partial h}{\partial y}\hat{y} \tag{3.1}$$

where $\vec{i}$ is the gradient vector and *h* is the head (i.e., water table elevation). Streamlines were calculated as everywhere-tangent to the gradient, or perpendicular to contour lines of *h*. The divergence of the gradient vector field was calculated using the following equation (Hunt, 1995):

$$div(\vec{i}) = \nabla \bullet \vec{i} = \frac{\partial i_x}{\partial x} + \frac{\partial i_y}{\partial y} \tag{3.2}$$

where div($\vec{i}$) is the divergence of $\vec{i}$. The operator div($\vec{i}$) is a scalar quantity with units of L^{-1}, and is essentially a measure of the change in gradient per unit length.

The divergence of a velocity vector field represents sources and sinks. With units of T^{-1}, div($\vec{v}$) represents the net flux (outflow minus inflow) through the surface of a unit volume. Due to continuity, the divergence of the velocity vector field for an incompressible fluid with no change in storage (e.g. saturated material) must be zero (Hunt, 1995). This also applies to a two-dimensional representation of an unconfined aquifer if the change in water table elevation over time is negligible. Velocity can be related to the gradient by:

$$\vec{v} = \frac{K}{\phi}\vec{i} \tag{3.3}$$

where $\vec{v}$ is the pore velocity, *K* is saturated hydraulic conductivity, and φ is porosity. Assuming *K* and φ are homogenous, then

$$div(\vec{v}) = \frac{\partial\left(\frac{K}{\phi} i_x\right)}{\partial x} + \frac{\partial\left(\frac{K}{\phi} i_y\right)}{\partial y} = \frac{K}{\phi}\left[\frac{\partial i_x}{\partial x} + \frac{\partial i_y}{\partial y}\right] = \frac{K}{\phi} div(\vec{i}) \tag{3.4}$$

If div($\vec{v}$) is zero, then div($\vec{i}$) must also be zero for an incompressible fluid with no change in storage. If div($\vec{i}$) is non-zero, then *K* and/or φ must be heterogeneous, or the change in water table elevation over time must be significant. We hypothesized that when the change in water table elevation over time was small (e.g. base flow conditions), the magnitude of div($\vec{i}$) was an indicator of the degree of aquifer heterogeneity at a point in space. Since heterogeneity in *K* was much greater than heterogeneity in φ (Kavvas and Karakas, 1995), it was assumed that *K* was the dominant source of heterogeneity affecting the divergence data.

A positive div($\vec{i}$) represents a higher gradient leaving a control volume than entering it. Perhaps this can be best illustrated with a case study. Consider a shallow unconfined aquifer with the water table illustrated in Figure 3.3. Arrows are streamlines showing the direction of flow, which are perpendicular to the contour lines. Assuming that the aquifer can be adequately represented by two-dimensional flow and that there is no change in storage, flow between two streamlines must be constant throughout that streamtube due to conservation of mass. In case (a), since the streamtubes have a constant area, the decreasing gradient must be caused by an increasing *K*. The control volume has a unit width and a unit length, and the arrows represent the gradient vector on each side. While an $\vec{i}$ of 0.001 m m^{-1} would be more reasonable, values near 10 m m^{-1} were chosen for clarity of demonstration. The divergence would be calculated as div($\vec{i}$) equal to -4 m^{-1}. A negative value for divergence indicates convergence. As this example demonstrates, gradient convergence indicates flow from an area of low *K* to an area of high *K*.

Case (b) is an example where the gradient is constant but the width of the stream tubes is increasing. Again, since flow must be constant within a streamtube, the increasing area must be caused by a decreasing *K*. Here, div($\vec{i}$) in the volume element is 9.5 m^{-1}. A positive divergence indicates flow from high *K* to low *K*.

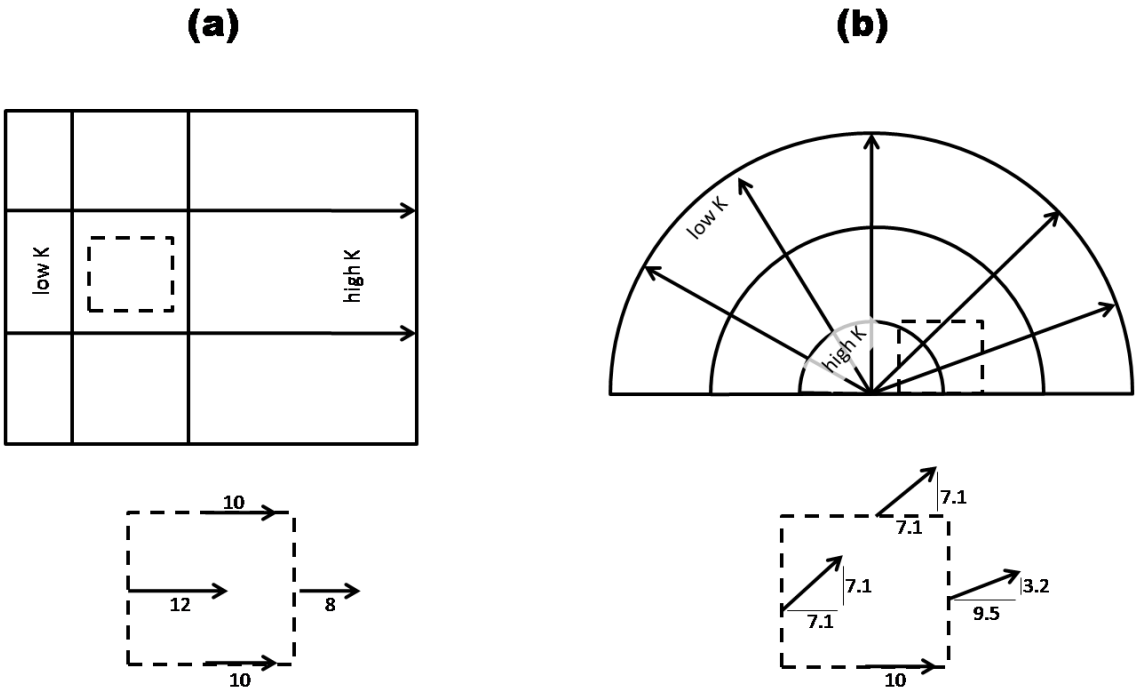

Figure 3.3. Case study for divergence calculations. Contour lines are water table elevations and arrows are streamlines. The gradient vectors are shown on each side of the control volumes. (a) Flow convergence, div($\vec{i}$) = -4 m^{-1}, and (b) flow divergence, div($\vec{i}$) = 9.5 m^{-1}.

Statistics of the div($\vec{i}$) were derived using the mean, median, standard deviation, and 5th and 95th percentiles. These statistics were correlated to the river stage during the six week monitoring period.

3.3.4. Direction as an Indicator of Transient Storage

The magnitude (R) and direction (θ) of the groundwater flow gradient at each point in the two-dimensional well field grid was derived using the following equations:

$$R = \sqrt{\left(\frac{\partial h}{\partial x}\right)^2 + \left(\frac{\partial h}{\partial y}\right)^2} \tag{3.5}$$

$$\theta = \tan^{-1}\left(\frac{\partial h / \partial y}{\partial h / \partial x}\right) \tag{3.6}$$

The arctangent function was in the range of $-\pi/2$ to $\pi/2$ radians. The direction (θ) in radians was then converted to a 0° to 360° scale with the appropriate conversion factor for each quadrant. Statistics of the R and θ were derived using the mean, median, standard deviation, and 5^{th} and 95^{th} percentiles, and these statistics were correlated to the stage during the six week monitoring period. Polar plots of the R and θ were created for specific flow events at both the Barren Fork Creek and Honey Creek field sites to investigate the change in the groundwater flow direction under baseflow and the rising limb, peak, and recession limb of streamflow hydrographs.

3.4. RESULTS AND DISCUSSION

3.4.1. Water Table Elevations and Streamlines

Patterns in the water table elevation contour plots and streamline plots at each site remained relatively similar during baseflow conditions, but changed during high flow events. Plots for baseflow conditions and at two points during the largest flow event at each site were selected to illustrate the range of flow patterns in the dataset (Figures 3.4 and 3.5). The highest gradients in the alluvial aquifer occurred during the rising limb of the hydrographs, when the stream stage was rising most quickly. The impact of aquifer heterogeneity could be seen qualitatively in the contour and streamline plots. For example, a PFP can be seen along the Barren

Fork Creek (Figure 3.4b) providing an inlet for stream water to enter the groundwater system. This area of focused recharge appears to be at point (80 m, 60 m), which is the location of the PFP that was studied previously (Fuchs et al., 2009; Heeren et al., 2010). Intuitively, the highest water table elevation should be at the top-center of the contour plot, at the up-gradient end of the stream; however, the highest water table elevation was in the PFP, where stream water could most readily enter the alluvial aquifer. At other times, the contour patterns indicated flow convergence zones (bottom center of Figure 3.4a and 3.4c), where a PFP appeared to be draining a large area of groundwater. At the Honey Creek site, there was a PFP that activated during the rising limb of flood events (Figure 3.5b and 3.5e), providing a convergence zone that drained a large area of groundwater to the northwest. The location of this PFP was consistent with previous electrical resistivity research at this site (Miller et al., 2010; Miller, 2012).

An interesting observation based on the water table elevation data was that the Barren Fork Creek was a losing stream at this field site, even during base flow and falling limb conditions (Figure 3.4). This illustrated the complexity of stream-aquifer interactions in these coarse gravel alluvial aquifers. We hypothesize a flow pattern where water regularly left the stream at one point within the study area, traveled through the aquifer, and reentered further downstream outside of the study area. This would be equivalent to a large-scale hyporheic flow path, with its activity dependent on stream stage.

3.4.2. Divergence as an Indicator of Subsurface Heterogeneity

Aquifer heterogeneity was quantified with divergence data which was a composite of radial flow (Figure 3.3b) and changing gradient along a flow path (Figure 3.3a). The results indicated that these effects often happen together. For example, a PFP that creates a divergence zone results in both radial flow and increasing gradient along the flow paths. The mean

divergence data were plotted over time relative to the stream stage at both the Barren Fork Creek and the Honey Creek field sites (Figure 3.6).

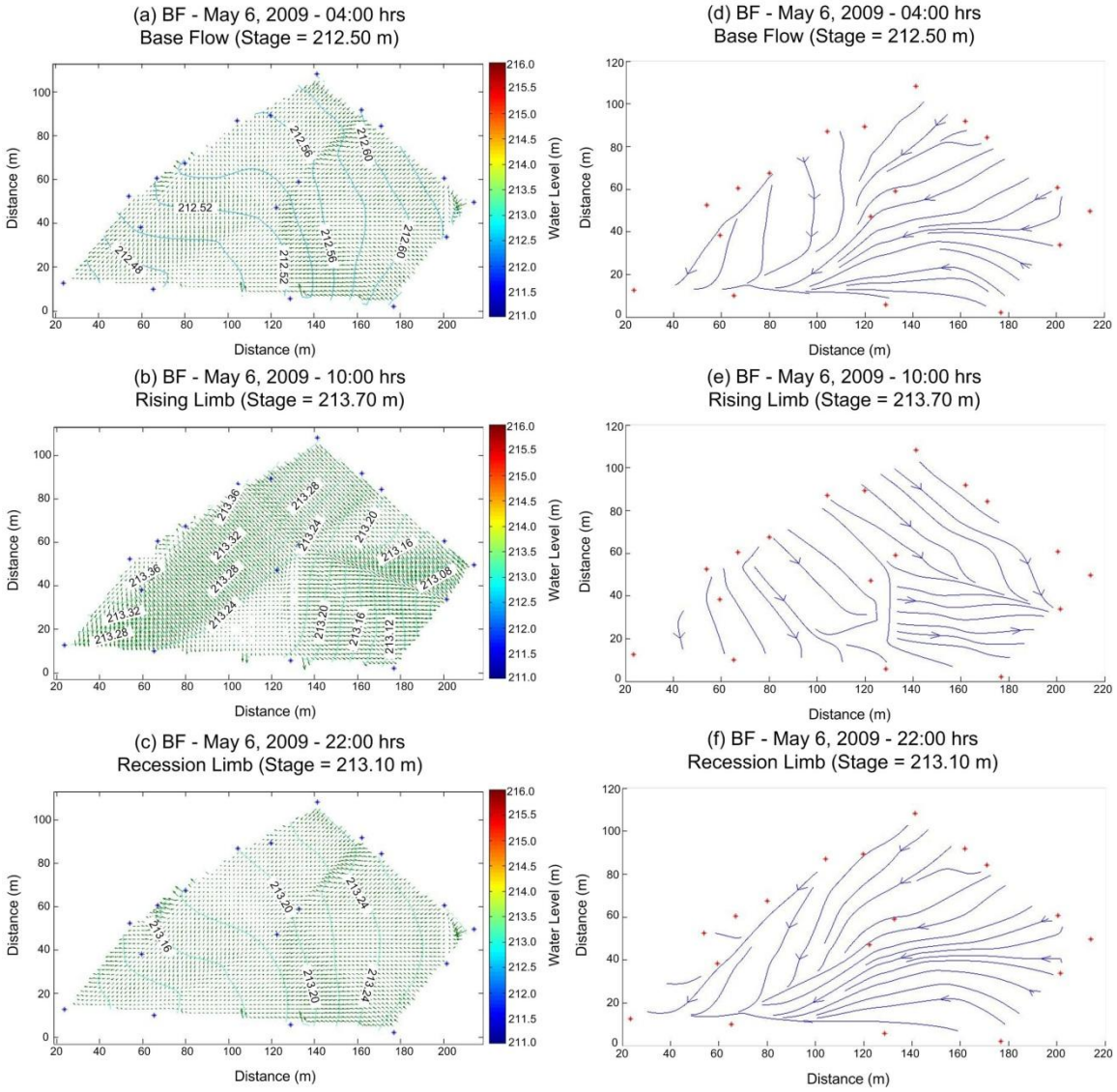

Figure 3.4. Water table elevation contour plots (a, b, and c) and streamlines (d, e, and f) for the Barren Fork Creek (BF) site during base flow (a and d), rising limb (b and e), and recession limb (c and f) of a streamflow hydrograph on May 6, 2009. The Barren Fork Creek is located at the top left corner of the plot.

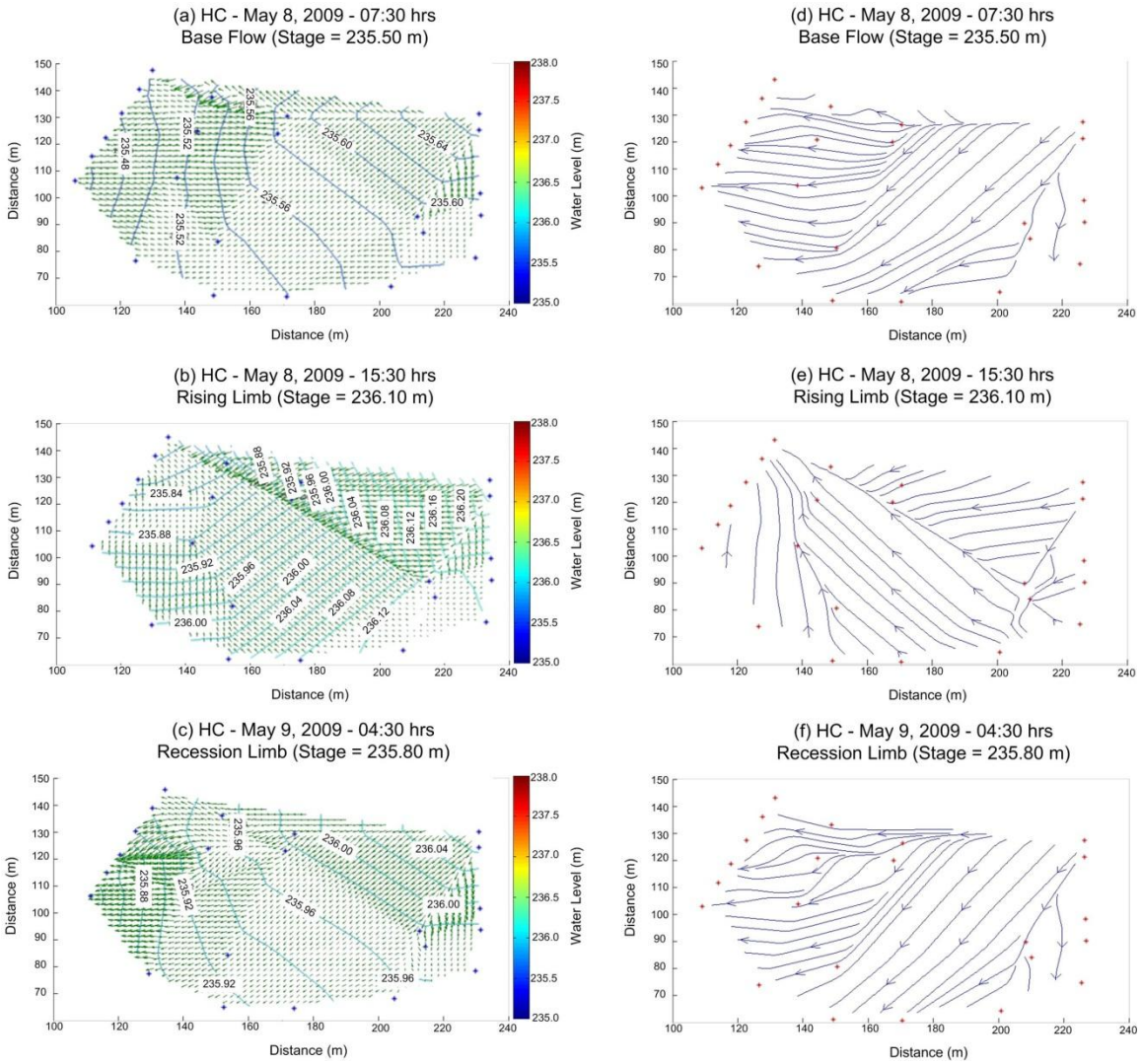

Figure 3.5. Water table elevation contour plots (a, b, and c) and streamlines (d, e, and f) for the Honey Creek (HC) site during base flow (a and d), rising limb (b and e), and recession limb (c and f) of a streamflow hydrograph on May 8-9, 2009. Honey Creek is located around the bend at the bottom of the plot.

During baseflow conditions, divergence provided a direct measure of aquifer heterogeneity since the change in water table elevation over time was small. At the Barren Fork Creek site, divergence during baseflow correlated well with stream stage. For example, during baseflow divergence became positive whenever the stream stage declined past 212.0 m. These divergence data also exhibited a negative correlation with stream stage at the Honey Creek site

during baseflow conditions. As the water table declined, layers of aquifer material became unsaturated and no longer affected flow patterns.

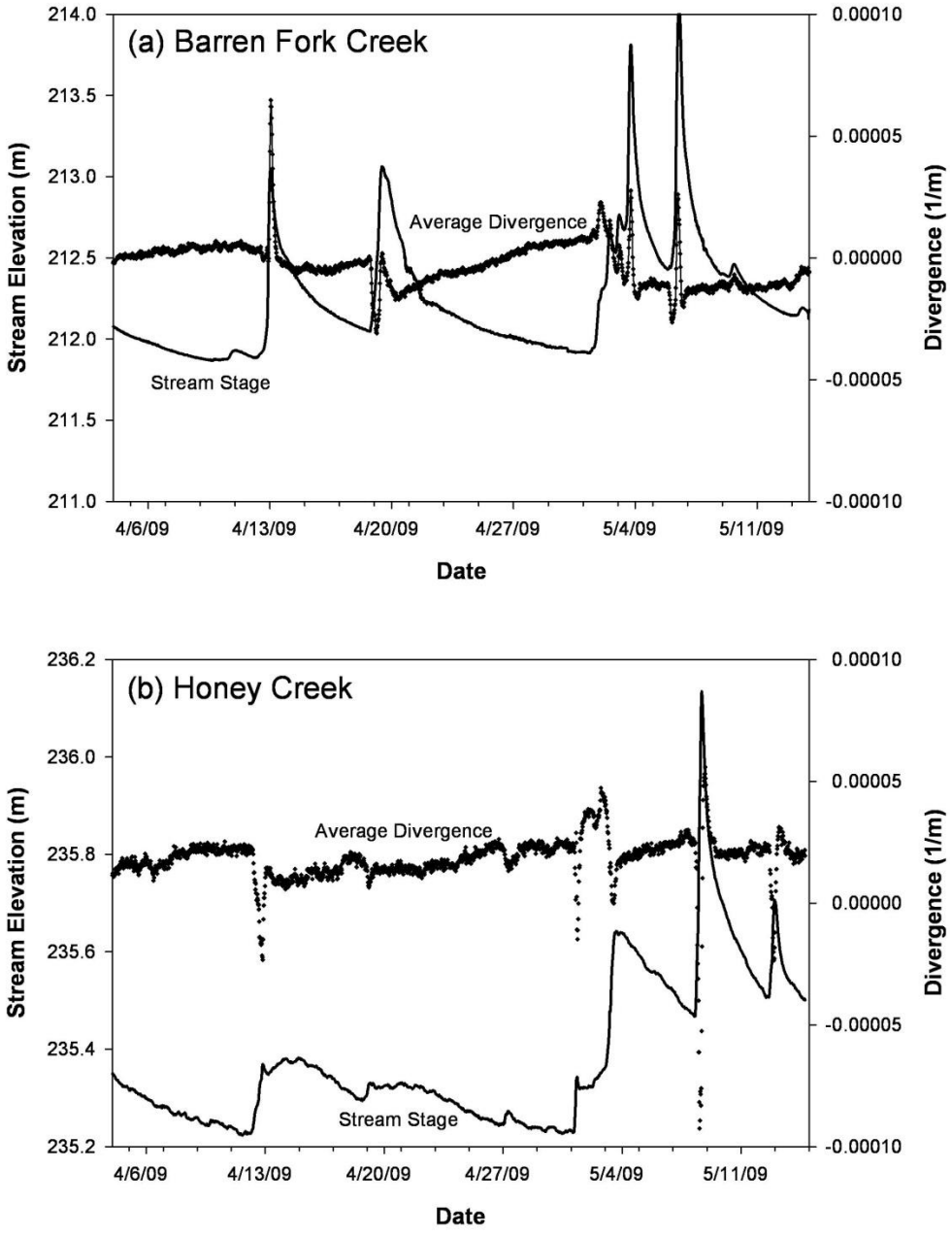

Figure 3.6. Divergence data for the Barren Fork Creek site (a) and the Honey Creek site (b). For scale, the May 6 event on the Barren Fork Creek had a peak flow of 250 $m^3 s^{-1}$, a 1.3 year recurrence interval event. The May 8 event on Honey Creek had a peak flow of 18 $m^3 s^{-1}$, a 1.7 year recurrence interval event.

During high flow events, the change in water table elevation over time may have become significant, in which case these divergence data would reflect both aquifer heterogeneity and change in storage (i.e., water table elevation). This was a confounding factor at the Honey Creek site. For example, on the rising limb of the May 8th event the mean divergence decreased to -9 x 10^{-5} m^{-1} (a large convergence), followed by an increase in divergence to 6 x 10^{-5} m^{-1}, before returning to baseflow levels of divergence (Figure 3.6). On the rising limb, measured divergence due to the rapidly changing water table would be negative. Since the mean divergence was negative during the rising limb, we were unable to determine whether it was primarily due to aquifer heterogeneity or the rapidly rising water table.

However, divergence data were not confounded during high flow events at the Barren Fork Creek site. Since the mean divergence was positive during the rising limb of high flow events, i.e. the rising water table contributed to gradient convergence, the impact of aquifer heterogeneity (divergence) was dominant over change in storage effects (convergence). Mean divergence levels in the groundwater approached 6 x 10^{-5} m^{-1} (Figure 3.6) during the rising limb of high flow events due to a PFP connected to the stream. This divergence zone, which allowed stream water to quickly enter the groundwater system, was the same PFP observed in the water table elevation data (Figure 3.4b). The activity of a convergence zone at the southwest corner of the site (Figure 3.4f) caused the mean divergence to decrease to -3 x 10^{-5} m^{-1} on the falling limb of high flow events at the Barren Fork Creek site.

It appeared that both the convergence zone PFP and the divergence zone PFP at the Barren Fork Creek site could be active at the same time. At baseflow both were active, but which one had the dominant effect on the mean divergence depended on the water table elevation. At higher stream stage, the convergence zone had a greater impact on groundwater flow, resulting in a negative mean divergence. At lower stream stages during baseflow, the divergence zone had a greater impact, resulting in a positive mean divergence.

3.4.3. Direction as an Indicator of Transient Storage

The average groundwater flow direction at each floodplain site also changed considerably between baseflow and storm events (Figure 3.7). At the Barren Fork Creek field site, the average direction in the floodplain was approximately southwest (200° to 220°) during baseflow conditions, but changed to a southeastern direction (300° to 320°) during large flow events (Figure 3.8). At the Honey Creek floodplain site, the average groundwater direction was southwest (210° to 220°) (i.e., across the meander bend and directed back towards the stream) during baseflow conditions. During storm events, the average direction changed to northwest (i.e., 130° to 150° or away from the meander bend) (Figure 3.9). The statistical range in groundwater direction increased across both of the two-dimensional well grids during flow events (Figures 3.8 and 3.9), suggesting that the flow patterns in these floodplains became more complex during high stream stage.

The changes in average groundwater direction indicated the occurrence of transient storage within the floodplain: groundwater flow direction changed as water moved rapidly into the floodplain during the rising limb of the streamflow hydrograph and then returned to its original average direction as water drained through a preferential flow pathway during the recession of the hydrograph (Figures 3.8 and 3.9). Similar to the flow divergence, the change in the direction at both field sites appeared to be a function of the rate of change in the stream stage, with higher rates of change correlating to greater variations in the average groundwater direction compared to the direction under baseflow conditions. In fact, the maximum deviation in average groundwater gradient from the average gradient under baseflow conditions occurred slightly before the peak of the streamflow hydrograph at both sites. The average groundwater gradient after the peak shifted quickly back to the average gradient during baseflow conditions (Figures 3.8 and 3.9).

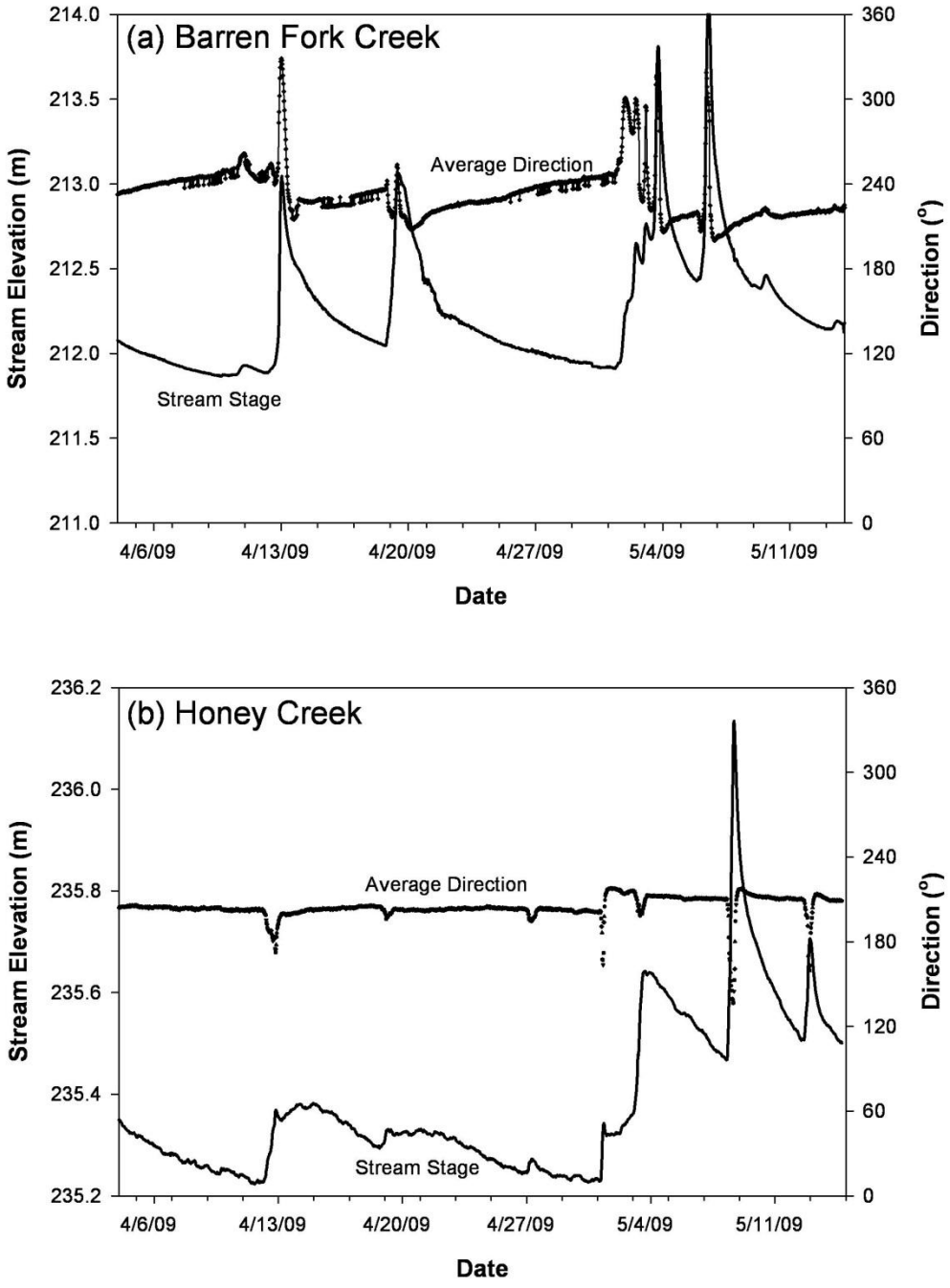

Figure 3.7. Average direction of the hydraulic gradient at the (a) Barren Fork and (b) Honey Creek field sites from April 4, 2009 to May 14, 2009.

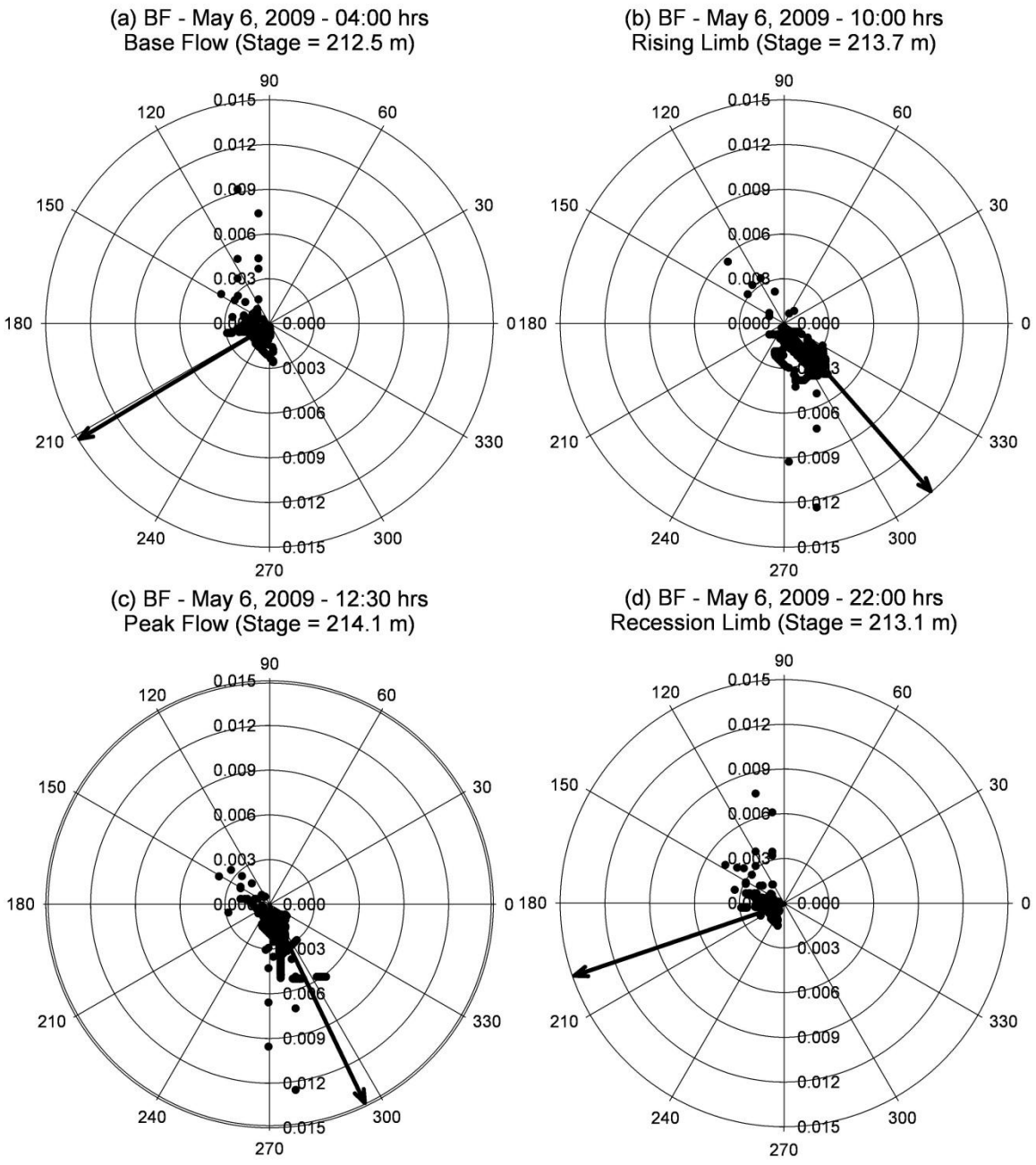

Figure 3.8. Polar plots of the hydraulic gradients during a hydrograph at the Barren Fork Creek (BF) field site on May 6, 2009. These polar plots are constructed with the magnitude and direction of the groundwater gradient for all points in the floodplain grid. The red line indicates the direction of the average groundwater gradient. (a) Base flow with an average groundwater gradient of 0.001 m/m at 211°, (b) rising limb with an average groundwater gradient of 0.003 m/s at 314°, (c) peak flow with an average groundwater gradient of 0.002 m/m at 295°, and (d) recession limb with an average groundwater gradient of 0.001 m/m at 200°.

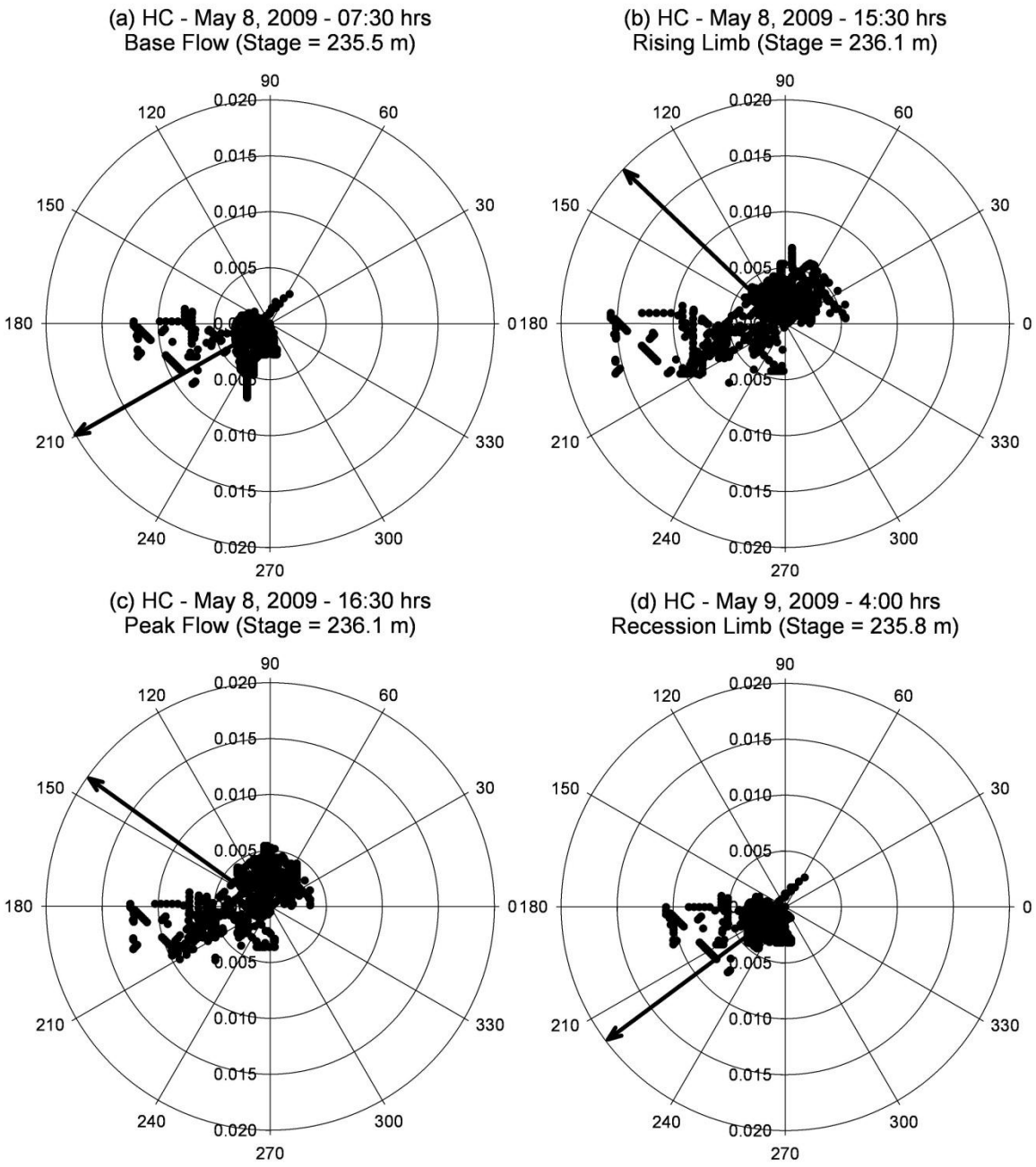

Figure 3.9. Polar plots of the hydraulic gradients during a hydrograph at the Honey Creek (HC) field site on May 8-9, 2009. These polar plots are constructed with the magnitude and direction of the groundwater gradient for all points in the floodplain grid. The red line indicates the direction of the average groundwater gradient. (a) Base flow with an average groundwater gradient of 0.003 m/m at 210°, (b) rising limb with an average groundwater gradient of 0.004 m/m at 136°, (c) peak flow with an average groundwater gradient of 0.003 m/m at 145°, and (d) recession limb with an average groundwater gradient of 0.003 m/m at 217°.

3.4.4. Research Implications

As discussed by Packman and Bencala (2000), the surface and subsurface hydrological interactions in these alluvial floodplains can be viewed from two different perspectives. The first is viewing the interaction from the stream. From this viewpoint, the interaction is commonly idealized using a transient storage model that simulates hyporheic storage in an aggregate fashion as a well-mixed but immobile system (Bencala and Walters, 1983). Harvey et al. (1996) and others have suggested this idealization captures rapid hyporheic transport (i.e., near streambed exchange) but cannot capture exchange with the more extensive alluvium. The groundwater divergence and direction results in this research further verify these conclusions and more intensely emphasize the importance of considering stream exchanges beyond the near-streambed zone (i.e., larger-scale transient storage) relative to changes in stream stage. Changes in discharge and stream stage are suggested to influence near-streambed transient storage (D'Angelo et al., 1993; Harvey and Bencala, 1993; Morrice et al., 1997; Worman et al., 2002; Zarnetske et al., 2007; Stofleth et al., 2008). However, as noted by Zarnestke et al. (2007), "…the overall understanding of how they [perturbations in discharge, elevation of channel stage, and water table] correlate to in-channel and hyporheic storage dynamics is still unclear", especially for larger-scale interactions with the alluvium. The presence of large-scale transient storage at high stream stage may have a direct impact on the transport of in-stream contaminant loads as the stream water interacts with the alluvial groundwater in floodplains throughout the watershed. Future work should be devoted to creating models capable of handling both the near-streambed and larger-scale transient storage to quantify implications of this larger-scale exchange on solute and contaminant transport in stream systems during both base flow and high flow conditions.

The second perspective is viewing the surface-subsurface interaction from the subsurface, which considers hyporheic exchange as the mixing of stream-derived and aquifer-derived water. This perspective relies heavily on the use of numerical groundwater flow models to describe

reach-scale groundwater flow pathways (Packman and Bencala, 2000; Poole et al., 2006). Particle tracking models may be used to determine the extent of penetration of stream-derived water into the aquifer (Wroblicky et al., 1998). The stream is commonly idealized as a boundary that derives subsurface flow. Of course any modeling effort is dependent on the ability to adequately parameterize input data and specify the appropriate boundary conditions. Also, groundwater heads are typically measured throughout the study area to calibrate the model. The most sensitive parameter in groundwater flow models and the subject of most calibration effort is the aquifer hydraulic conductivity. The divergence and direction results from the two floodplain studies reported in this research indicate the necessity of considering horizontal zones of aquifer heterogeneity and anisotropy within alluvial floodplains to adequately simulate larger-scale PFPs over a range of water table elevations. Heterogeneity has been modeled by assuming a distribution of hydraulic conductivity and that the distribution is randomly distributed in space (Gotovac et al., 2009). However, the non-random nature of the heterogeneity has been confirmed by variograms performed on hydraulic conductivity data in previous research at these alluvial sites (Miller et al., 2010; Miller, 2012). These PFPs are hypothesized to be buried gravel bars, resulting in long, continuous zones of high conductivity (Heeren et al., 2010). Also, groundwater heads measured for flow calibration should be measured during both baseflow and high stream stage events when the PFPs activate. It is important to appropriately identify potential PFPs prior to installation of observation wells for monitoring groundwater levels. Electrical resistivity imaging was used in this research to locate observation well sites at areas of potential flow convergence and divergence. Neglecting PFPs and their stage-dependent activation may limit the amount of useful information derived from groundwater flow models due to an inappropriate representation of the flow system.

3.5. SUMMARY AND CONCLUSIONS

The assumptions of uniform, homogeneous stream/aquifer interaction and only localized, near-streambed hyporheic interactions were not appropriate in the studied alluvial floodplains. The activity of preferential flow pathways depended on the elevation of the water table and the interaction between the stream and the groundwater. It appeared that preferential flow pathways acted as divergence zones, allowing stream water to quickly enter the groundwater system, or as flow convergence zones draining a large groundwater area. A method was developed to quantify aquifer heterogeneity using divergence of the water table gradient. During base flow conditions, non-zero results indicated areas of spatial heterogeneity in saturated hydraulic conductivity consistent with previous research. During high flow events, divergence was a measure of both aquifer heterogeneity and the rapidly changing water table elevation (aquifer storage). At the Barren Fork Creek site, stream water consistently flowed into the alluvial aquifer, even during base flow conditions. Transient storage occurred in these alluvial floodplains systems as highlighted by the fact that the average groundwater flow direction at each floodplain site changed considerably between baseflow and storm events. Such transient storage may have a direct impact on the transport of in-stream contaminant loads as the stream water interacts with the alluvial groundwater along floodplains throughout the watershed.

This research was limited by the cubic interpolation used to determine the distribution of head between wells; future research should use a process based groundwater model to determine a physically sound distribution of head on which to calculate divergence and direction. Transient zone storage models should be modified to consider the larger scale (i.e., beyond near-streambed) and stage-dependent storage observed in this research. Furthermore, more research needs to be performed in additional alluvial floodplain sites with coarse, gravel material to document the occurrence of these rapid exchange flow pathways and their impact on contaminant fate and transport.

3.6. ACKNOWLEDGMENTS

This research is based upon work supported by the Oklahoma Conservation Commission with a U.S. Environmental Protection Agency Region VI Section 319 grant. The author acknowledges Mr. Dan Butler of the Oklahoma Conservation Commission and Mr. Bill Berry for providing access to the alluvial floodplain properties. Dr. Garey Fox, Oklahoma State University, and Amanda K. Fox, Private Consultant, developed and ran the Matlab routine. Dr. Dan Storm, Ron Miller, and Aaron Mittelstet, Biosystems and Agricultural Engineering, Oklahoma State University, also contributed significantly to this chapter. The author acknowledges Sharla Lovern and Jason Walker, Biosystems and Agricultural Engineering, Oklahoma State University, for assisting with field work.

CHAPTER IV

STAGE-DEPENDENT TRANSIENT STORAGE OF PHOSPHORUS IN ALLUVIAL FLOODPLAINS[2]

4.1. ABSTRACT

Models for contaminant transport in streams commonly idealize transient storage as a well-mixed but immobile system. These transient storage models capture rapid (near-stream) hyporheic storage and transport, but do not account for large scale, stage-dependent interaction with the alluvial aquifer. The objective of this research was to document transient storage of phosphorus (P) in coarse gravel alluvium potentially influenced by large-scale, stage dependent preferential flow pathways (PFPs). Long-term monitoring was performed at floodplain sites adjacent to the Barren Fork Creek and Honey Creek in northeastern Oklahoma. Based on results from subsurface electrical resistivity mapping which was correlated to hydraulic conductivity data, observation wells were installed both in higher hydraulic conductivity and lower hydraulic conductivity subsoils. Water levels in the wells were monitored over time, and water samples were obtained from the observation wells and the stream to document P concentrations at

[2] Published in *Hydrological Processes*
Heeren, D. M., G. A. Fox, R. B. Miller, D. E. Storm, A. R. Mittelstet, A. K. Fox, C. J. Penn, and T. Halihan. 2011. Stage-dependent transient storage of phosphorus in alluvial floodplains. *Hydrol. Process.* 25(20): 3230-3243, doi: 10.1002/hyp.8054.

multiple times during high flow events. Contour plots indicating direction of flow were developed using water table elevation data. Contour plots of total P concentrations showed the alluvial aquifer acting as a transient storage zone, with P-laden stream water heterogeneously entering the aquifer during the passage of a storm pulse, and subsequently reentering the stream during baseflow conditions. Some groundwater in the alluvial floodplains had total P concentrations that mirrored the streams' total P concentrations. A detailed analysis of P forms indicated that particulate P (i.e., P attached to particulates greater than 0.45 μm) was a significant portion of the P transport. This research suggests the need for more controlled studies on stage-dependent transient storage in alluvial systems.

4.2. INTRODUCTION

Increased nutrient loads have resulted in several adverse impacts on surface water quality, including excessive algal growth, and fish kills across the United States and especially in the Illinois River Basin (Andrews et al., 2009). Lake Eucha, a source of water for Tulsa, Okla., suffered from drinking water taste and odor issues that were attributed to algal production (Blackstock, 2003). Nitrogen is a concern, but phosphorus (P) is generally considered the limiting nutrient in most surface water systems (Daniel et al., 1998). While optimum crop growth requires a range of P above 0.2 mg/L, preventing surface water enrichment generally requires P to be below 0.03 mg/L (Pierzynski et al., 2005). In fact, surface waters in the Ozark ecoregion in particular may have a threshold closer to 0.01 mg/L (D.E. Storm, 2012, personal communication). Scientists and engineers need to identify critical nutrient source areas and transport mechanisms within a catchment in order to protect and enhance drinking water systems, recreation activities, and aquatic ecosystems. Subsurface contaminant transport may be important in highly conductive soils (Lacas et al., 2005), even for a highly sorbing contaminant such as P (Turner and Haygarth, 2000; Fuchs et al., 2009).

Although numerous studies have documented subsurface P transport from agricultural fields with tile drainage (Sims et al., 1998; Turner and Haygarth, 2000; Djodjic et al., 2004; Kleinman et al., 2004; Nelson et al., 2005; Hively et al., 2006), limited subsurface P transport studies have been conducted in other hydrologic settings and the transport mechanisms are generally less understood compared to transport by surface runoff (Gachter et al., 1998; Stamm et al., 1998; Heathwaite and Dils, 2000). From research on four grassland soils, Turner and Haygarth (2000) documented that subsurface P transport, primarily in the dissolved form, can occur at concentrations that could cause eutrophication. When assessing long-term risk of P loss from waste-amended soils, Nelson et al. (2005) indicated that P leaching and subsurface transport should be considered. In addition, other researchers have emphasized the importance of colloidal transport for P movement (Broberg and Persson, 1988), as P adsorbs to small particles capable of being transported through soil pore spaces in the subsurface (Haygarth et al., 1997; Addiscott et al., 2000; de Jonge et al., 2004; Fuchs et al., 2009).

There have been a few studies conducted in which observation wells were used to monitor the movement of nutrients in alluvial floodplains (Vanek, 1993; Cooper et al., 1995; Carlyle and Hill, 2001; Fuchs et al., 2009; Thompson and McFarland, 2010). Studies have shown high P availability for groundwater transport due to saturation of the riparian zone (Cooper et al., 1995) and near streambank sediment (Thompson et al., 2010). Monitoring 12 wells in a lake riparian zone, Vanek (1993) noted groundwater P concentrations ranging from 0.4 to 11 mg/L with an average of 2.6 mg/L. Carlyle and Hill (2001) monitored the behavior of P in the subsurface in a river riparian zone and suggested that riparian areas can become saturated with P. They documented higher soluble reactive P (SRP) concentrations (0.10 to 0.95 mg/L) in areas having soils with higher hydraulic conductivities buried under topsoils. Exchange of water and P between the stream and gravel subsoils is distributed across the entire river channel but enhanced in preferential pathways (Malard et al., 2002). There is a need for additional studies devoted to

understanding both groundwater flow patterns and P transport through the subsurface of alluvial floodplains.

One approach for simulating contaminant transport during the interaction between streams and alluvial aquifers is through a transient storage zone model, with the transient storage zone commonly idealized as a well-mixed but immobile system (Bencala and Walters, 1983). Harvey et al. (1996) suggested that this idealization captures rapid hyporheic storage and transport (i.e., near streambed exchange) but cannot capture exchange with the more extensive alluvium. Changes in discharge and stream stage are suggested to influence near-streambed transient storage (D'Angelo et al., 1993; Morrice et al., 1997; Hart et al., 1999; Worman et al., 2002; Zarnetske et al., 2007; Stofleth et al., 2008). However, as noted by Zarnestke et al. (2007), "…the overall understanding of how they [perturbations in discharge, elevation of channel stage, and water table] correlate to in-channel and hyporheic storage dynamics is still unclear", especially for larger-scale interactions with the alluvium. The presence of large-scale transient storage at high stream stages may have a direct impact on the transport of in-stream contaminant loads as the stream water interacts with the alluvial groundwater in floodplains throughout the watershed.

It is well known that paleochannels, or linear deposits of coarse-grained sediments, exist across floodplains and link modern channel flows to distal floodplain areas (Stanford and Ward, 1992; Poole et al., 1997; Amoros and Bornette, 2002; Naiman et al., 2005). Hydrologic pathways become complex with deposits of coarse alluvium (Naiman et al., 2005). Poole et al. (2002) characterized a coarse alluvial aquifer on the Middle Fork Flathead River in Montana, with a localized hydraulic conductivity on the order of 10,000 m/d. Preferential flow paths (PFPs) were identified with 20% of the river's flow entering the aquifer in one area and reemerging downstream. Also, paleochannels in the vadose may become active once the stream stage has reached a specific elevation to transmit flow. Preferential flow through paleochannels would

result in complex, larger-scale flow patterns that would be considered beyond the scale and definition of hyporheic zone flow. However, limited data has been reported on P transport through these floodplain-scale PFPs.

Large-scale preferential flow and transient storage become more significant in streams adjacent to highly conductive alluvial aquifers. For example, the Ozark ecoregion of Missouri, Arkansas, and Oklahoma is approximately 62,000 km2 and is characterized by gravel bed streams that have migrated substantially over time yielding many paleochannels throughout the ecoregion. The erosion of carbonate bedrock (primarily limestone) by slightly acidic water has left a large residuum of chert gravel in Ozark soils, with floodplains generally consisting of coarse, chert gravel overlain by a mantle (1 to 300 cm) of gravelly loam or silt loam. The same processes have resulted in karst topography, including caves, springs, sink holes, and losing streams (Neill et al., 2003; Davis et al., 2005).

The objective of this research was to document large scale, stage-dependent transient storage of P in coarse alluvial aquifers potentially influenced by PFPs. An extensive body of literature exists for near-stream transient storage but only limited data has been published on larger-scale transient storage. In this research, transient storage includes storage in both perpetually and variably saturated substrates, the latter of which is often referred to as bank storage. While the long-term monitoring was performed in the Ozark ecoregion, similar hydrogeologic conditions exist in gravel bed streams and their associated shallow alluvial aquifers worldwide.

4.3. METHODS AND MATERIALS

4.3.1. Alluvial Floodplain Sites

The alluvial floodplain sites were located in the Ozark ecoregion of northeastern Oklahoma (Figure 3.1). The Barren Fork Creek site (Figure 4.1a, latitude: 35.90°, longitude:

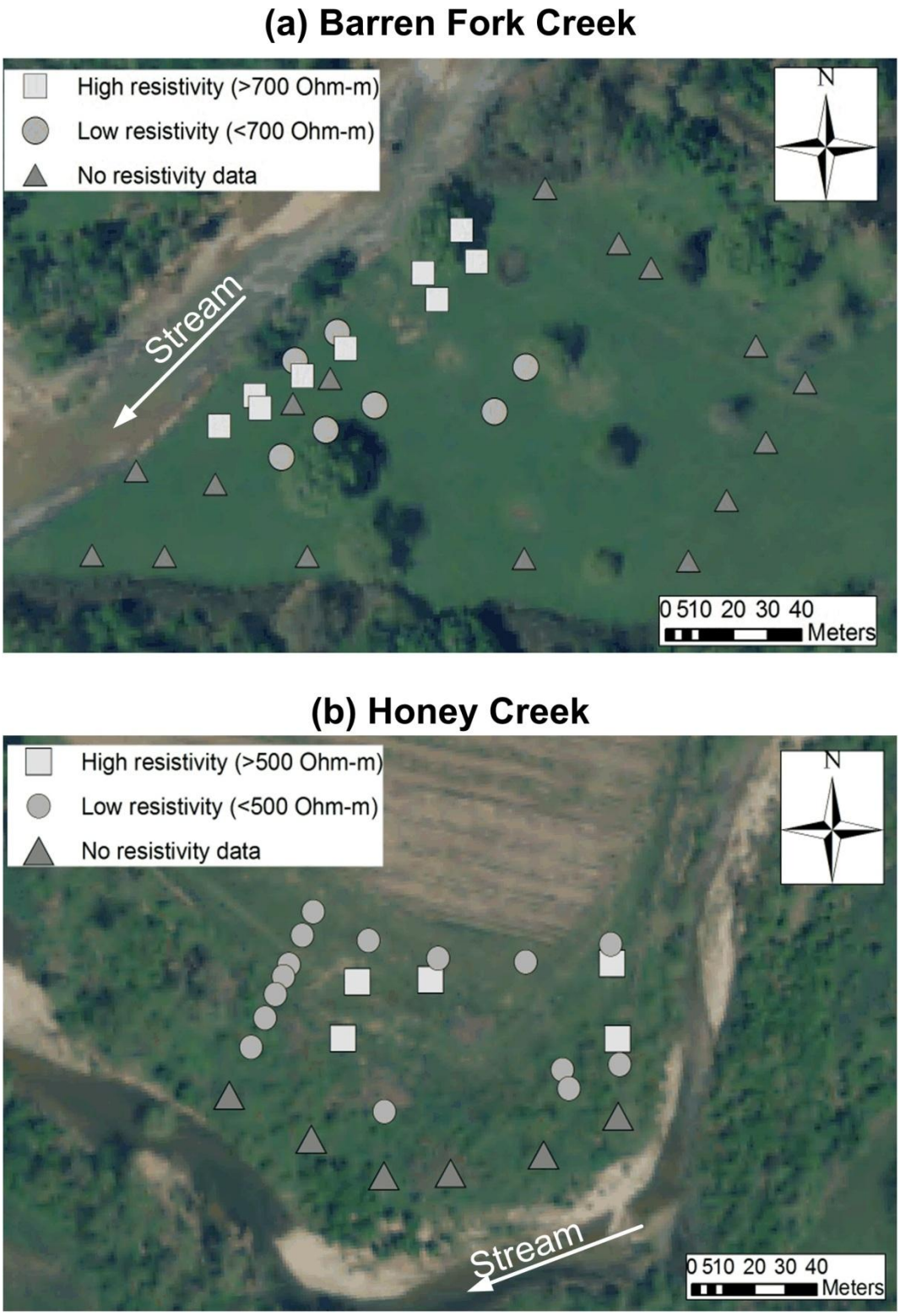

Figure 4.1. Observation well locations overlain on aerial images (NAIP, 2008) for the Barren Fork Creek site (a) located near Tahlequah, Oklahoma, and the Honey Creek site (b) located near Grove, Oklahoma. Most wells were located based on electrical resistivity data, with high resistivity (greater than 700 Ω-m) subsoils considered to have potential for preferential flow.

-94.85°) was immediately downstream of the Eldon Bridge U.S. Geological Survey (USGS) gage station 07197000. With a watershed size of 845 km^2, the Barren Fork Creek site was a fourth order stream with a historical median discharge of 3.6 m3 s^{-1} and. The study area at the Barren Fork Creek was located on the outside of a meander bend which was being actively eroded by the stream. The Honey Creek site (Figure 4.1b, latitude: 36.54°, longitude: -94.70°) was also located immediately downstream of a USGS gage station (07189542). As a third order stream, the Honey Creek site had a 0.54 m^3 s^{-1} historical median discharge and a 150 km^2 watershed. The riparian area on Honey Creek was located on the inside of a meander bend, an area likely to be aggradational.

The Barren Fork Creek site was a hay field with a Mehlich III soil test P (STP) of 33 mg/kg in the top 15 cm and had not received fertilizer for several years. The Honey Creek study site was composed of both forest and grassland. Adjacent to a tree farm, the area had received fertilizer in the past resulting in a current STP of 60 mg/kg in the top 15 cm. Fuchs et al. (2009) reported a P sorption maximum of 125 mg kg^{-1} and a binding energy of 0.048 L mg^{-1} for a Langmuir isotherm performed on the fine material (i.e. < 2.0 mm) in the alluvial aquifer at the Barren Fork Creek site. The degree of P saturation (i.e., P / [Al + Fe]) was found to be 4 to 8% based on ammonium oxalate extractions. Redox conditions were not expected to be a concern for characterizing P fate and transport because of the lack of anaerobic conditions due to the high porosity and excessive drainage of both the soil and subsurface materials in Ozark floodplains. For example, dissolved oxygen (DO) of the groundwater at the Barren Fork Creek site (measured with a ProODO DO meter, YSI Inc., Yellow Springs, Ohio) ranged from approximately 8 mg/L near the creek to 4 mg/L up to 100 m from the creek.

The soils of both floodplain sites were classified as Razort gravelly loam underlain with alluvial gravel deposits. Thickness of the loam ranged from 0.5 to 1.0 m at the Barren Fork Creek site and from 0.1 to 0.5 m at the Honey Creek site. Soil hydraulic studies on these soil types have shown

that subtle morphological features can lead to considerable differences in soil water flow rates (Sauer and Logsdon, 2002). Fuchs et al. (2009) described some of the soil and hydraulic characteristics of the Barren Fork Creek floodplain site, including estimates of hydraulic conductivity for the gravel subsoil between 140 and 230 m d^{-1} based on falling head trench tests. Heeren et al. (2010) performed a tracer injection into a PFP, identified as a buried gravel bar, at the Barren Fork site. Local transient storage was observed as evidenced by the elongated tails of breakthrough curves in some observation wells due to physical heterogeneity in the aquifer materials.

4.3.2. Electrical Resistivity Mapping and Observation Well Installation

Geophysics has been widely used for subsurface mapping (Pellerin, 2002; Robinson et al., 2008). Resistivity mapping involves measuring the electrical properties of near-surface earth materials, which vary with grain size, mineral type, solute content of pore water, and pore-space saturation. Apparent electrical resistivity is calculated at several locations in a two-dimensional profile by carefully measuring the voltage generated by a known electrical current using four electrodes in contact with the soil. Miller et al. (2012) collected electrical resistivity data using a SuperSting R8/IP Earth Resistivity Meter (Advanced GeoSciences Inc., Austin, TX) with a 56-electrode array. The profiles at the Barren Fork Creek site employed electrode spacings of 0.5 to 2.5 m with associated depths of investigation ranging from 7.5 to 25.0 m, respectively. The Honey Creek site utilized a 1-m spacing, with an associated depth of investigation of approximately 10 m. The area of interest in each study site, which was less than 5 m below the ground surface, was well within the ERI depth of investigation. The resistivity sampling and subsequent inversion utilized a proprietary routine devised by Halihan et al. (2005), which produced higher resolution images than conventional techniques. Electrical resistivity results showed subsurface heterogeneity at both floodplain sites (Figure 4.2). One of the high resistivity

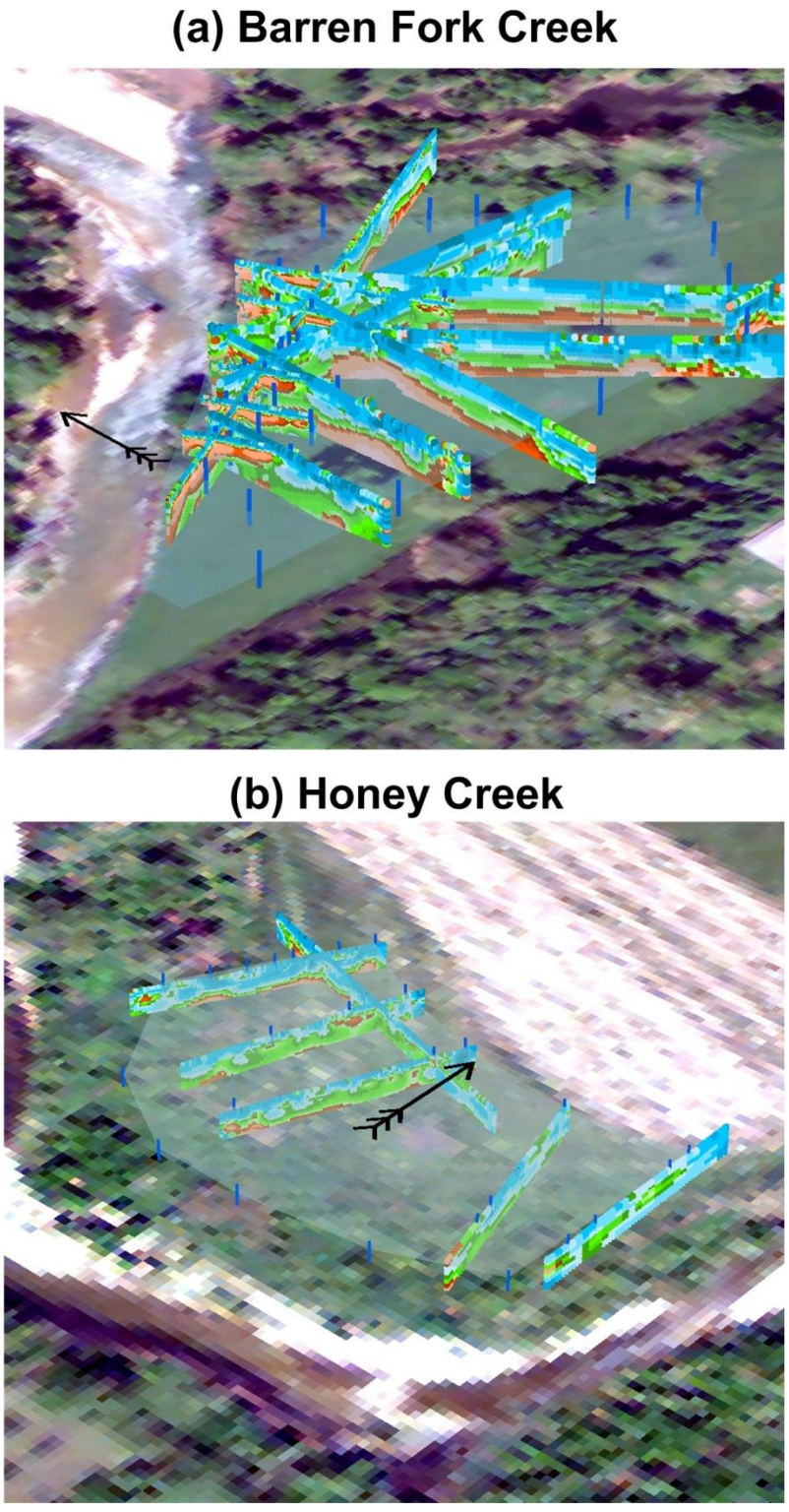

Figure 4.2. Barren Fork Creek (a) and Honey Creek (b) vertical (5m) electrical resistivity profiles which have been positively correlated (r^2 = 0.73) to saturated hydraulic conductivity (Miller et al., 2010; Miller, 2012). Blue is low resistivity (less than 375 Ω-m); green is medium; and orange is high (greater than 700 Ω-m). The shaded areas demarcate well fields, with blue lines indicating observation well locations. The black arrows show true north; aerial images are from NAIP, 2008.

areas at the Barren Fork Creek site matched a PFP observed in previous research (Fuchs et al., 2009; Heeren et al., 2010).

Using a borehole permeameter specifically designed for coarse gravel subsoils (Miller et al., 2011) to measure saturated hydraulic conductivity in situ, Miller et al. (2012) established a positive correlation between electrical resistivity and hydraulic conductivity for the Barren Fork Creek and Honey Creek floodplain sites. Based on that correlation and the previous electrical resistivity results (Heeren et al., 2010; Miller et al., 2010; Miller, 2012), observation wells were located in both higher electrical resistivity (possible PFP) and lower electrical resistivity subsoils (Figures 4.1 and 2). In this research, a PFP was defined as a zone of high hydraulic conductivity in the subsoil that has potential for rapid transport of water and solutes.

A Geoprobe Systems drilling machine (6200 TMP, Kejr, Inc., Salina, KS) was used to install observation wells in the alluvial floodplains with a 2.0 to 3.0 m screened section at the base. Depth to refusal for installed wells ranged from 4.0 m to greater than 5.0 m at the Barren Fork Creek site and from 2.5 to 3.5 m at the Honey Creek site. Bentonite clay was placed at the top of the well casing to prevent surface runoff from entering the borehole. Well locations were surveyed using a TOPCON HiperLite Plus global positioning system configured with a base station and rover unit (4 cm accuracy). These data were corrected for positional errors using the National Geodetic Survey Online Positioning User Service (OPUS). Since the water table elevation data were more sensitive to measurement error than horizontal position, a laser level was used to determine the elevation at the top of each well (1 cm accuracy).

4.3.3. Long-Term Monitoring for Groundwater Flow Patterns

At each site, 24 observation wells were instrumented with automated water level loggers (HoboWare, Onset Computer Corp., Cape Cod, MA, water level accuracy of 0.5 cm) to monitor water pressure and temperature at five minute intervals from April 2009 to April 2010. One

logger was placed above the water table at each site to account for changes in atmospheric pressure. Reference water table elevations, obtained with a water level indicator, were then calculated. The logger data were processed with HoboWare Pro software, which accounted for changes in atmospheric pressure as well as changes in water density due to temperature and produced water table elevation data (1 cm accuracy).

Water table elevation data were analyzed with Matlab (The Mathworks, Natick, MA). Using 30-minute intervals, a cubic interpolation was performed to determine the head for grid points in the two-dimensional well field. Contour maps were plotted with equipotential lines using a 2-cm interval. While streamlines were not necessarily perpendicular to contour lines due to anisotropy and unsteady flow during high flow events, the contour plots did indicate general flow patterns in the groundwater system. Patterns in groundwater contours were investigated at both baseflow conditions and during storm events. Data from the local USGS gage stations were also used in the analysis.

4.3.4. Phosphorus Sampling and Testing

Water samples from observation wells were collected during multiple high flow events using a peristaltic pump. Samples were obtained at seven different times (September 2009 and March 2010) from the stream and 19 to 23 observation wells at the Barren Fork Creek site and at six different sampling times (October 2009 and March 2010) from the stream and 21 observation wells at the Honey Creek site (Figure 4.3, Table 4.1). The number of observation wells at the Barren Fork Creek site decreased over time due to rapid streambank erosion (Midgley et al., 2011). High flow events were of particular interest because stream P concentrations generally increase with streamflow in these watersheds (Andrews et al., 2009). While samples were collected from the top of the water table (i.e., upper 10 cm) in order to avoid sediment in the bottom of the wells, water in the well was assumed mixed during pumping. Water samples were

stored on ice and transported back to the laboratory for analysis. After digestions with the sulfuric acid-nitric acid method (Pote et al., 2009), total P concentrations were determined colorimetrically (Murphy and Riley, 1962) with a spectrophotometer (Spectronic 21D, Milton Roy, Ivyland, PA).

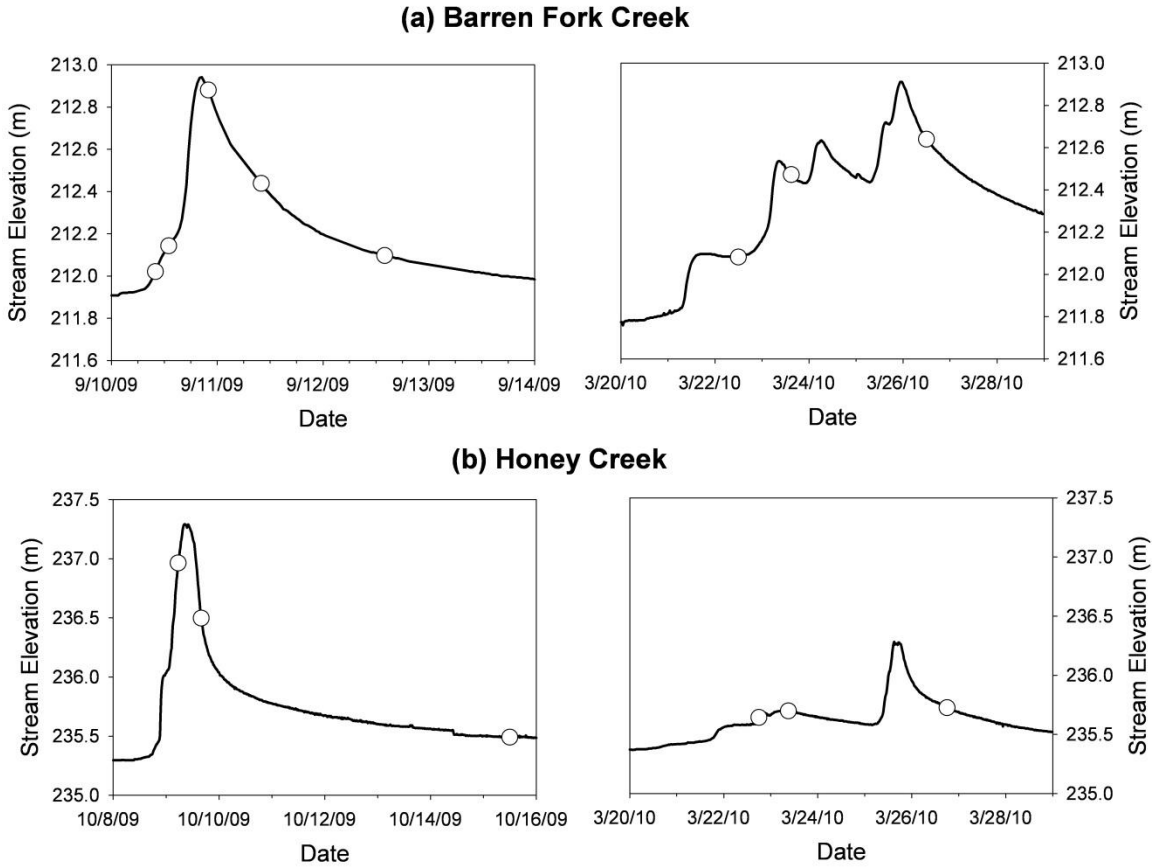

Figure 4.3. Hydrographs for the Barren Fork Creek (a) and Honey Creek (b) field sites based on upstream gage stations. Circles designate dates of water table contour plots and phosphorus sampling from the observation wells and streams. Note that samples were not collected for the first point on the Honey Creek hydrograph, but the water table data was included to illustrate groundwater flow during rising limb conditions.

Contour plots of total P concentration were generated with Matlab (The Mathworks, Natick, MA). A cubic interpolation was performed to determine the P concentration for grid points in the two-dimensional well field with a contour interval of 10 μg/L P. Kriging, which attempts to express trends suggested in the underlying data (Cressie, 1991), was also considered as a geostatistical technique for interpolating the P data. Developed using Surfer 8 (Golden

Software, Inc., Golden, CO), variograms were used to quantitatively assess the spatial continuity in the data, but consistent trends were not observed in the data due to the complex nature of the alluvial deposits. Also, any spatial relationships in the variograms may have been obscured by the asymmetrical distribution along with the limited number of observation wells. Therefore, the cubic interpolation was selected as the best visual presentation of the data.

Table 4.1. Hydrologic data and total phosphorus (P) concentrations (mg/L as P) for each sampling time. Size of the flow event is characterized by its recurrence interval. Groundwater concentrations are characterized by the median and interquartile range (IQR). Percent particulate phosphorus is the mean of the groundwater samples.

Site	Date	Time	Runoff Source	Stream Stage (m)	Hydro-graph Position	Peak Flow (m^3s^{-1})	Interval (yr)	Total P (mg/L) Groundwater Median	Groundwater IQR	Stream	Particulate P* (%)
Barren Fork Creek	9/10/09	10:00	Rainfall	212.0	Rising	86	1.1	0.02	0.03	0.02	--
	9/10/09	13:00	Rainfall	212.1	Rising	86	1.1	0.01	0.01	0.03	--
	9/10/09	22:00	Rainfall	212.9	Peak	86	1.1	0.01	0.02	0.07	--
	9/11/09	10:00	Rainfall	212.4	Falling	86	1.1	0.02	0.03	0.08	--
	9/12/09	14:00	Rainfall	212.1	Falling	86	1.1	0.02	0.02	0.04	--
	3/22/10	12:00	Snowmelt	212.1	~Rising	48	1.05	0.03	0.01	0.03	30
	3/23/10	15:00	Snowmelt	212.5	Falling	48	1.05	0.04	0.02	0.20	36
	3/26/10	12:00	Rainfall	212.6	Falling	85	1.1	0.02	0.03	0.21	53
Honey Creek	10/09/09	16:00	Rainfall	236.5	Falling	81	6	0.05	0.03	0.16	--
	10/15/09	12:00	Rainfall	235.5	Baseflow	81	6	0.05	0.03	0.07	--
	3/22/10	18:00	Snowmelt	235.6	Rising	6.1	1.1	0.05	0.02	0.11	35
	3/23/10	9:00	Snowmelt	235.7	Peak	6.1	1.1	0.05	0.02	0.10	34
	3/26/10	18:00	Rainfall	235.7	Falling	24	1.7	0.05	0.04	0.11	55

* Not measured for 2009 samples

Samples collected in 2010 were further analyzed to determine P forms. Filtration with a 0.45 μm filter (Millipore mixed cellulose ester membranes, Fisher Scientific, Waltham, Mass.) was used to remove particulates greater than 0.45 μm. Filtered samples were tested with the spectrophotometer for dissolved reactive P and an Inductively Coupled Plasma – Optical Emission Spectrometer (ICP-OES, Arcos, SPECTRO Analytical Instruments, Kleve, Germany) for total dissolved P. The minimum detection limit was 0.01 mg/L P for both the spectrophotometer and the ICP-OES.

4.4. RESULTS AND DISCUSSION

4.4.1. Groundwater Flow Patterns

Patterns in the water table elevation contour plots at the Barren Fork Creek and Honey Creek field sites during the 12 month observation period remained relatively consistent during baseflow conditions, but changed during high flow events. Plots for times at which P samples were collected, as well as two additional times to illustrate rising limb stream conditions, illustrate the range of groundwater flow patterns in the dataset (Figures 4.4 to 4.8).

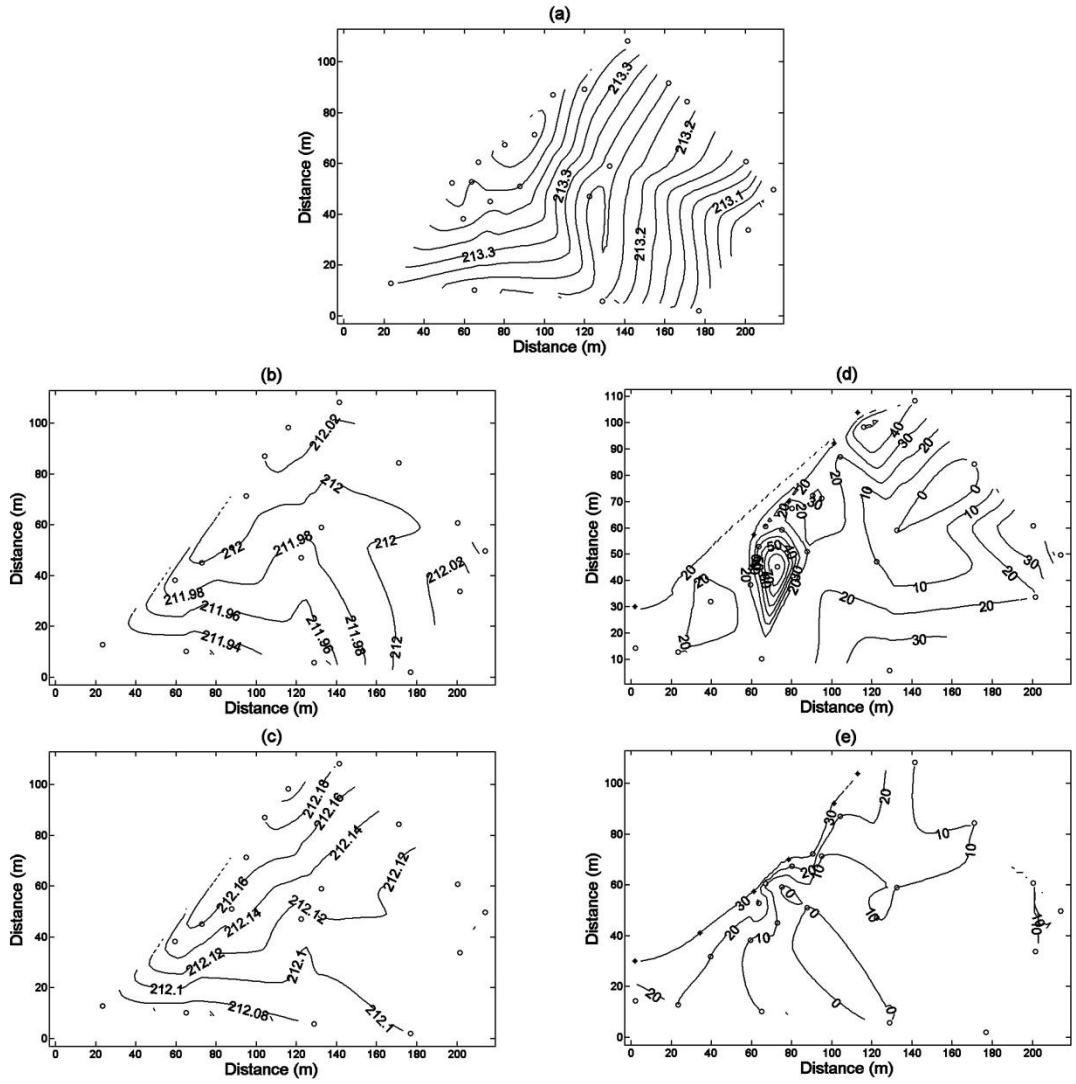

Figure 4.4. Water table contour plot (a) for the Barren Fork Creek site during the rising limb of the May 6, 2009, high flow event before significant streambank erosion occurred (Midgley et al., 2011). Water table (b-c) and total phosphorus (d-e) concentration (µg/L as P) contour plots for the first (b,d) and second (c,e) sampling times during the rising limb of the September 10, 2009, high flow event. Interpolations are based on measured data from wells (circles) and the stream (stars). See Table 4.1 and Figure 4.3 for more information on hydrologic conditions at the time of sampling.

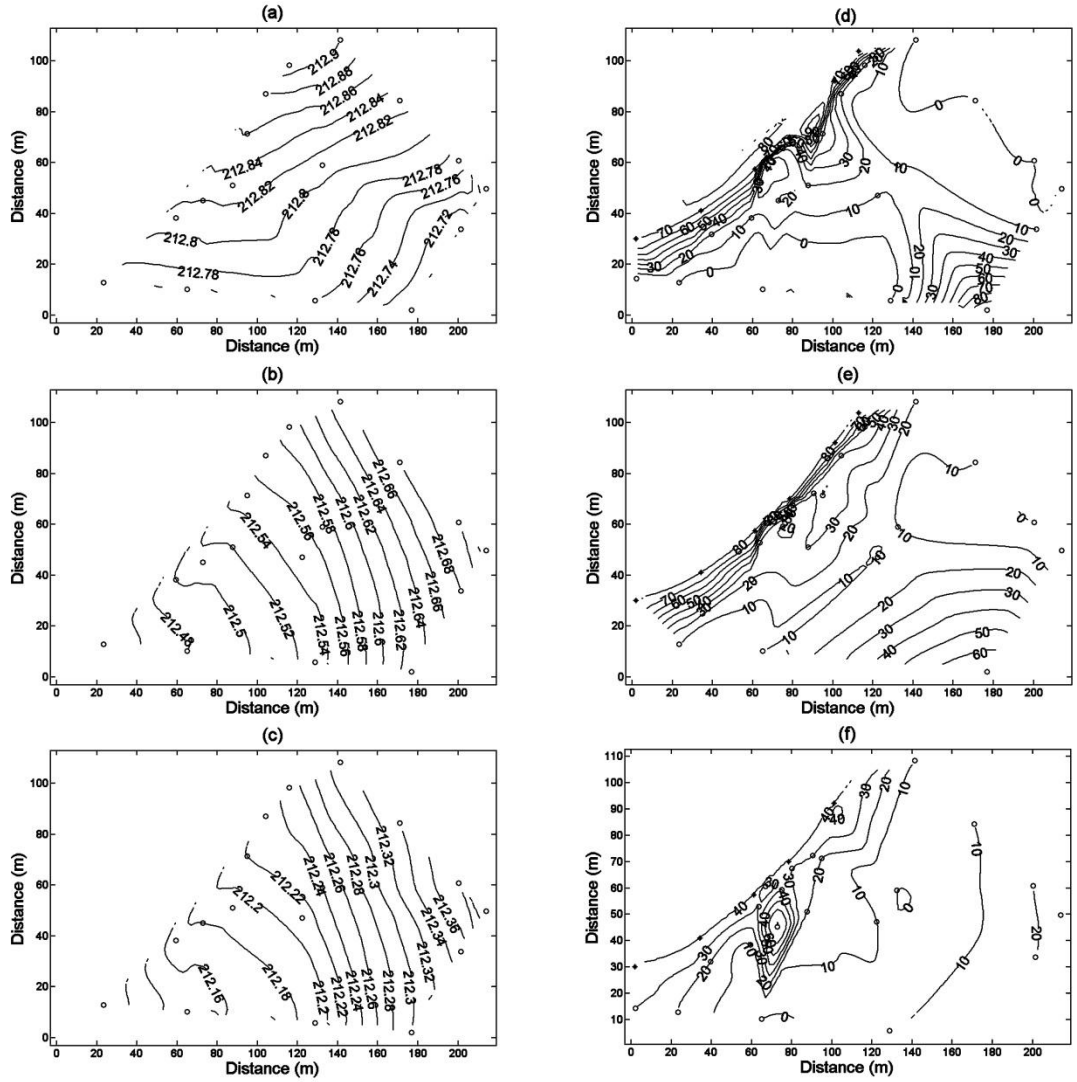

Figure 4.5. Water table (a-c) and total phosphorus (d-f) concentration (µg/L as P) contour plots for the Barren Fork Creek site during the peak (a,d) and the first (b,e) and second (c,f) sampling times of the recession limb of the September 10, 2009, high flow event. Interpolations are based on measured data from wells (circles) and the stream (stars). See Table 4.1 and Figure 4.3 for more information on hydrologic conditions at the time of sampling.

The highest gradients in the alluvial aquifers occurred during the rising limbs of the hydrographs (Figure 4.4a and 4.7a), when the stream stage was rising most quickly. The average groundwater gradient after the peak (Figures 4.5a and 4.6c for the Barren Fork Creek site; Figures 4.7b and 4.8b for the Honey Creek site) shifted quickly back to the average gradient during baseflow conditions (Figures 4.5c and 4.7c).

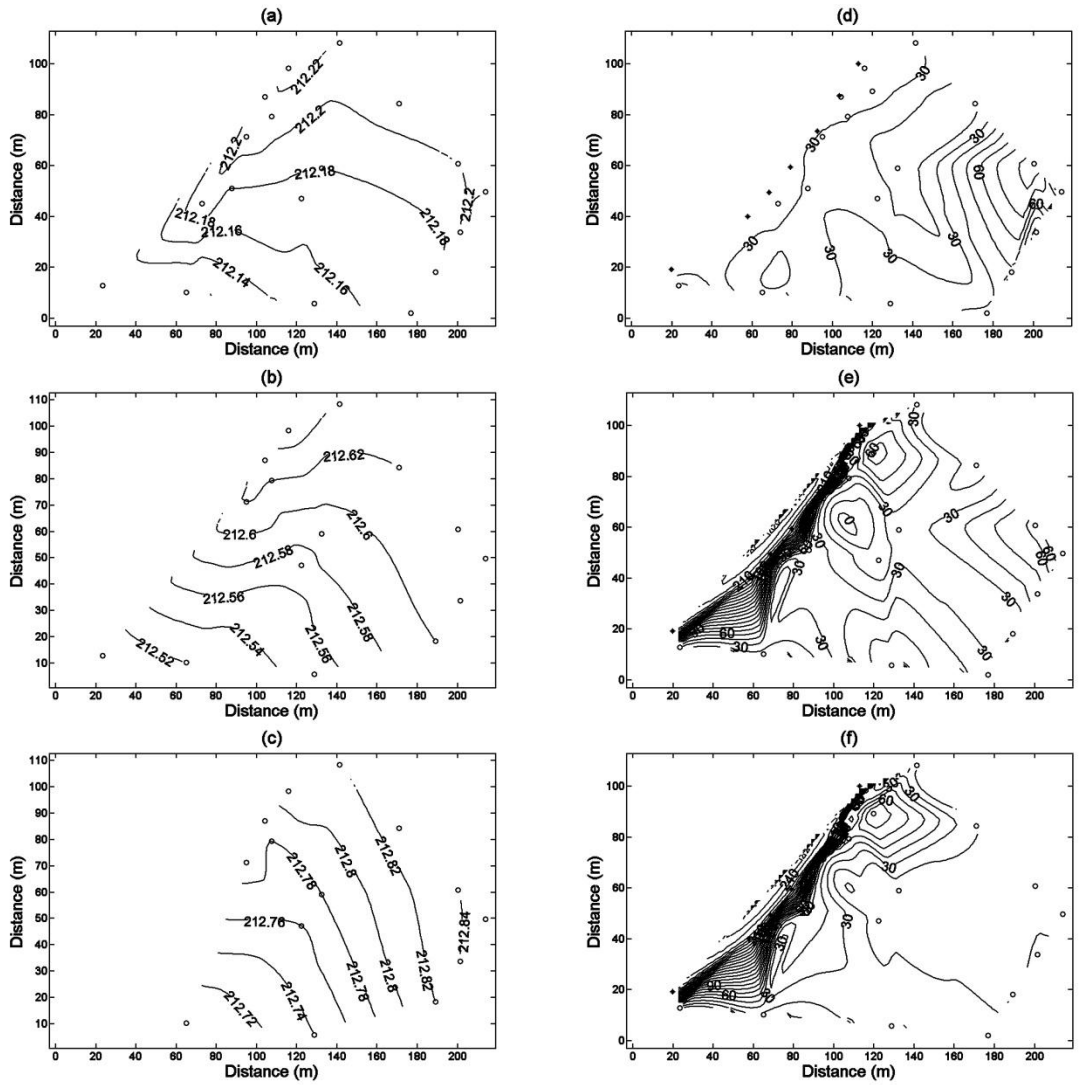

Figure 4.6. Water table (a-c) and total phosphorus (d-f) concentration (µg/L as P) contour plots for the Barren Fork Creek site during the rising limb (a,d) and the recession limb (b,e) of the March 23, 2010, high flow event and the recession limb (c,f) of the March 25, 2010, high flow event. Interpolations are based on measured data from wells (circles) and the stream (stars). See Table 4.1 and Figure 4.3 for more information on hydrologic conditions at the time of sampling. The loss of observation wells (c) is due to rapid streambank erosion rates (Midgley et al., 2011).

Flow directions in the groundwater changed considerably between base and peak flows, suggesting that the floodplains acted as transient storage zones, rapidly storing and releasing water during passage of a storm pulse. At the Barren Fork Creek field site, the average direction in the floodplain was approximately southwest (200° to 220°) during baseflow conditions (Figure 4.5c) (i.e. away from the stream in the direction of flow), but changed to a southeastern direction

(300° to 320°) (i.e. away from the stream opposite of the stream flow direction) during large flow events (Figure 4.4a to 4.4c).

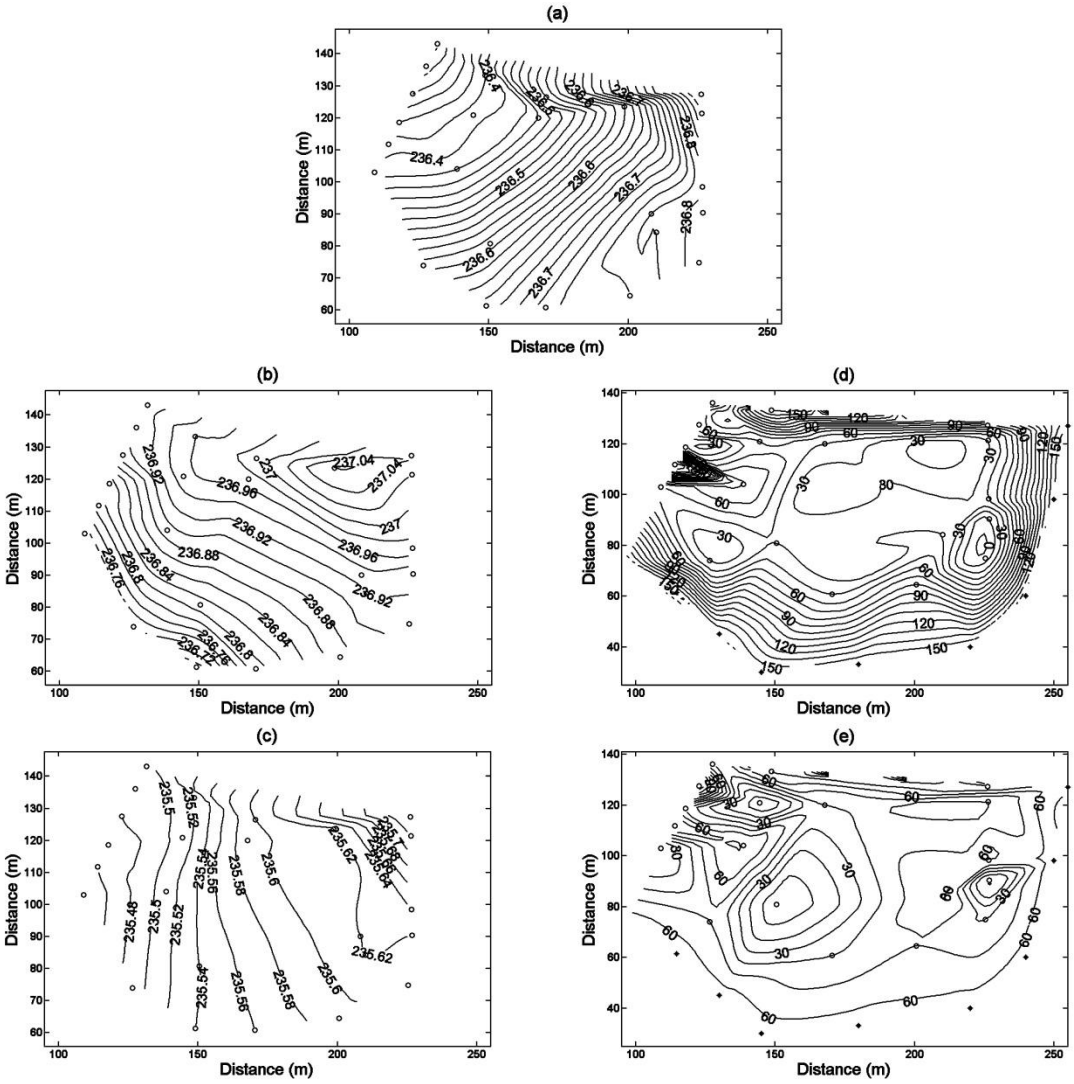

Figure 4.7. Water table (a-c) and total phosphorus (d-e) concentration (µg/L as P) contour plots for the Honey Creek site during the rising limb (a), recession limb (b,d) and baseflow (c,e) of the October 9, 2009, high flow event. Interpolations are based on measured data from wells (circles) and the stream (stars). See Table 4.1 and Figure 4.3 for more information on hydrologic conditions at the time of sampling.

At the Honey Creek floodplain site, the average groundwater direction was southwest (210° to 220°) (i.e., across the meander bend and directed back towards the stream) during

baseflow conditions (Figure 4.7c). During storm events, the average direction changed to northwest (i.e., 130° to 150° or away from the meander bend) (Figure 4.7a).

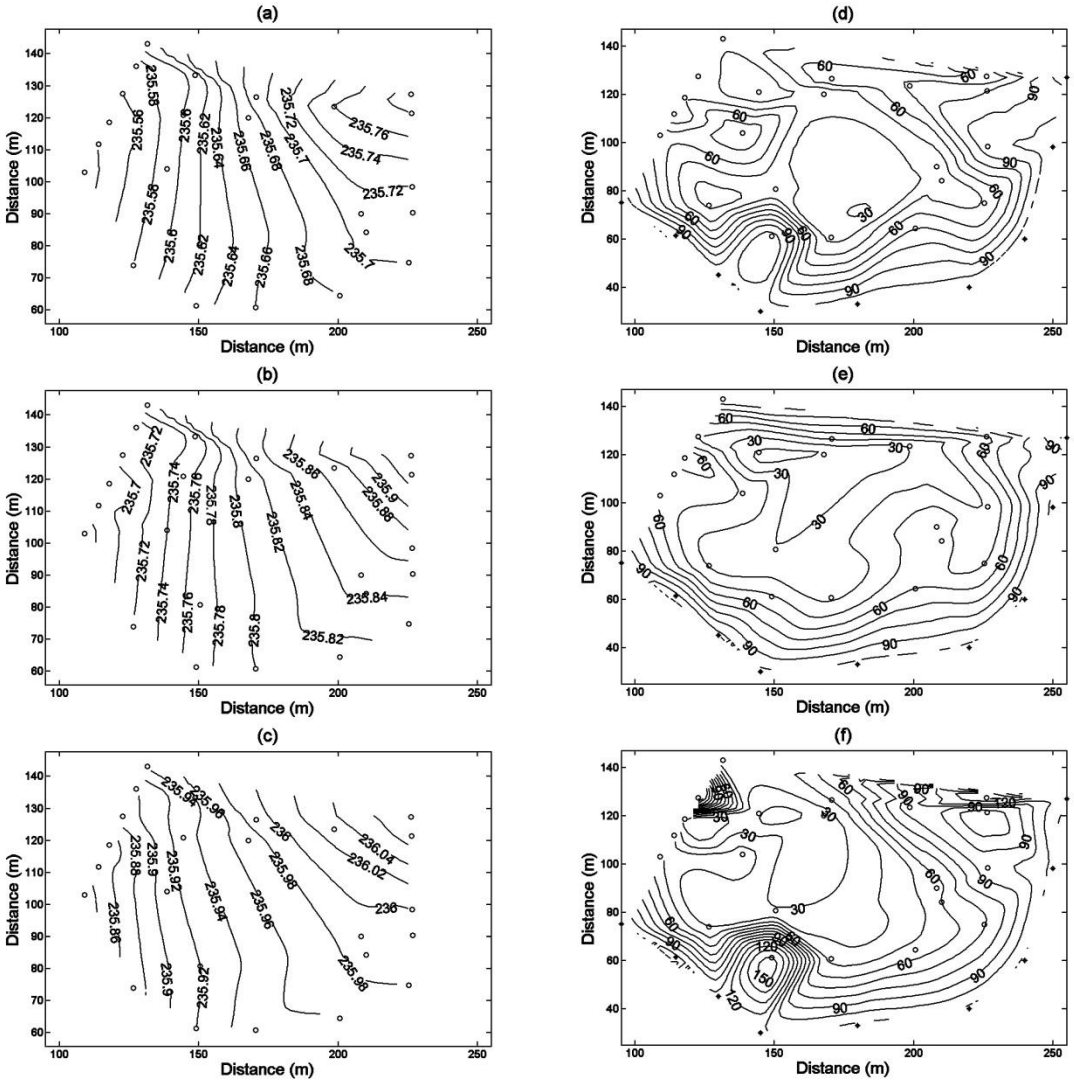

Figure 4.8. Water table (a-c) and total phosphorus (d-f) concentration (µg/L as P) contour plots for the Honey Creek site during the rising limb (a,d) and peak (b,e) of the March 23, 2010, high flow event and the recession limb (c,f) of the March 25, 2010, high flow event. Interpolations are based on measured data from wells (circles) and the stream (stars). See Table 4.1 and Figure 4.3 for more information on hydrologic conditions at the time of sampling.

The change in the direction at both field sites appeared to be a function of the rate of change in the stream stage, with higher rates of change correlating to greater variations in the average groundwater direction compared to the direction under baseflow conditions. The changes

in average groundwater direction indicated the occurrence of transient storage within the floodplain: groundwater flow direction changed as water moved rapidly into the floodplain during the rising limb of the streamflow hydrograph and then returned to its original average direction as water drained during the recession of the hydrograph.

Besides stream-aquifer interactions, the impact of aquifer heterogeneity could also be seen in the water table contour plots. The primary source of heterogeneity was expected to be saturated hydraulic conductivity, a parameter which spans several orders of magnitude, but it is acknowledged that spatial variability in porosity and aquifer depth also contributes to non-uniform flow patterns. While streamlines were not necessarily perpendicular to contour lines due to anisotropy and unsteady flow during high flow events, the contour plots did indicate general flow patterns in the groundwater system.

Flow patterns showed groundwater areas, potentially PFPs, acting as flow convergence (i.e., draining a large groundwater area) or divergence (i.e., allowing stream water to quickly enter the groundwater system) zones. For example, a zone of focused recharge can be seen along the Barren Fork Creek (Figure 4.4a) providing an inlet for stream water to enter the groundwater system. This divergence zone was at point (80 m, 60 m) (Figure 4.4a compared to Figure 4.2a), which is the location of the PFP investigated in previous research (Fuchs et al., 2009; Heeren et al., 2010) and was evident in the electrical resistivity datasets. While the buried gravel bar also extends to the northeast (see high resistivity wells in Figure 4.1a), the divergence zone in the flow data during rising stream stage conditions occurs where the PFP intersects the stream (Figure 4.4a). Intuitively, the highest water table elevation should be at the top-center of the contour plot (150 m, 110 m), at the upgradient end of the stream; however, the highest water table elevation was in the possible PFP, where stream water could most readily enter the alluvial aquifer. This possible PFP was not visible in the contour patterns at later dates (Figures 4.4b to 4.4c and 4.5a to 4.5c) since much of the area was removed due to streambank erosion between May and

September, 2009 (Midgley et al., 2011). Another divergence zone was observed at the Honey Creek site (220 m, 120 m) (Figure 4.8a to 4.8c). The correlation with electrical resistivity (Figure 4.2b) was less obvious in this case.

At other times, the contour patterns indicated flow convergence zones draining a large area of groundwater. For example, at the Honey Creek site, there was a zone between points (160 m, 125 m) and (210 m, 120 m) (Figure 4.7a), which drained a large area of groundwater to the west-northwest. The location was consistent with the location of previously hypothesized PFPs based on electrical resistivity data (Miller et al., 2010; Miller, 2012), including the high contrast in electrical (and hydraulic) properties between the two wells near point (170 m, 125 m) (Figure 4.7a compared to Figure 4.2b). The activity of this convergence zone depended on stream stage. That is, it was hypothesized that one or more PFPs were positioned in the vadose zone and began to rapidly transport water when the water table reached their elevation. This convergence zone became hydraulically activated sometime before the water table reached an elevation of 236.5 m (Figure 7a). It must also have been activated in Figure 7b (with a water table elevation of 237 m) but its impact on groundwater flow patterns may have been masked due to flow being generally perpendicular to the high conductivity zone during the falling limb of the hydrograph. Thus, the potential impact of one or more PFPs on flow was hypothesized to be a function of both stream stage and stream-aquifer interactions. The stage-dependent convergence zone at Honey Creek was more active in 2009 due to the 6-yr recurrence interval event, compared to the less than 2-yr recurrence interval events in 2010 (Figure 4.3). While the impact of specific PFPs was difficult to quantify with this data set, such results emphasize the stage-dependent nature of focused recharge/discharge in these systems and more work should be devoted to understanding the occurrence and activation of alluvial flow pathways.

4.4.2. Phosphorus Concentrations

Water samples from observation wells were collected during multiple high flow events (Figure 4.3) with peak flows from one to two orders of magnitude greater than median flow rates (Table 4.1) and were subsequently analyzed for total P concentrations (Figures 4.4 to 4.8). During baseflow conditions, groundwater P concentrations were typically 0.01 to 0.04 mg/L and 0.02 to 0.06 mg/L at the Barren Fork Creek and Honey Creek field sites, respectively. Groundwater P concentrations rose during high flow events and were generally highest where stream water was entering the groundwater system and decreased with distance downgradient from the stream (Figures 4.5d, 4.5e, 4.6e, 4.6f, 7d, and 4.8d to 4.8f). The decrease in P concentrations farther into the aquifer is likely due to sorption of the P onto the fine material in the gravel, as well as dilution with the groundwater. Even though total P concentrations decreased as stream water moved through the aquifer, transient storage was occurring in the alluvial aquifer as seen in the significant levels of P leaving the study area (and presumably re-entering the stream). Total P concentrations of groundwater leaving the well field often exceeded 0.037 mg/L, which is the standard set for Oklahoma Scenic Rivers (OWRB, 2010), which include the Barren Fork Creek (a tributary to the Illinois River).

During high flow events, the maximum P concentrations measured in the groundwater were approximately a factor of five over background levels, reaching 0.20 mg/L at the Barren Fork Creek site and 0.25 mg/L at the Honey Creek field site. Although total P concentrations generally decreased as alluvial groundwater traveled further from the stream, in some of the groundwater domain rapid transport of P occurred with concentrations at or near the P concentration in the streams during larger storm events. For example, one or more possible PFPs located at (220 m, 120 m) on the Honey Creek site facilitated transport of P into the floodplain (Figures 4.8d-f). At the Barren Fork Creek site, well 28 (at point (180 m, 0 m) in Figure 4.5d and 5e) was 100 m from the stream and had P concentrations similar to the stream P concentrations.

Well 28 was located adjacent to an abandoned stream channel that runs along a bluff; it was hypothesized that a buried lateral gravel bar served as a flow and transport pathway (Heeren et al., 2010). All zones of high electrical resistivity and therefore high hydraulic conductivity (possible PFPs) did not always show rapid P transport as these pathways must be hydraulically activated and connected to a source of P for preferential transport to occur. With limited spatial and temporal data throughout the saturated aquifer material, it was difficult to quantify the impact of specific PFPs on P transport. However, this research demonstrates that preferential transport does occur and that it should be further investigated using three-dimensional P sampling in the alluvial material (Vadas et al., 2007).

Possible sources of P in the groundwater included stream-aquifer interaction, P leaching from the topsoil due to rainfall infiltration, P-laden runon (from upland runoff) infiltration, and existing P in upgradient groundwater. The water table elevation data (Figures 4.4 to 4.8) suggest that the source of P was primarily P-laden stream water entering the alluvial aquifer. Background concentrations in the aquifer during baseflow conditions (less than 0.06 mg/L, Figures 4.4d and 4.7e) were low compared to the high total P concentrations observed during high flow events. Due to the low intensity agricultural practices at each site, the topsoil was not expected to be a significant source of P to the groundwater. While the equilibrium P concentrations (based on STP data) for the top 15 cm of soil was likely higher than measured groundwater P concentrations, subsequent layers of loam were expected to have ample sorption sites available to remove P before leachate entered the aquifer. The timing of increases in groundwater P concentrations, which matched times of rising streamflow instead of times of rainfall, also indicated that any increases in P from leaching was insignificant.

To determine whether P concentrations in the observation wells varied with depth at the Barren Fork Creek site, low-flow sampling using a peristaltic pump was used on March 23, 2010, to collect samples at both the top of the water table (i.e., upper 10 cm) and from 2.0 m below the

water table. In most wells, P concentrations were similar at both depths. However, in well 28 (at point (180 m, 0 m) in Figure 4.6e), the 2-m sample had a P concentration of 0.19 mg/L (compared to 0.04 mg/L at the top of the water table), which approached the level of P in the stream. These concentrations suggested that this PFP was at a particular elevation, near the bottom of the alluvium. The high concentrations in well 28 may have been due to P-laden runon infiltration (upland runoff has been observed cascading over the bluff in that area). However, the increasing P concentration with depth indicates lateral preferential transport from the stream instead of downward transport from the soil surface. Future work needs to address the three-dimensional nature of subsurface P transport.

Suspended colloids and sediment often possess particulate P; therefore high total P concentrations tended to correspond with samples that were visibly cloudy. Differences between total dissolved P and dissolved reactive P were negligible, indicating that organic P, if present, was only a minimal portion of the dissolved P. Particulate P (defined in this research as P attached to particulates greater than 0.45 μm) was calculated as the difference between total P (unfiltered) and dissolved reactive P (filtered). Using dissolved reactive P instead of total dissolved P (measured with the ICP) was justified due to negligible amount of dissolved organic P. Percent particulate P was calculated as the ratio of the particulate P to total P, and ranged in the groundwater from 0 to 100%, with means from 30 to 55% (Table 4.1). Due to the shallow depth of water in a few of the wells (wells further from the creek) at the Honey Creek site, the cloudiness in some samples may have been due to agitated sediment from the bottom of the well. However, even the deep wells (wells closer to the creek) at Honey Creek occasionally yielded cloudy samples from the top of the water table (e.g. well W at point (160 m, 60 m) in Figures 4.8d and 4.8f) indicating colloidal transport of P in the groundwater.

Groundwater total P concentrations were also summarized by the median and interquartile range (Table 4.1). A general linear model was performed on total P data for wells

that were placed in subsoils with electrical resistivity data available (Figure 4.1). Differences between high resistivity and low resistivity wells were statistically significant (α=0.05) in all four datasets (Table 4.2). While not all PFPs transmitted high levels of P, enough of them were hydraulically activated (water table above the elevation of the PFP) and connected to a source of P to result in a significant correlation between high resistivity and P transport. In this case, the source of P was P-rich stream water infiltrating the groundwater system. A source of error in the correlation could be imperfect identification of high hydraulic conductivity zones with the electrical resistivity data. The general linear model was also used to compare differences between wells close to the stream and wells far from the stream. The distance from the stream was a statistically significant variable (α=0.05) in two of the four data sets. This was consistent with the observation of P generally moving into the aquifer but with the movement of the plume being retarded due to sorption and dilution.

Table 4.2. Comparison of total phosphorus concentrations between wells close to and far from the stream and between high (>700 Ω-m) and low resistivity observation wells. Probability is the significance of a linear model.

		Probability	
Site	Year	Distance From Stream	Electrical Resistivity
Barren Fork Creek	2010	0.03	<0.01
Barren Fork Creek	2009	0.19	<0.01
Honey Creek	2010	<0.01	0.04
Honey Creek	2009	0.61	0.01

4.4.3. Research Implications

As discussed by Packman and Bencala (2000), the surface and subsurface hydrological interactions in these alluvial floodplains can be viewed from two different perspectives. The first is viewing the interaction from the stream. From this viewpoint, the interaction is commonly idealized using a transient storage model that simulates hyporheic storage in an aggregate fashion as a well-mixed but immobile system (Bencala and Walters, 1983). The groundwater flow and

transport results in this research demonstrate exchange with the more extensive alluvium that would not be accounted for in near streambed models. The presence of large-scale transient storage at high stream stage may have a direct impact on the transport of in-stream contaminant loads as the stream water interacts with the alluvial groundwater in floodplains throughout the watershed. Future work should be devoted to creating models capable of handling both the near-streambed and larger-scale transient storage to quantify implications of this larger-scale exchange on solute and contaminant transport in stream systems during both base flow and high flow conditions.

The second perspective is viewing the surface-subsurface interaction from the subsurface, which considers hyporheic exchange as the mixing of stream-derived and aquifer-derived water. This perspective relies heavily on the use of numerical groundwater flow models to describe reach-scale groundwater flow pathways (Packman and Bencala, 2000; Poole et al., 2006). Particle tracking models may be used to determine the extent of penetration of stream-derived water into the aquifer (Wroblicky et al., 1998). The stream is commonly idealized as a boundary that derives subsurface flow. The most sensitive parameter in groundwater flow models and the subject of most calibration effort is the aquifer hydraulic conductivity. The flow and transport results from the two floodplain studies reported in this research indicate the necessity of considering horizontal zones of aquifer heterogeneity and anisotropy within alluvial floodplains to adequately simulate larger-scale transient storage over a range of water table elevations. Heterogeneity has been modeled by assuming a distribution of hydraulic conductivity and that the distribution is randomly distributed in space (Gotovac et al., 2009). However, the non-random nature of the heterogeneity has been confirmed by variograms performed on hydraulic conductivity data in previous research at these alluvial sites (Miller et al., 2010; Miller, 2012). Higher electrical resistivity areas were hypothesized to be buried gravel bars, resulting in long, continuous zones of high conductivity (Heeren et al., 2010). Also, groundwater heads measured for flow calibration

should be measured during both baseflow and high stream stage events when the zones activate. It is important to appropriately identify potential PFPs prior to installation of observation wells for monitoring groundwater levels.

Due to their close proximately and connectedness to streams, agricultural areas of gravelly floodplains may need to be managed differently than those of upland areas. While surface runoff is considered to be the primary transport mechanism for P, subsurface transport through coarse subsoil to gravel bed streams would be a source of P not alleviated by current conservation practices (e.g., riparian buffers) aimed at surface runoff P loads. Though a highly sorbing contaminant, this research shows P being rapidly transported through coarse gravel subsoils. In these well managed sites, P leaching from the topsoil was not a significant source of P to the groundwater; therefore improvements in land management would likely have a minimal effect on subsurface P transport. However, intense agricultural management makes up a significant portion of the land-use in the Ozark ecoregion due to the presence of a poultry industry, and P leaching may be a significant source of P to the groundwater at these sites due to high STP levels throughout the soil profile. Also, the depth of the loam soil layer, which provides an opportunity for leachate to be filtered before reaching the gravel, ranges from 1 to 300 cm in the Oklahoma Ozark floodplains, and generally increases with increasing stream order. At one site in Pumpkin Hollow north of Tahlequah, OK, the loam is less than 2 cm and would provide only minimal P attenuation before runoff enters the alluvial aquifer. Ongoing research aims to quantify P leaching through loam soils of various depths. If P is found to leach through loam soil and to rapidly travel through gravel aquifers to streams, then new best management practices should be developed to halt or prevent the buildup of high STP levels in gravelly floodplains.

4.5. CONCLUSIONS

This research demonstrated significant interaction of both water and P between the stream and the aquifer. The coarse gravel aquifer acted as a transient storage zone, allowing large volumes of P-laden stream water to quickly enter the groundwater system during high flow events and to subsequently exfiltrate to the stream during baseflow conditions. Future work should be devoted to creating models capable of handling both the near streambed and larger-scale transient storage to quantify implications of this larger-scale exchange on solute and contaminant transport in stream systems during both base flow and high flow conditions.

Particulate P was a significant portion of total P in these coarse gravel aquifers. Stage-dependent preferential flow pathways appeared to transport water and P rapidly from the stream through the groundwater system, with some groundwater having total P concentrations that mimicked stream concentrations. However, the impact of specific preferential flow pathways on P transport was not explicit due to the low spatial and time resolution of P samples throughout the saturated aquifer material. Future work should include a well-controlled tracer study examining the impacts of preferential pathways on flow and transport. Additionally, more work needs to be done to characterize subsurface P transport when leaching from the topsoil is a significant source.

4.6. ACKNOWLEDGEMENTS

This material is based upon work supported by the Oklahoma Conservation Commission with a U.S. Environmental Protection Agency Region VI 319 grant. The author acknowledges Mr. Dan Butler and Mr. Bill Berry for providing access to the alluvial floodplain properties. Dr. Halihan has a managed conflict of interest with Oklahoma State University regarding the use of ERI developments.

CHAPTER V

COMPARISON OF SUBSURFACE AND SURFACE RUNOFF PHOSPHORUS TRANSPORT RATES IN ALLUVIAL FLOODPLAINS[3]

5.1. ABSTRACT

Phosphorus (P) loading to streams can occur by both surface runoff and subsurface transport, with subsurface P transport often assumed negligible. Groundwater P concentrations in alluvial aquifers can be significant, especially in preferential flow paths (PFPs). The objectives of this research were to quantify subsurface P transport rates at two sites in northeastern Oklahoma and to compare them with surface runoff P transport rates. Ozark ecoregion study sites were adjacent to the Barren Fork Creek and Honey Creek in northeastern OK, USA. Each site, instrumented with twenty-four observation wells, was monitored for several months for both groundwater levels and P concentrations. Using the flow and P concentration data, Monte Carlo simulations with Darcy's Law and a P transport rate equation were used to calculate the distributions of subsurface P transport rates across a transect within the well field containing a single identified PFP. Total subsurface P transport rates, through both the non-PFP flow domain

[3] Published as part of the following article in *Agriculture, Ecosystems, and Environment*
Mittelstet, A. R., D. M. Heeren, D. E. Storm, G. A. Fox, M. J. White, and R. B. Miller. 2011. Comparison of subsurface and surface runoff phosphorus transport rates in alluvial floodplains. *Agric. Ecosyst. Environ.* 141: 417-425.

and a single PFP, were estimated to be 0.04 kg yr^{-1} and 0.03 kg yr^{-1} for the Barren Fork Creek and Honey Creek field sites, respectively. Subsurface transport rates were compared with results from concurrent research, which used a hydrologic model, the Pasture Phosphorus Management Calculator (PPM Plus), to derive surface runoff P transport rates. Monte Carlo simulations for surface runoff P transport rates with PPM Plus resulted in average total P surface runoff transport rates of 0.07 kg yr^{-1} for the Barren Fork Creek site and 0.08 kg yr^{-1} for the Honey Creek site. For the groundwater at these floodplains, the P source was P-laden stream water flowing into the alluvial aquifer and a minimal quantity of P leaching from the surface. Results indicated that the subsurface P transport rates for small (3 ha) alluvial floodplain sites in the Ozark ecoregion were at least 0.03 to 0.04 kg yr^{-1}, although subsurface P transport rates may be higher in cases with greater numbers of PFPs and where the subsurface is connected to a larger P source.

5.2. INTRODUCTION

Phosphorus (P) is a necessary nutrient for terrestrial and aquatic plants, yet over-application of organic and/or inorganic fertilizers to agricultural fields can result in elevated Soil Test Phosphorus (STP) levels and can lead to eutrophication in receiving streams and reservoirs (Daniel et al., 1998). While optimum crop growth requires a range of P above 0.2 mg/L, preventing surface water enrichment generally requires P to be below 0.03 mg/L (Pierzynski et al., 2005). In fact, surface waters in the Ozark ecoregion in particular may have a threshold closer to 0.01 mg/L (D.E. Storm, 2012, personal communication). One such area of concern is eastern Oklahoma and western Arkansas (White et al., 2009; Andrews et al., 2009) where poultry litter is often applied based on nitrogen requirements, resulting in excessive P application. Sharpley at al. (2003) noted that feed imported to support concentrated poultry production has resulted in a net increase of nutrients in the region. After export of poultry products, what remains in the region is nutrient rich poultry litter, which is bulky and expensive to export. Therefore, the poultry litter is often applied to nearby pastures, including those in floodplains, as an inexpensive fertilizer. Over

time excessive application can result in elevated STP with an increased potential for P transport to streams and reservoirs.

Nonpoint source P pollution became a major focus in the 1970's and 1980's after it was discovered that reducing point source pollution did not significantly improve water quality in many watersheds (Crowder and Young, 1988). Compared to point source load reduction, nonpoint source load reduction is much more difficult and complex (Sims and Sharpley, 2005). The design and implementation of agricultural conservation practices to reduce P in runoff, such as buffer strips, riparian zones, terracing, and cover crops, are site specific and may be difficult to implement as economic, social, and political considerations affect farmers' willingness to adopt and maintain these practices (Sharpley et al., 2003; Sims and Sharpley, 2005). As in the 1970's and 1980's when the focus was on the easily measurable and reducible point sources, implementation of riparian buffer zones and other conservation practices currently focus on the more easily understood and observed surface runoff mechanism (Lacas et al., 2005; Popov et al., 2005; Reichenberger et al., 2007; Poletika et al., 2009; Sabbagh et al., 2009).

While surface runoff is considered to be the primary transport mechanism for P (Gburek et al., 2005), subsurface transport through coarse subsoil to gravel bed streams may be significant and represents a source of P not alleviated by current conservation practices (e.g., riparian buffers). Although conservation practices can reduce P loss in surface runoff, the movement of subsurface P and its contribution to the receiving stream system may also need to be considered. Studies have shown that subsurface nutrient transport can be significant in soils with preferential flow pathways (PFPs) (McCarty and Angier, 2001; Polyakov et al., 2005; Fuchs et al., 2009; Heeren et al., 2010, 2011) and limited soil sorption capacity (Carlyle and Hill, 2001; Polyakov et al., 2005).

Subsurface P transport from agricultural fields with tile drainage is well documented (Sims et al., 1998; Stamm et al., 1998; Heathwaite and Dils, 2000; Kleinman et al., 2004), but the research on subsurface P transport in other contexts is less developed (Gachter et al., 1998; Turner and Haygarth, 2000; Djodjic et al., 2004; Nelson et al., 2005). For example, from research on four grassland soils, Turner and Haygarth (2000) documented that subsurface P transport, primarily in the dissolved form, can occur at concentrations that could cause eutrophication. When assessing long-term risk of P loss from waste-amended soils, Nelson et al. (2005) indicated that P leaching and subsurface transport should be considered.

There have been studies conducted in which observation wells were used to monitor the movement of P in alluvial floodplains under natural conditions (Vanek, 1993; Cooper et al., 1995; Carlyle and Hill, 2001; Thompson and McFarland, 2010). Studies have shown high P availability for groundwater transport due to P saturation of the riparian zone (Cooper et al., 1995) and near streambank sediment (Thompson and McFarland, 2010). Monitoring 12 wells in a lake riparian zone, Vanek (1993) noted groundwater P concentrations ranging from 0.4 to 11 mg L^{-1} with an average of 2.6 mg L^{-1}. Carlyle and Hill (2001) monitored the behavior of P in the subsurface in a river riparian zone and suggested that riparian areas can become saturated with P. They documented higher soluble reactive P (SRP) concentrations (0.10 to 0.95 mg L^{-1}) in areas having soils with higher hydraulic conductivities buried under topsoils. Due to the changes in redox potential, they suggested that riparian areas might actually be contributing to the release of P to subsurface flow (Carlyle and Hill, 2001).

A growing body of research addresses P transport in the Ozark ecoregion, which is characterized by gravel bed streams and coarse gravel alluvial aquifers overlain with a mantle (1-300 cm) of silt loam. Storm et al. (2009), using the Soil and Water Assessment Tool (SWAT) (Arnold et al., 1998) to model the Illinois River basin in eastern Oklahoma and western Arkansas, estimated that of the entire nonpoint source P load to Lake Tenkiller, 7% was derived from

baseflow contributions compared to 22% from poultry litter via surface runoff contributions. On an alluvial floodplain site along the Barren Fork Creek, Fuchs et al. (2009) used a trench to inject P into the groundwater flow system and found it to be rapidly transported in a PFP with minimal attenuation. Heeren et al. (2010) used geophysical methods to characterize the PFP as a buried gravel bar, and performed a larger scale tracer test that demonstrated the impact of the subsurface physical heterogeneities on solute transport.

The objectives of this research were to utilize groundwater table elevation, STP, and subsurface P concentration data from the Barren Fork Creek and Honey Creek floodplain sites in northeastern Oklahoma to (1) quantify distributions in subsurface P transport rates across a transect within the well field in both PFP and non-PFP domains using Monte Carlo simulations, (2) to estimate distributions of surface runoff P transport rates based on Monte Carlo simulations of the Pasture Phosphorus Management Calculator (PPM Plus) (White et al., 2009; White et al., 2010), and (3) to compare the subsurface and surface runoff P transport rates at each site.

5.3. MATERIALS AND METHODS

5.3.1. Barren Fork Creek and Honey Creek Floodplain Sites

The two floodplain sites were located in the Ozark ecoregion of northeastern Oklahoma (Figure 3.1). The Barren Fork Creek (Figure 5.1, latitude: 35.90°, longitude: -94.85°) and Honey Creek sites (Figure 5.2, latitude: 36.54°, longitude: -94.70°) were immediately downstream of U.S. Geological Survey (USGS) gage stations 07197000 and 07189542, respectively. With a watershed size of 845 km^2, the Barren Fork Creek site had a median daily flow of 3.6 $m^3 s^{-1}$ and was a fourth order stream. Honey Creek, a third order stream, had a 0.54 $m^3 s^{-1}$ median daily flow and a 150 km^2 watershed. Both floodplain sites consisted of alluvial gravel deposits underlying a mantle of topsoil (Razort gravelly loam). The Barren Fork site's topsoil thickness ranged from 0.5 to 1.5 m (Figure 5.3). The alluvial floodplain consisted of a hay field with no fertilizer applied in

recent years and had an area of 2.7 ha with a 0.004% slope. The Honey Creek site had a topsoil thickness ranging from 0.1 to 0.5 m (Figure 5.3) and had not received poultry litter application for over ten years. The site had a 0.01% slope and a total area of 3.2 ha, of which 1.5 ha was forest along the stream and the remainder was a hay field.

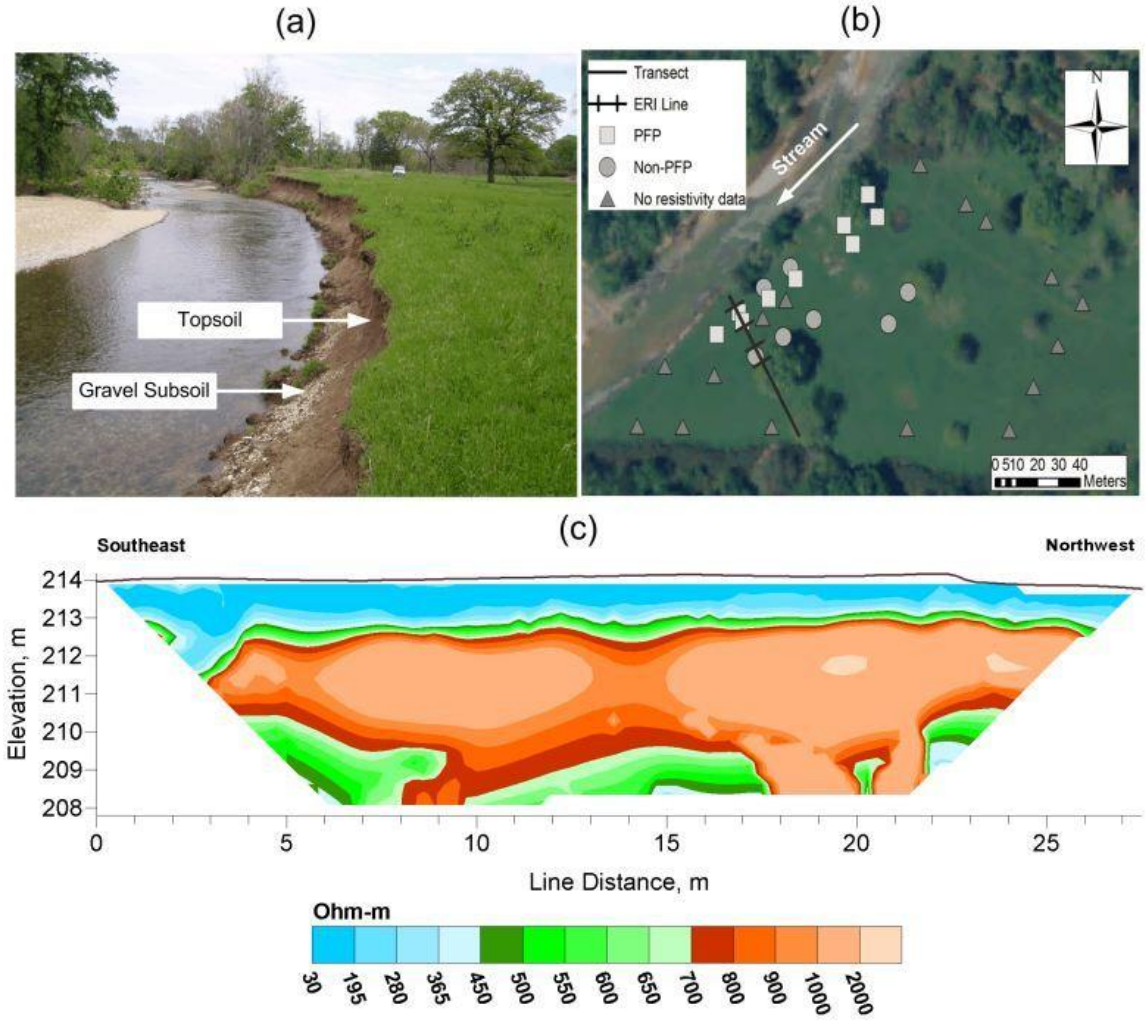

Figure 5.1. (a) The Barren Fork Creek field site near Tahlequah, OK, USA is a hay field where the floodplain consists of coarse chert gravel overlain by a mantle (50 to 150 cm) of topsoil. (b) Observation wells were located in both preferential (PFP) and non-preferential (non-PFP) flow areas based on electrical resistivity imaging. Arrow indicates stream flow direction. (c) Electrical resistivity profile through the groundwater transect for which P transport rates were calculated. Electrical resistivity at this field site has been positively correlated to saturated hydraulic conductivity (Miller et al., 2010; Miller, 2012).

5.3.2. Soil Sampling

The STP levels in the soils were quantified by collecting 15-cm soil cores from approximately 30 locations within each of the floodplain sites. These 30 soil cores were composited, mixed, and three subsamples were analyzed for STP by the Soil, Water, and Forage Analytical Laboratory at Oklahoma State University. Testing consisted of adding 20 mL of Melich 3 extraction to 2 g soil samples, shaking for 5 minutes, filtering, and then analyzing for P with inductively coupled plasma spectrometry (ICP).

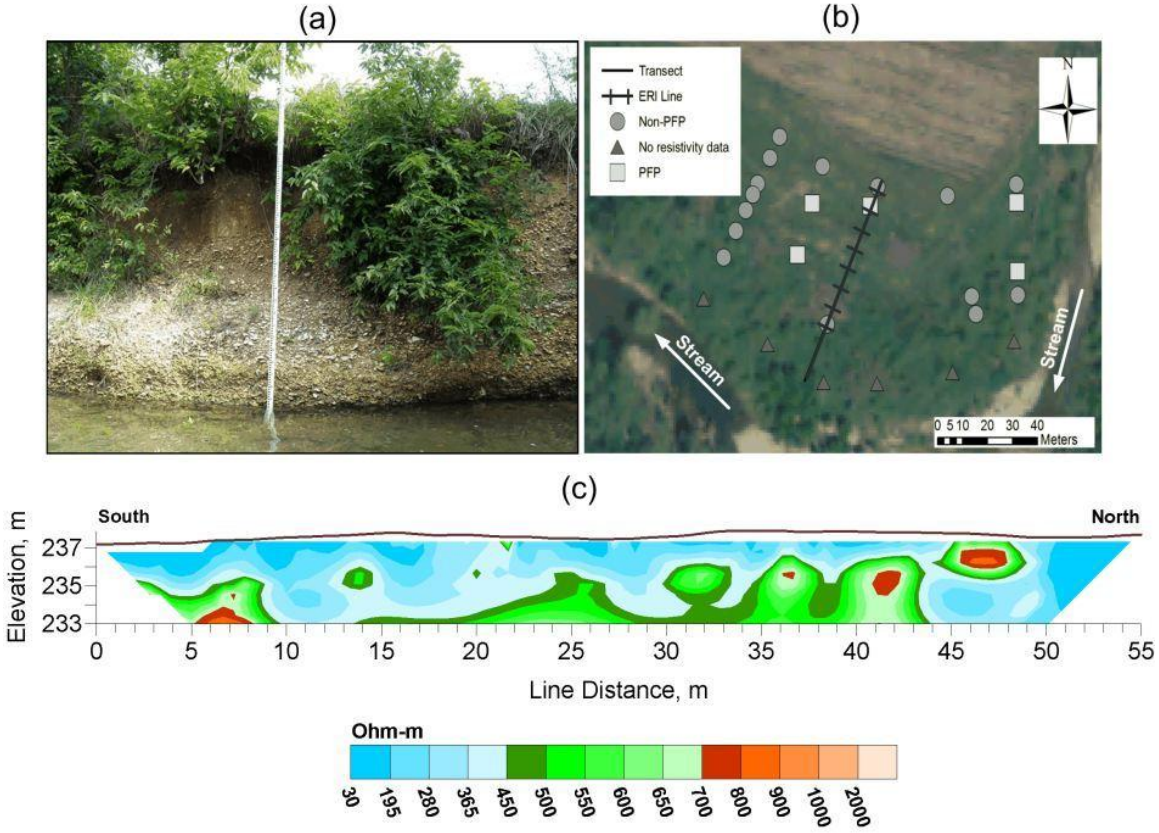

Figure 5.2. (a) The Honey Creek field site near Grove, OK, USA is an orchard with a riparian buffer where the floodplain consists of coarse chert gravel overlain by a mantle (10 to 50 cm) of topsoil. (b) Observation wells were located in both preferential (PFP) and non-preferential (non-PFP) flow areas based on electrical resistivity imaging. Arrows indicate stream flow direction. (c) Electrical resistivity profile through the groundwater transect for which P transport rates were calculated. Electrical resistivity at this field site has been positively correlated to saturated hydraulic conductivity (Miller et al., 2010; Miller, 2012).

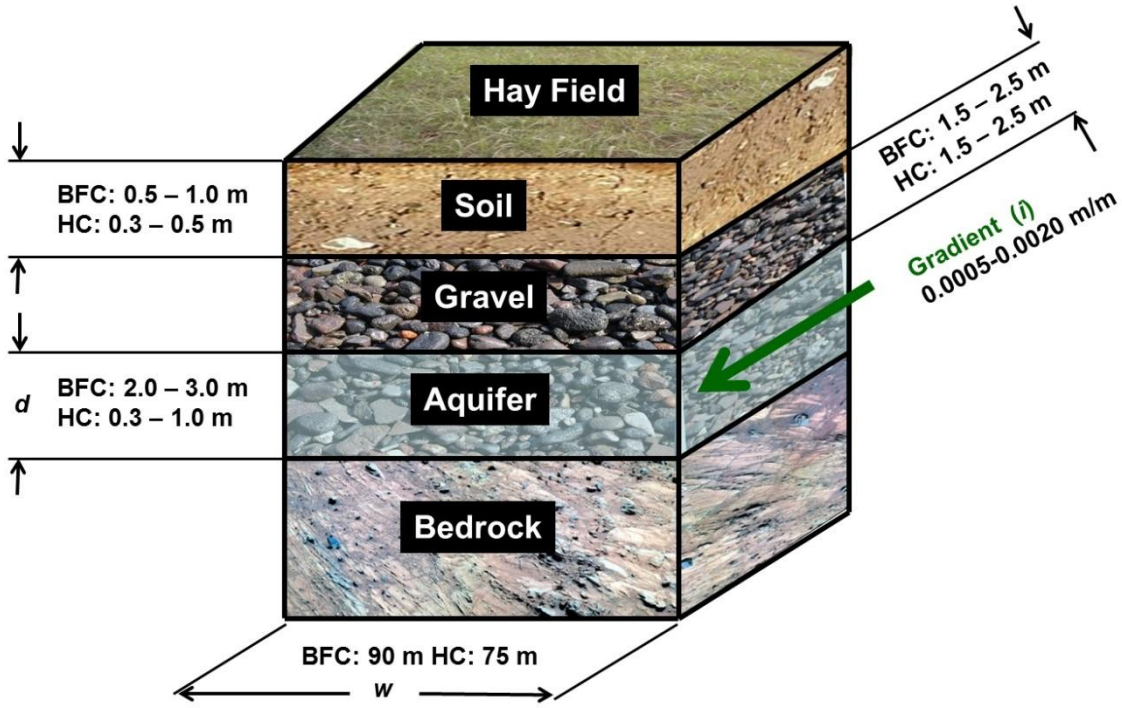

Figure 5.3. Typical soil profile at the Barren Fork Creek (BFC) and Honey Creek (HC) alluvial floodplain sites, including depth (*d*) and width (*w*) of aquifer. Preferential flow paths (PFP) in the vadose zone become activated as the water table rises due to an influx of stream water during high flow events.

5.3.3. Water Levels and Subsurface P Sampling

Based on previous geophysical research (Heeren et al., 2010, 2011; Miller et al., 2010; Miller, 2012), 24 observation wells were installed at each site. Geophysics has been widely used for subsurface mapping (Pellerin, 2002; Robinson et al., 2008). Resistivity mapping involves measuring the electrical properties of near-surface earth materials, which vary with grain size, mineral type, solute content of pore water, and pore-space saturation. Electrical resistivity is calculated at several locations in a two-dimensional profile by carefully measuring the voltage of a known electrical current between two electrodes in contact with the soil. Miller et al. (2012) collected electrical resistivity data using a SuperSting R8/IP Earth Resistivity Meter (Advanced GeoSciences Inc., Austin, TX) with a 56-electrode array (see Figures 5.1c and 5.2c for examples). The profiles employed electrode spacings of 0.5 to 2.5 m with associated depths of investigation

ranging from 7.5 to 25.0 m, respectively. The resistivity sampling and subsequent inversion utilized a proprietary routine devised by Halihan et al. (2005), which produced higher resolution images than conventional techniques.

Using a vadose zone borehole permeameter designed for coarse gravel (Miller et al., 2011), a positive correlation between electrical resistivity and hydraulic conductivity was established for the Barren Fork Creek and Honey Creek floodplain sites (Miller et al., 2010; Miller, 2012). Based on that correlation and the previous electrical resistivity results (Heeren et al., 2010, 2011; Miller et al., 2010; Miller, 2012), observation wells were located in both high hydraulic conductivity (one or more possible preferential flow pathways or PFPs) and low hydraulic conductivity (non-PFP) subsoils (Figures 5.1b and 5.2b). In this research, a PFP is defined as a region of high hydraulic conductivity in the vadose zone that has potential for rapid transport of water and solutes when saturated by a high water table.

A Geoprobe Systems drilling machine (6200 TMP, Kejr, Inc., Salina, KS) was used to install observation wells in the alluvial floodplains with a 2.0 to 3.0 m screened section at the base. Depth to refusal for installed wells ranged from 4.0 m to greater than 5.0 m at the Barren Fork Creek site and from 2.5 to 3.5 m at the Honey Creek site. Bentonite clay was placed at the top of the well casing to prevent surface runoff from entering the borehole.

Observation wells were instrumented with automated water level loggers (HoboWare, Onset Computer Corp., Cape Cod, MA) to monitor water pressure and temperature at five minute intervals. One logger was placed above the water table at each site to account for changes in atmospheric pressure. Reference water table elevations, obtained with a water level indicator, were then calculated. The logger data were processed with HoboWare Pro software, which accounted for changes in atmospheric pressure as well as changes in water density due to temperature. Contour plots of water table elevation were generated with MATLAB (The

Mathworks, Natick, MA) (Figures 5.4a and 5.4c). The local USGS gage stations were used to analyze stream stage.

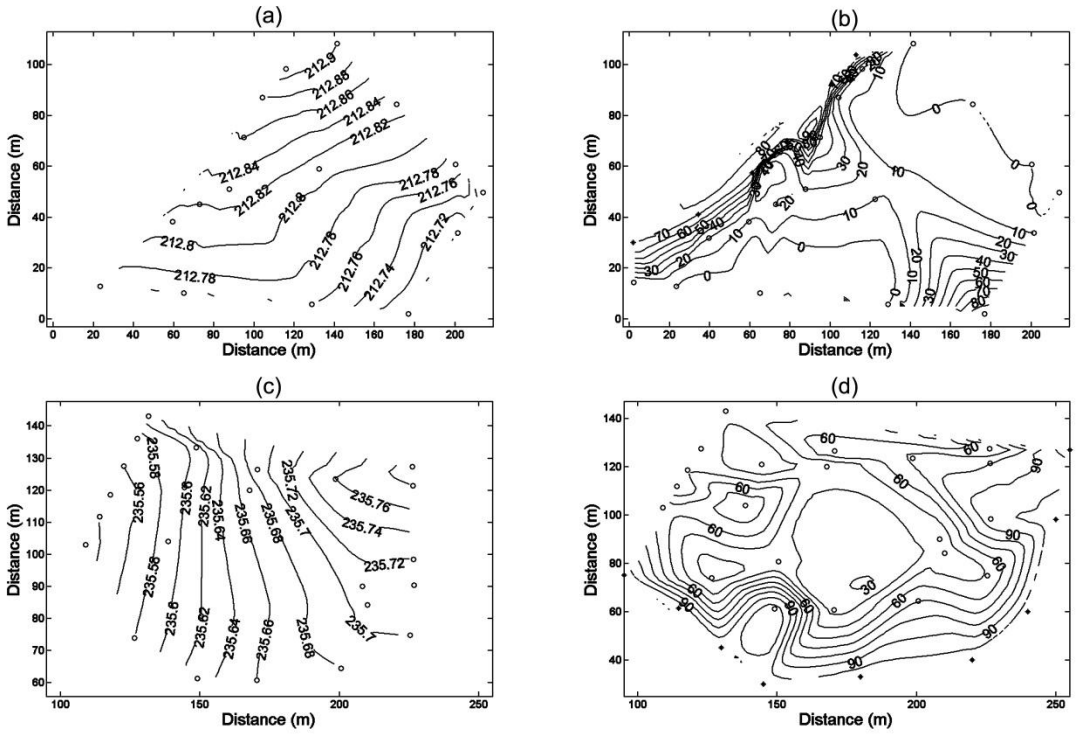

Figure 5.4. Water table ((a) (c)) and total phosphorus ((b) (d)) concentration (µg L^{-1} as P) contour plots for the Barren Fork Creek ((a) (b)) and Honey Creek ((c) (d)) sites. Barren Fork Creek data are from the peak of the 10 September 2009 high-flow event and Honey Creek data are from the rising limb of the 23 March 2010 high-flow event. Interpolations are based on measured data from wells (circles) and the stream (stars). Figures are adapted from Heeren et al. (2011).

Using a peristaltic pump, water samples were collected from the stream and observation wells during both baseflow and high flow events (Table 5.1), preserved on ice, and transported back to the laboratory for analysis. High flow events were of particular interest because stream P concentrations generally increase with streamflow in these watersheds (Andrews et al., 2009). The samples were digested based on the sulfuric acid-nitric acid method (Pote et al., 2009), and total P concentrations were determined colorimetrically (Murphy and Riley, 1962; EPA Method 365.2) with a spectrophotometer (Spectronic 21D, Milton Roy, Ivyland, PA). Contour plots of total P concentration were generated with MATLAB (The Mathworks, Natick, MA) (Figure 5.4b

and 5.4d). More details of water level monitoring and P results are presented in Heeren et al. (2011).

Table 5.1. Stream flow data and groundwater total phosphorus concentrations (μg L^{-1} as P) for PFP and non-PFP wells for each sampling time during the study period.

Site	Date (Month/Day/Year)	Time	Hydrograph Position	Mean Daily Flow ($m^3 s^{-1}$)	Median Total P Concentration PFP (μg L^{-1})	Median Total P Concentration non-PFP (μg L^{-1})
Barren Fork Creek[a]	9/10/09	10:00	Rising Limb	35	30	20
	9/10/09	13:00	Rising Limb	35	20	10
	9/10/09	22:00	Peak	35	30	10
	9/11/09	10:00	Falling Limb	44	40	20
	9/12/09	14:00	Falling Limb	23	30	10
	3/22/10	12:00	~Rising Limb	17	30	30
	3/23/10	15:00	Falling Limb	39	50	30
	3/26/10	12:00	Falling Limb	62	50	30
Honey Creek[a]	10/09/09	16:00	Falling Limb	41	40	50
	10/15/09	12:00	Baseflow	2.9	40	60
	3/22/10	18:00	Rising Limb	4.2	80	50
	3/23/10	9:00	Peak	5.5	40	60
	3/26/10	18:00	Falling Limb	9.2	40	50

[a] Data adapted from Heeren et al. (2011).

5.3.4. Subsurface Phosphorus Transport Rates

At each site, one of the electrical resistivity lines that identified a PFP was chosen as the transect (extended to the boundary of the well field) across which transport rates were calculated (Figures 5.1 and 5.2). The subsurface P transport rate was defined as the average annual subsurface P rate crossing the selected transect within the observation well field. Subsurface P transport rate was calculated by first determining the average groundwater flow based on Darcy's Law:

$$Q = qA = -K\frac{\partial h}{\partial x}wd = |Ki|wd \tag{5.1}$$

where Q is the groundwater discharge ($L^3\ T^{-1}$), q is the Darcy velocity ($L\ T^{-1}$), h is the groundwater head (L), x is the distance along the direction of flow (L), A is the cross-sectional area (L^2), w is the width of the monitored transect or groundwater flow domain (L), d is the depth of the aquifer (L), and i is the average groundwater gradient ($L\ L^{-1}$) (Figure 5.3). Note that this equation was applied separately to a single, identified PFP and the remaining non-PFP groundwater domains within the selected transect, using the site specific w and d of each domain. The annual subsurface P transport rate, m_p ($M\ T^{-1}$), was then calculated using the following mass transport equation:

$$m_P = Q \times TP \times n_d \tag{5.2}$$

where TP is the total P concentration ($M\ L^{-3}$) measured from observation wells in the PFP and non-PFP domains, and n_d is the number of days per year in which each groundwater flow domain was activated.

A Monte Carlo simulation was performed using 10,000 realizations of subsurface P transport rates due to uncertainty in six variables, with the distributions and statistics shown in Table 5.2. Following McKay (1995) and Fox et al. (2010), a uniform distribution was used for input parameters with an absence of experimental values to inform a probability distribution. A normal distribution after a Box Cox transformation was used to quantify K throughout the observation well field, based on electrical resistivity measurements correlated to point measurements of K as reported in Miller et al. (2010, 2011) and Miller (2012). At the Barren Fork Creek site, subsoils with electrical resistivity values greater than 700 Ω-m (correlating to a hydraulic conductivity of 74 m d^{-1}) were considered to be a PFP. At the Honey Creek floodplain, which is a smaller scale alluvial system, an electrical resistivity of 500 Ω-m (correlating to a hydraulic conductivity of 53 m d^{-1}) was considered to be the demarcation between PFP and non-PFP subsoils. The aquifer width, w, was held constant for each field site for the non-PFP domain,

but varied for the PFP domain assuming a uniform distribution. The w of the PFP was based on the identification of the PFP within ERI data for the transect at each site (Figures 5.1c and 5.2c). The distribution for *d* was assumed uniform for both PFP and non-PFP domains. The ranges in d for the non-PFP domains were identified based on typical baseflow water table elevations combined with depth to refusal during well installation and electrical resistivity mapping at each field site as reported in Miller et al. (2010) and Miller (2012). The ranges in d for PFPs were determined based on the high *K* zones in the ERI data for each transect (Figures 5.1c and 5.2c).

Table 5.2. Statistics for input parameters used in the Monte Carlo simulations of subsurface P transport rates at the Barren Fork Creek (BFC) and Honey Creek (HC) field sites.

Parameter	Site	Flow Domain	Input Distributions for Monte Carlo[a]
Saturated Hydraulic Conductivity ($m\ d^{-1}$)	BFC	Non-PFP	Normal after power function (λ^b =-0.62); μ_x^c=0.13; σ_x^c=0.04
		PFP	Normal after power function (λ=-0.62); μ_x=0.13; σ_x=0.04
	HC	Non-PFP	Normal after power function (λ=0.23); μ_x=2.3; σ_x=0.17
		PFP	Normal after power function (λ=0.23); μ_x=2.3; σ_x=0.17
Groundwater Gradient ($m\ m^{-1}$)	BFC	Non-PFP	Uniform; Min=0.0005; Max=0.0015
		PFP	Uniform; Min=0.0005; Max=0.0015
	HC	Non-PFP	Uniform; Min=0.0010; Max=0.0020
		PFP	Uniform; Min=0.0020; Max=0.0040
Aquifer Depth (m)	BFC	Non-PFP	Uniform; Min=2.0; Max=3.0
		PFP	Uniform; Min=2.0; Max=3.0
	HC	Non-PFP	Uniform; Min=0.25; Max=1.0
		PFP	Uniform; Min=0.5; Max=2.0
Domain Width (m)	BFC	Non-PFP	Fixed; 65
		PFP	Uniform; Min=15; Max=20
	HC	Non-PFP	Fixed; 75
		PFP	Uniform; Min=3.0; Max=4.0
Total Phosphorus Concentration ($\mu g\ L^{-1}$)	BFC	Non-PFP	Uniform; Min=10; Max=40
		PFP	Uniform; Min=30; Max=90
	HC	Non-PFP	Uniform; Min=20; Max=60
		PFP	Uniform; Min=60; Max=80
Activity (d)	BFC	Non-PFP	Fixed; 365
		PFP	Lognormal; μ_x=2.47; σ_x=0.91
	HC	Non-PFP	Fixed; 365
		PFP	Lognormal; μ_x=2.01; σ_x=1.03

[a] Note that unique distributions were used for the preferential flow (PFP) and non-preferential flow (non-PFP) domains.
[b] λ= exponent for the power transformation of the original distribution.
[c] μ_x , σ_x = mean and standard deviation for the normal and lognormal distributions.

The non-PFP domain was assumed active for 365 days; therefore, a fixed value was used for these calculations. The PFP activity was quantified based on the minimum mean daily flow that resulted in PFP activation during the study period, which is shown for each site in Figure 5.4. P can be seen preferentially entering the aquifer at point (90 m, 70 m) at the Barren Fork Creek site (Figure 5.4b) and at point (230 m, 110 m) at the Honey Creek site (Figure 5.4d).While the impacts of the PFPs aren't visible in the flow data at these particular times (Figures 5.4a and 5.4c), the PFPs (identified in electrical resistivity data) must be activated as evidenced by the high P concentrations. The requirements for PFP activation were the mean daily flows at these sampling times (Table 5.1), which were 35 and 4.2 $m^3 s^{-1}$ for the Barren Fork Creek and Honey Creek field sites, respectively. The lognormal n_p parameter distribution was derived from 60 yr and 12 yr of daily mean streamflow measurements by the USGS at the Barren Fork Creek and Honey Creek sites, respectively. The P transport rate was highly dependent on n_d. Uniform distributions were used for *i* and *TP* with unique *i* and *TP* for the PFPs and non-PFPs. The *i* and *TP* distributions were derived from groundwater levels and P concentrations measured in the observation well fields as well as particular PFPs (Figure 5.4) with generally higher *i* and *TP* for the PFP domains due to their activation during storm events (Heeren et al., 2011).

5.3.5. Surface Runoff Phosphorus Transport Rates

Concurrent research (Mittelstet et al., 2011) used a hydrologic model, the Pasture Phosphorus Management Calculator (PPM Plus) (White et al., 2009; White et al., 2010), to derive the average annual P loss from the Barren Fork Creek and Honey Creek field sites. PPM Plus is based on the Soil and Water Assessment Tool (SWAT) (Arnold et al., 1998), a product of more than 30 years of model development by the U.S. Department of Agriculture, Agricultural Research Service. PPM Plus was parameterized for actual land use at each site: low intensity agricultural production for pasture without cattle grazing or poultry litter application. The only agricultural activity was hay removal scheduled for August. Due to uncertainty in several

variables, a Monte Carlo simulation was performed with 10,000 realizations on six variables, similar to the method used for producing distributions of subsurface P transport rates.

5.4. RESULTS AND DISCUSSION

As noted by Heeren et al. (2011), the assumptions of uniform, homogeneous stream/aquifer interaction and only localized near-streambed water exchanges were not relevant for the two studied alluvial floodplains (Figure 5.4). The activity of preferential flow pathways depended on the elevation of the water table and the interaction between the stream and the groundwater. The average groundwater flow direction at each floodplain site changed considerably between baseflow and storm events, and the highest water table gradients in the alluvial aquifer occurred during the rising limb of the hydrographs, when the stream stage was rising most quickly. It appeared that preferential flow pathways acted as divergence zones, allowing stream water to quickly enter the groundwater system during rising limbs of streamflow hydrographs, or as flow convergence zones draining a large groundwater area during the falling limbs of streamflow hydrographs. At the Barren Fork Creek site, a PFP at point (90 m, 70 m) (Figures 5.4a and 5.4b) was found to act as a divergence zone, allowing stream water to preferentially flow into the alluvial aquifer. A large convergence zone occurred at the Honey Creek site directing water through the subsurface near the northern boundary of the meander bend or the upper left corner of the well field (Figures 5.4c and 5.4d).

The floodplain STP levels at the Barren Fork site ranged between 28.5 and 30.5 mg kg^{-1} with an average of 29.5 mg kg^{-1} and standard deviation of 1.00 mg kg^{-1}. The STP range at the Honey Creek site was 51.5 to 55.0 mg kg^{-1} with an average of 53.2 mg kg^{-1} and a standard deviation of 1.76 mg kg^{-1}. The Honey Creek site possessed a higher average STP due to historical poultry litter applications on the floodplain. These STP levels suggested minimal P leaching through the topsoil layers in these floodplains; therefore, the main source of P measured in the

observation wells was most likely from P-laden stream water entering the floodplain, an assertion supported by the groundwater elevation and P data.

As discussed in Heeren et al. (2011), water samples from observation wells were collected during multiple high flow events (Table 5.1) with peak flows from one to two orders of magnitude greater than median flow rates and were subsequently analyzed for total P concentrations (Figure 5.4). During both baseflow and high flow conditions, groundwater P concentrations in the non-PFP domain were typically 10 to 40 μg L^{-1} and 20 to 60 μg L^{-1} at the Barren Fork Creek and Honey Creek field sites, respectively. It should be noted that some of the TP concentrations in the non-PFP wells at the Honey Creek site (Table 5.1) may be artificially elevated due to samples containing agitated sediment from the bottom of wells with very shallow water depths (wells furthest from the creek). The P concentrations were generally highest where stream water was entering the groundwater system and decreased with distance down-gradient from the stream. In activated PFPs, the P concentrations during high flow events were as high as 90 μg L^{-1} at the Barren Fork Creek site and 80 μg L^{-1} at the Honey Creek field site. P can be seen preferentially entering the aquifer at point (90 m, 70 m) at the Barren Fork Creek site (Figure 5.4b) and at point (230 m, 110 m) at the Honey Creek site (Figure 5.4d). Potential PFPs were also observed at points (180 m, 0 m) and (150, 60) in the P data at the Barren Fork Creek (Figure 5.4b) and Honey Creek (Figure 5.4d) sites, respectively.

Based on the Monte Carlo simulation of the subsurface P transport rate (Equations 5.1 and 5.2), the estimated median annual subsurface P transport rate for the non-PFP flow domain at the Barren Fork Creek field site was 0.04 kg yr^{-1} (Figure 5.5a). This compared to a median of 0.003 kg yr^{-1} from the single PFP. The median total P transport rate from surface runoff based on the PPM Plus Monte Carlo simulations was 0.07 kg yr^{-1} from the current conditions (low intensity scenario) and 9.9 kg yr^{-1} with litter application and cattle grazing (high intensity scenario). For the Honey Creek site, the estimated median annual subsurface P transport rate was 0.03 kg yr^{-1} in the

non-PFP domain and 0.0004 kg yr^{-1} in the single PFP (Figure 5.5b). These results compared to 0.08 kg yr^{-1} of surface P runoff based on the low intensity scenario (low agricultural production)

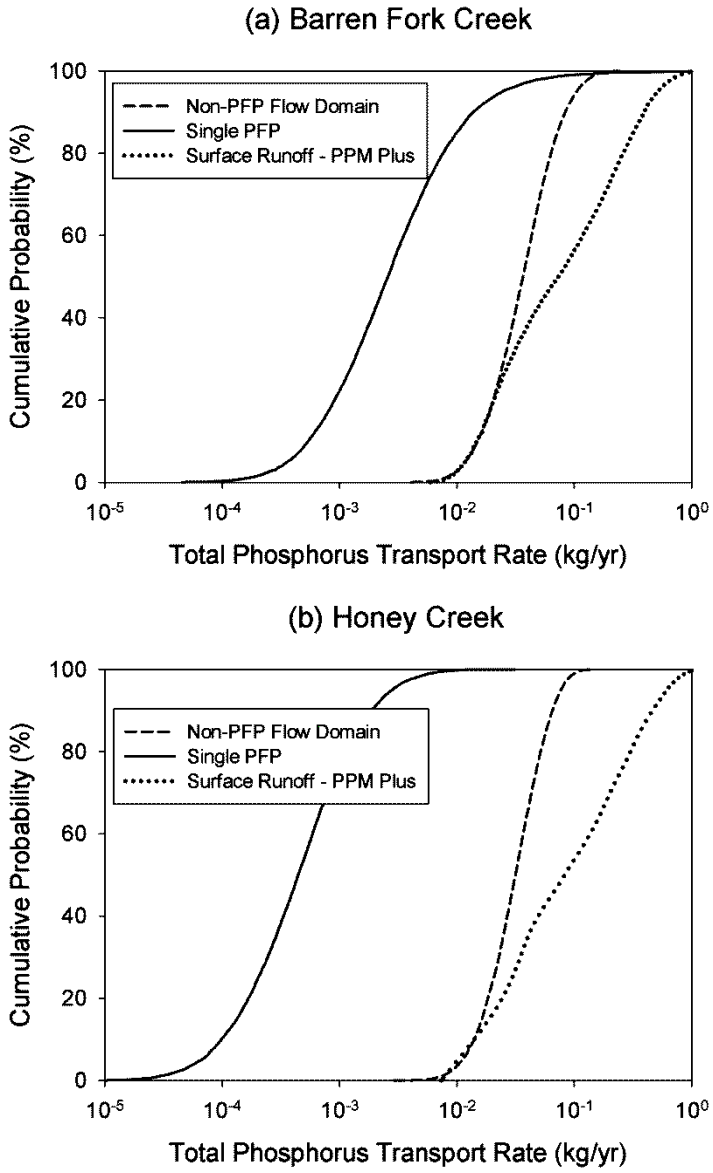

Figure 5.5. Total phosphorus transport rate due to subsurface transport generated based on Monte Carlo analyses and total phosphorus transport rates in surface runoff based on PPM Plus simulations at the Barren Fork Creek and Honey Creek field sites under low intensity agricultural production. PFP = preferential flow pathway; non-PFP = non-preferential subsurface flow.

and 6.3 kg yr^{-1} of surface P runoff based on the high intensity scenario (high agricultural production). The Honey Creek site had a smaller subsurface P transport rate due to a smaller

aquifer cross-sectional area (both in terms of *d* and *w*) and *K* compared to the Barren Fork Creek site. Also the size of the PFP was larger at the Barren Fork Creek site making the P transport rate higher than at Honey Creek. As stream order increases, *d* and *K* increase due to larger gravel deposits. Based on a Mann-Whitney rank sum test, median values between the surface P transport rate and non-PFP subsurface P transport rate were significantly different ($p < 0.001$) for both field sites.

The surface runoff P transport rates based on the low and high agricultural production at the Barren Fork and Honey Creek sites from PPM Plus ranged from 0.03 to 3.6 kg ha^{-1} yr^{-1} (Mittelstet et al., 2011) and were within the range of observed total P loss (0.02 to 4.6 kg ha^{-1} yr^{-1}) from previous studies at twelve field sites in eastern Oklahoma (Storm et al, 2007; White et al., 2009). The modeling results were also consistent with field measurements of total P loss observed by Romeis et al. (2011). They reported measured total P yields from commercial poultry-pasture headwater streams ranging from 0.03 to 3.17 kg ha^{-1} over an 18 to 22 month sampling period. They also summarized the range in P yield (0.1 to 17.8 kg ha^{-1} yr^{-1}) from field-scale studies of P transfer from poultry manure-amended pastures in the literature.

The subsurface P transport rate was on the same order of magnitude relative to the surface runoff P transport rate for current site conditions, yet was small compared to the simulation with poultry litter application and cattle grazing. Though the total P transport rate was small in the PFP due to the small area and number of active days, it may provide rapid unimpeded transport from the surface to the stream at high STP sites. In areas where there is a larger number of PFPs and/or during years where the PFP remains active for longer periods of time, the PFPs will provide a larger P transport rate. For example, the P transport rate at the 99^{th} percentile of the Monte Carlo simulation was 0.10 kg yr^{-1} in the single PFP at the Barren Fork Creek, or 136% of the median surface runoff P transport rate from low intensity conditions.

The Illinois River, of which the Barren Fork Creek is a tributary, may have a deeper aquifer, higher *K*, and larger PFPs, resulting in a higher subsurface P transport rate. Therefore, as the stream order increases, the significance of subsurface P transport rates and PFPs may also increase. A need exists for additional research to scale-up the observations at these individual floodplains sites to the watershed scale, which will require future research at additional floodplain sites in larger-order stream systems. Of course, a difficulty that exists is identifying and documenting the number and size of PFPs within these alluvial floodplains. Geophysical techniques such as electrical resistivity imaging used by Miller et al. (2012) will be invaluable in future floodplain investigations.

These results also suggest that the subsurface P transport rate of alluvial floodplains with one PFP in the Ozark ecoregion may be at least 0.01 to 0.10 kg yr^{-1} and perhaps even higher in cases where the subsurface is connected to a larger source of P. While the source of P in the groundwater at these well managed sites was limited to minimal surface P and P-laden stream water entering the alluvial aquifer, this research demonstrated that coarse gravel subsoils have a capacity to transport as much P as the surface runoff (i.e., the Barren Fork Creek site). The field data used in this analysis did not include floodplains with poultry litter application or cattle production. Also, upland areas may contribute P to these floodplains through P-laden surface runoff or from the subsurface through karst features typical of the Ozark ecoregion. Further work is needed to quantify P transport in cases with such additional P sources.

5.5. CONCLUSIONS

Research has shown that subsurface P contributions can be significant in riparian zone soils with spatial variability in hydraulic conductivity, preferential flow pathways, and limited sorption capacity. This study estimated subsurface P transport rates as quantified by annual P rates crossing a transect within two groundwater systems, with uncertainty parameters quantified

through Monte Carlo simulation. The subsurface P transport rate was compared to surface runoff rates based on simulations of PPM Plus. Results suggested that the subsurface P transport rates were significant compared to surface runoff P rates at low intensity agricultural field sites. Though the subsurface contributions were small compared to the PPM Plus simulations with more intensive land use, floodplains with poultry litter application or cattle grazing may have a corresponding increase in subsurface P transport. The field sites in this study had low agricultural intensity; therefore, the calculated subsurface P transport included a minimal amount of P leaching from the surface. Future work needs to quantify P leaching through the soil from a surface P source and determine whether this significantly elevates levels of subsurface P transport. It is also hypothesized that as stream order increases, the significance of subsurface P transport rate and preferential flow pathways increase.

5.6. ACKNOWLEDGMENTS

This material is based upon work supported by the U.S. Environmental Protection Agency Region VI, Oklahoma Conservation Commission, Oklahoma Agricultural Experiment Station, and Oklahoma State University College of Agricultural Sciences and Natural Resources. The author acknowledges Mr. Dan Butler and Mr. Bill Berry for providing access to the alluvial floodplain property. Amanda K. Fox, Stillwater, OK, is acknowledged for her assistance with the MATLAB software. Dr. Chad Penn, Oklahoma State University, assisted with analysis of phosphorus data, and Dr. Todd Halihan, Oklahoma State University, assisted with the electrical resistivity surveying. The author also acknowledges Grant Graves, Katie Beitz, Jorge Guzman, and Jesi Lay, Biosystems and Agricultural Engineering, and Elliot Rounds, Plant and Soil Sciences, Oklahoma State University, for assisting with field and laboratory work.

CHAPTER VI

BERM METHOD FOR QUANTIFICATION OF INFILTRATION AND LEACHING AT THE PLOT SCALE IN HIGH CONDUCTIVITY SOILS

6.1. ABSTRACT

Measuring infiltration and leaching at the plot scale is difficult, especially for high hydraulic conductivity soils. Infiltration rate has been indirectly calculated at the plot scale by comparing surface runoff to rainfall. Direct measurement of infiltration and leaching beyond the point scale is typically limited to locations where land forming has been performed, e.g. infiltration ponds and fields with basin irrigation. The standard method for field measurement of infiltration is a double ring infiltrometer, which is limited in size (typically 30 cm diameter). In this research, a new method is proposed that uses a temporary berm constructed of a water filled 15 cm diameter vinyl hose with the edges sealed to the soil using bentonite. The berm is capable of confining infiltration plot areas of various sizes (e.g. 1 m by 1 m and 3 m by 3 m areas in this research). Water tanks (0.8 m^3 and 4.9 m^3) and gravity flow were used to supply water and tracers to the plots. A constant head was maintained within the plot automatically using float valves for lower flow rates and manually with a gate valve for higher flow rates. Observation wells were installed 0.5 m outside the plot to monitor for water table rise and tracers that leached into the groundwater. The procedure was tested on soils ranging from silt loam to coarse gravel with

measured infiltration rates ranging from 5 to 70 cm/hr. Guidelines are provided for tank size and refilling frequency for field experiments. In addition, numerical simulations were performed to estimate time of response in wells for various soil and experimental design conditions.

6.2. INTRODUCTION

Physical properties of porous media tend to be highly variable in space until a representative elementary volume (REV) is reached (Brown et al., 2000). It is unknown how well point measurements of infiltration scale up to the plot or field scale. Sisson and Wierenga (1981) considered the effect of double ring infiltrometer diameter (up to 127 cm) on steady-state infiltration, and found increasing variability with smaller ring sizes. Lai and Ren (2007) also found that larger double ring infiltrometers (>80 cm) were necessary in order to reduce variability in infiltration results. Massman (2003) found that hydraulic conductivities measured with flood tests in infiltration basins were up to two orders of magnitude higher or lower than hydraulic conductivities determined from air conductivity or estimated from grain size parameters.

Measuring infiltration rates and/or leaching of tracers at a larger scale, however, is difficult, especially for high hydraulic conductivity soils where large volumes of water are required. The standard method for field measurement of infiltration is a double ring infiltrometer (ASTM D3385-09), with the inner ring typically limited to a diameter of 30 cm. Infiltration rate has been indirectly calculated at the plot scale by comparing surface runoff to simulated rainfall (Fiedler et al., 2002) or run-on (Sarkar et al., 2008). Direct measurement of infiltration on a plot or field scale is typically limited to locations where land forming has been performed, e.g. infiltration ponds (Massman, 2003) and fields with basin irrigation.

The objective of this research was to develop a straightforward method for directly quantifying infiltration rates at the plot scale in high hydraulic conductivity soils. A secondary objective was to use a conservative tracer to investigate solute transport.

6.3. METHODS AND MATERIALS

6.3.1. Field Site for Application and Testing

Both 1 m by 1 m and 3 m by 3 m berms were tested at an alluvial floodplain site located adjacent to Pumpkin Hollow Creek in the Ozark ecoregion of northeastern Oklahoma (latitude: 36.02°, longitude: -94.81°) (Figure 3.1). As a small tributary of the Illinois River, Pumpkin Hollow Creek was a first order ephemeral stream in its upper reaches. At the field site, the floodplain was 120 to 130 m across, with a watershed area of 15 km^2. The land use at the site was pasture used for cattle. Ozark floodplains generally consist of coarse chert gravel overlain by a mantle (1 to 300 cm) of gravelly loam or silt loam (Heeren et al., 2011). The Pumpkin Hollow field site was a combination of Razort gravelly loam and Elsah very gravelly loam, although infiltration experiments were limited to the Razort gravelly loam soils. Topsoil thickness ranged from 0 to 3 cm, and bulk densities of the cohesive material were in the range of 1.3 to 1.5 g cm^{-3}.

6.3.2. Berm Installation, Hydraulics, and Sampling

The berm was constructed of four sections of 15 cm vinyl hose attached to four 90° elbows constructed from 15 cm steel pipe (Figure 6.1). Each elbow had an air vent and one elbow had a gate valve with a garden hose fitting for water. The vinyl hoses were secured to the elbows with stainless steel hose clamps and sealed with silicone sealant. The berms were then partially filled with water to add weight, but excess pressure was avoided to ensure the vinyl did not separate from the elbows.

Plots were located on relatively level areas in an attempt to maintain uniform water depths. Larger plots required shallower slopes to ensure that the entire plot could be inundated without overflowing the berm. The vinyl hose was placed around the perimeter of the infiltration gallery in a shallow trench (3 to 5 cm) cut through the surface thatch layer to minimize lateral

flow at the surface. A thick bead of liquid bentonite was also placed on the inside and outside of the berm to create a seal between the berm and the soil.

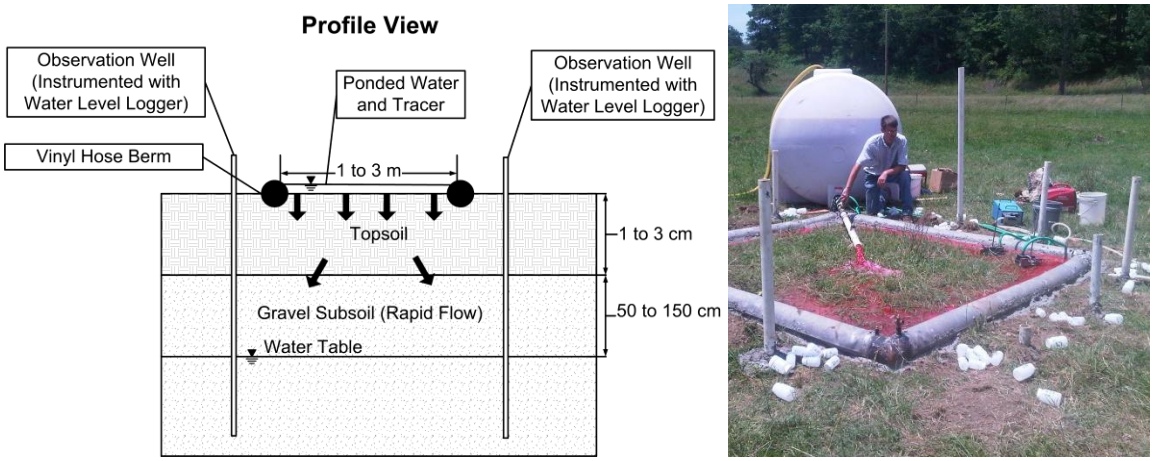

Figure 6.1. Berm infiltration method, including vinyl berms to contain water-tracer solution and observation wells for collecting groundwater samples: design (left) and implementation at the Pumpkin Hollow floodplain site in eastern Oklahoma (right).

High-density polyethylene tanks, 4.9 and 0.76 m^3, were used for the 3 m by 3 m and the 1 m by 1 m plots, respectively, to mix water and a potassium chloride tracer. Tanks were instrumented with automated water level data loggers with an accuracy of 0.5 cm (HoboWare U20, Onset Computer Corp., Cape Cod, MA) to monitor water depth (pressure) and temperature at one minute intervals. An additional water level data logger was used to monitor atmospheric pressure. Logger data were processed with HoboWare Pro software, which adjusted for changes in atmospheric pressure and water density. Tank water depth over time was used to calculate flow rate with a volumetric rating curve.

A combination of 5.1 cm diameter Polyvinyl chloride (PVC) pipe with a manual gate valve and vinyl garden hoses with float valves were used to deliver gravity fed water from the tanks to the plots. For low flow rates, one to two garden hoses with float valves were sufficient. When higher flow rates were required to achieve the desired constant head, flow was dominated by the larger PVC pipe and the garden hoses with float valves were relatively ineffective. For

these cases a fine-adjustment gate valve was required to manually control the flow rate to achieve a relatively constant head in the plots. When a tank was nearly empty, flow was temporarily stopped while water and tracer was added to the tank. Chloride was used as a conservative tracer with injection concentrations 20 to 30 times background levels. Depth in each plot area was monitored with a water level data logger. Heads were limited by the diameter of the berm and varied spatially according to the topography within the plot.

A Geoprobe Systems drilling machine (6200 TMP, Kejr, Inc., Salina, KS), which has been found to be effective in coarse gravel soils (Heeren et al., 2011; Miller et al., 2011), was used to install four to twelve observation wells around each plot. Boreholes were sealed with liquid bentonite to avoid water leaking down the hole. Observation wells were instrumented with water level data loggers. Reference water table elevations, obtained with a water level indicator and laser level data for each well, were then calculated. Water table elevation data had an accuracy of 1 cm. Low flow sampling with a peristaltic pump was used to collect water samples from the top of the water table, which ranged from 50 to 150 cm below ground surface. Both well and plot water samples were collected and tested for chloride concentration with ion chromatography which had a minimum detection limit of 0.16 mg/L.

6.3.3. Finite Element Modeling

Porous media flow from hypothetical 1 m by 1 m infiltration plots were simulated using HYDRUS-3D (Šimůnek et al., 2006) for three different soil types: sand, loam, and silt. This method was not expected to be used on soils finer than silt. HYDRUS is a finite element model for simulating two- and three-dimensional movement of water, heat, and multiple solutes in variably saturated media (Šimůnek et al., 2006; Akay et al., 2008). The HYDRUS code numerically solves the Richards equation for saturated-unsaturated water flow (Šimůnek et al., 2006).

The finite element grid consisted of triangular prism elements spaced equally every 25 cm in the horizontal, lateral, and vertical directions. The simulation domain consisted of a 1 m by 1 m constant head infiltration plot centered within a 10 m by 10 m area with a 3-m deep soil profile (Figure 6.2). All cells on the surface of the simulation domain outside the infiltration plot were no-flux boundaries. A constant head boundary condition was used to simulate the infiltration plot with constant heads ranging from 2.54 to 15.24 cm. The initial water table depth was varied between simulations, which included depths of 1.0, 2.0, and 2.5 m below ground surface. Below the water table, a no flux boundary condition was specified for the shell and bottom of the simulation domain to simulate the presence of a regional groundwater system. Above the water table, the shell boundary condition was a possible seepage face (Figure 6.2). At the water table depth, observation nodes were added to the simulation domain located at various distances (0 to 450 cm) away from the edge of the infiltration plot.

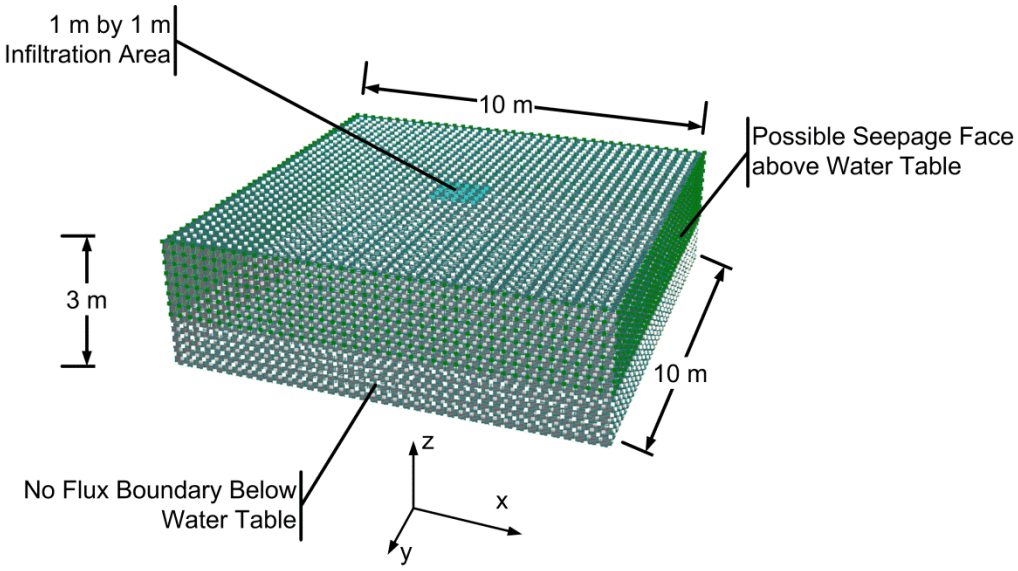

Figure 6.2. Simulation domain for HYDRUS-3D modeling of hypothetical infiltration experiments with a 1 m by 1 m infiltration plot.

The van Genuchten-Mualem model (van Genuchten, 1980) was used to describe the water retention, $\theta(h)$, and conductivity, $K(h)$, functions for the assumed homogeneous soil matrix:

$$\theta(h) = \begin{cases} \theta_r + \dfrac{\theta_s - \theta_r}{\left[1 + |\alpha h|^n\right]^m} & h < 0 \\ \theta_s & h \geq 0 \end{cases} \quad (6.1)$$

$$K(h) = K_s S_e^l \left[1 - (1 - S_e^{1/m})^m\right]^2 \qquad m = 1 - 1/n, \quad n > 1 \quad (6.2)$$

where is the effective saturation; α (L^{-1}), n, and l are empirical parameters; θ_s is the saturated water content (L3L-3); θ_r is the residual water content (L^3L^{-3}); and K_s (LT^{-1}) is the saturated hydraulic conductivity. Hydraulic parameters for the sand, loam, and silt soils were acquired from the soil catalog in HYDRUS, derived from Carsel and Parrish (1988), in order to represent average values for these different textural classes (Table 6.1).

Table 6.1. Soil properties for the sand, loam, and silt soils simulated by HYDRUS-3D for the hypothetical 1 m by 1 m infiltration experiments. Soil properties were from the soil catalog for the textural classes in HYDRUS (Šimůnek et al., 2006).

Soil Type	Residual Water Content, θ_r ($cm^3\ cm^{-3}$)	Saturated Water Content, θ_s ($cm^3\ cm^{-3}$)	α* (cm^{-1})	n*	Saturated Hydraulic Conductivity, K_s ($cm\ min^{-1}$)	Pore-Connectivity Parameter, l
Sand	0.045	0.430	0.145	2.68	0.495	0.5
Loam	0.078	0.430	0.036	1.56	0.017	0.5
Silt	0.034	0.460	0.016	1.37	0.004	0.5

*Empirical constants.

HYDRUS simulations were conducted to determine the time at which a detectable water table rise, defined as 1 cm, was observed in the observation nodes. This information was used to correlate the response time in observation wells installed next to the infiltration plot relative to the soil type, head in the infiltration plot, distance the observation well was installed from the infiltration plot edge, and the water table depth.

6.4. RESULTS AND DISCUSSION

Based on the two 1 m by 1 m plots and two 3 m by 3 m plots, infiltration rates ranged from 5 to 70 cm/hr, indicating considerable heterogeneity in the infiltration rates of the Pumpkin Hollow floodplain due to the occurrence of gravel outcrops. Measured infiltration rates were greater than the estimated permeability of the limiting layer reported by the U.S. Natural Resources Conservation Service (NRCS) for Cherokee County, Oklahoma (NRCS, 2012), which ranged from 1.5 to 5 cm/hr for the Razort gravelly loam soil. This difference indicates the need for larger scale field measurements of infiltration rate. For example, soil survey measurements may represent a typical soil pedon but miss gravel outcrops or large macropores which may be infrequent but have a disproportionate impact on infiltration.

This method was successful in quantifying high infiltration rate soils (i.e., gravels) even for large 3 m x 3 m plots, and lower infiltration rates could be easily measured. Larger plot sizes may require excessively large tanks, and thus continuous pumping and dosing to inject tracers directly into the pump hose may provide a better alternative for adequate mixing.

Figure 6.3 shows the relationship between flow rate and the time to empty the tank, which can be used to aid the design of infiltration experiments. For example, one of the 3 m by 3 m plots had a quasi-steady state infiltration rate of 6.3 cm/hr, which required an average flow rate of 9.5 L/min. According to Figure 6.3, the tank will need to be refilled every 8 hr for a 4.9 m^3 tank. Actual times to empty the tank after quasi-steady state was reached were 6.5, 6.0, and 8.0 hr, which is consistent with the fact that refills were performed before the tank was completely empty.

A constant head assumption was considered valid if the water depth in the infiltration plot was within 1.5 cm of the mean depth. All experiments met this requirement for 85 to 92 percent of the time (Figure 6.4). Float valves were reliable and effective, allowing the system to run

automatically for several hours at a time. Manual gate valves required attentive monitoring in order to be effective.

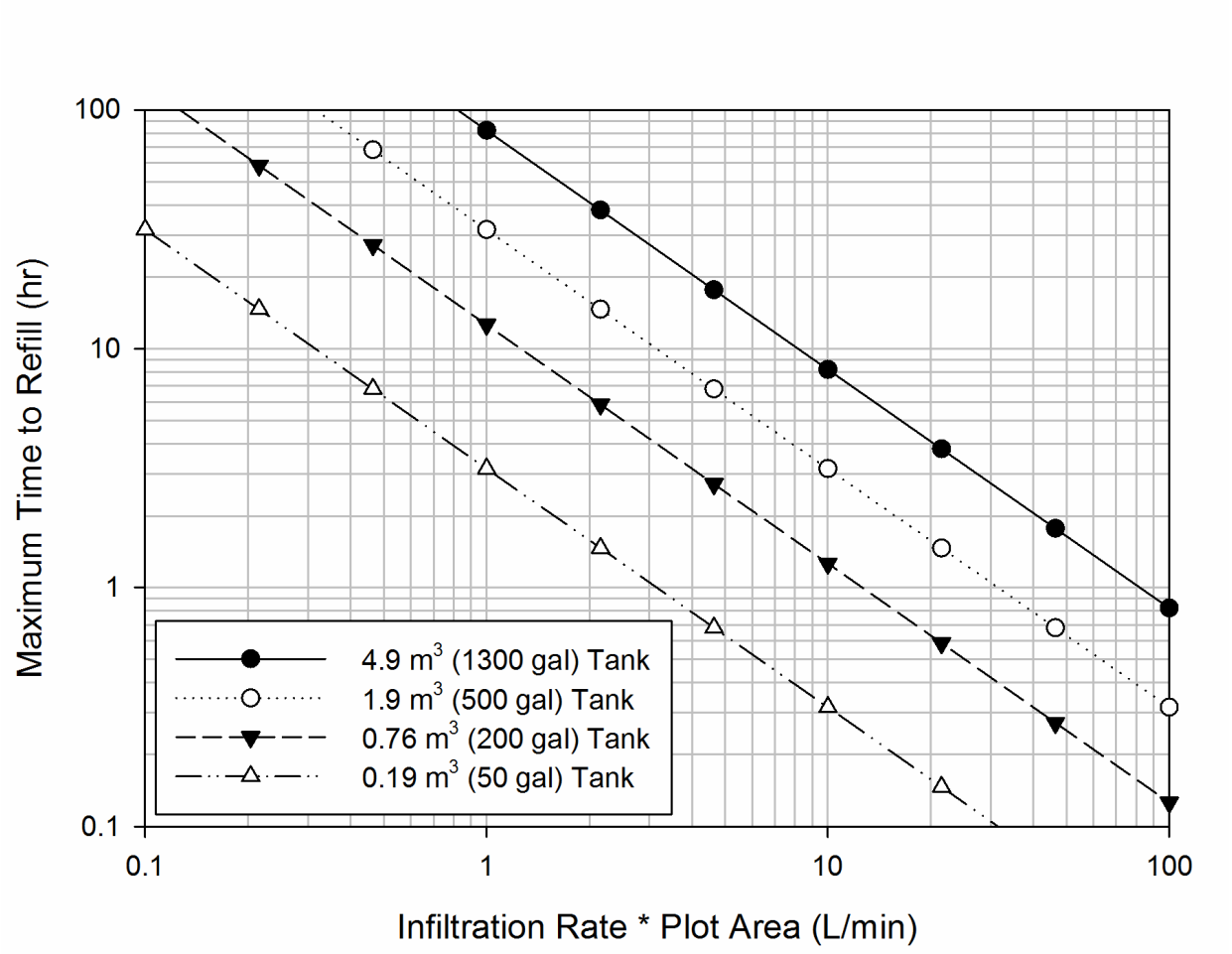

Figure 6.3. Relationship between expected infiltration flow rate and time to empty water tank for different size water tanks.

Observed response times based on chloride detection in groundwater wells (located 0.5 m from the edge of the berm) ranged from 18 minutes (coarse gravel outcrop) to more than 32 hours. All plots had at least some wells where chloride was never detected above background levels (duration of experiments ranged from 3 to 32 hours), again indicating significant heterogeneity within the floodplain soils.

Modeled response times using HYDRUS-3D were more dependent on water table depth than distance from the plot edge. In sand and coarser soils (Figure 6.5), response times were predicted to be less than 200 minutes (approximately 3 hrs), even with a deep water table (250 cm) and observation wells installed as much as 4 m from the edge of the infiltration plot. For silt and finer soils, experiments would need to be conducted for multiple days when sampling from a groundwater table 200 cm below ground surface (Figure 6.5), unless significant macroporosity is present.

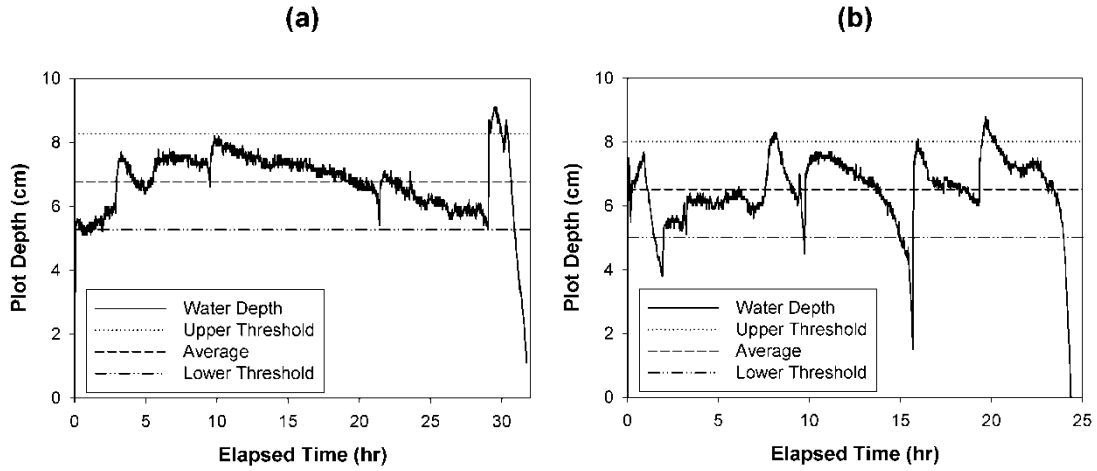

Figure 6.4. Measured plot water depth over time for a 1 m by 1 m plot with flow controlled primarily by an automatic float valve (a) and for a 3 m by 3 m plot with flow controlled primarily by a manual gate valve (b). Water depths were within 1.5 cm of the mean depth 92% (left) and 89% (right) of the time, meeting the prescribed requirements for constant head infiltration (add ASTM Standard reference here).

6.5. CONCLUSIONS

This research successfully demonstrated an innovative method for quantifying infiltration rates and leaching in highly conductive gravelly soils at the plot scale, maintaining a constant head at least 85% of the time during experiments. Guidelines have been provided for future infiltration experiments. The berm infiltration method allows investigations of various plot sizes and was demonstrated to be capable of measuring infiltration rates ranging from 5 to 70 cm/hr. Larger plot sizes may require continuous pumping and tracer injection directly into the pump

hose instead of using tanks for mixing. Numerical modeling indicated that experimental times in homogeneous soils were more dependent on water table depth than well distance from the plot edge, especially for coarser soils. Experimental durations may be less than 200 minutes in sand and coarser soils to multiple days for silt and finer soils.

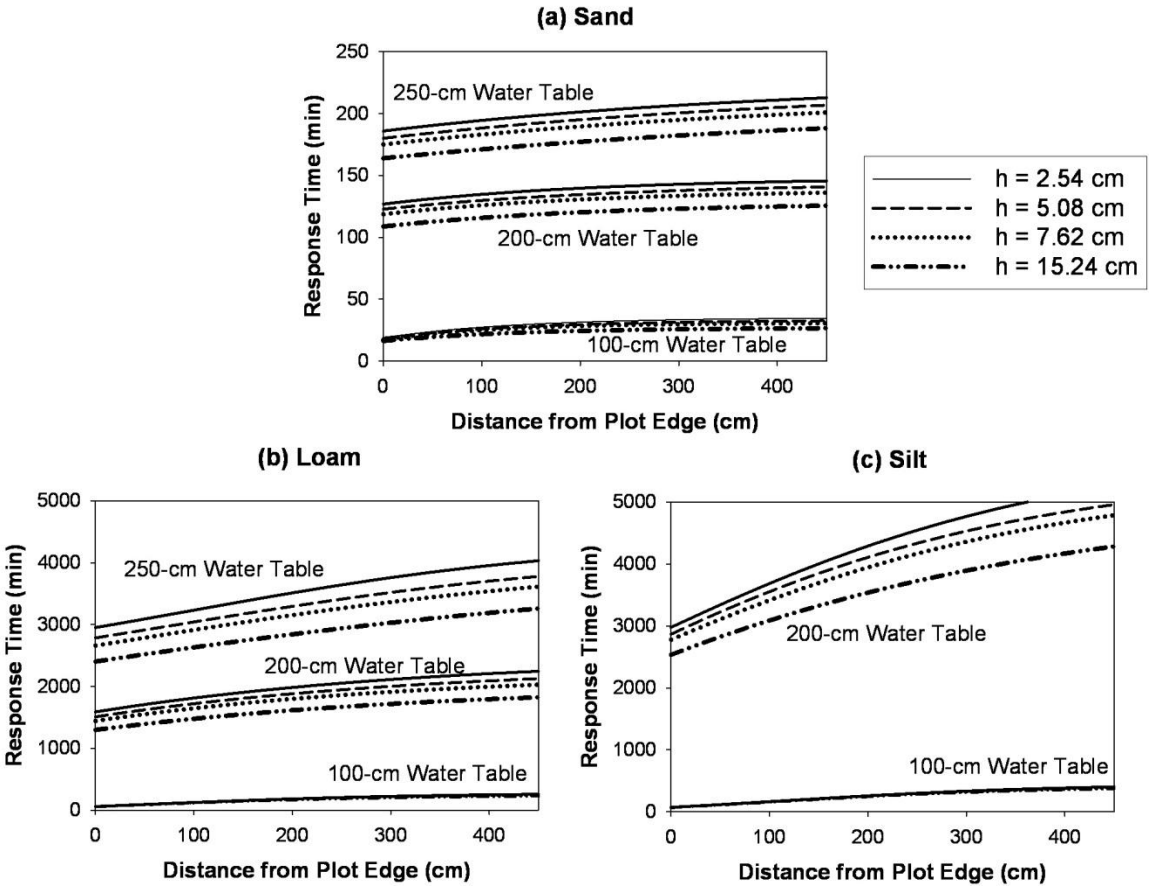

Figure 6.5. HYDRUS-3D predicted response times in observation wells installed next to infiltration plots as a function of soil type, head in the infiltration plot (h), distance the observation well was installed from the infiltration plot edge, and the depth to water table.

6.6. ACKNOWLEDGEMENTS

The project described in this publication was supported by Grant/Cooperative Agreement Number G10AP00137 from the United States Geological Survey. Its contents are solely the responsibility of the authors and do not necessarily represent the official views of the USGS. This material was also developed under STAR Fellowship Assistance Agreement no. FP-917333

awarded by the U.S. Environmental Protection Agency (EPA). It has not been formally reviewed by EPA; thus the views expressed in this paper are solely those of the author and EPA does not endorse any products or commercial services mentioned in this paper. The author also acknowledges Mrs. Shannon Robertson for providing access to the alluvial floodplain property. Drs. Garey A. Fox and Daniel E. Storm also contributed significantly to the HYDRUS modeling and the development of the berm design.

CHAPTER VII

QUANTIFICATION AND HETEROGENEITY OF INFILTRATION AND PHOSPHORUS LEACHING AT THE PLOT SCALE

7.1. ABSTRACT

In order to protect drinking water systems and aquatic ecosystems, all critical nutrient source areas and transport mechanisms need to be characterized. It is hypothesized that hydrologic heterogeneities (e.g., macropores and gravel outcrops) in the subsurface of floodplains play an integral role in impacting flow and contaminant transport between the soil surface and shallow alluvial aquifers. Infiltration is often assumed to be uniform at the field scale, but this neglects the high spatial variability common in anisotropic, heterogeneous alluvial-floodplain soils. In the Ozark ecoregion, for example, the erosion of carbonate bedrock (primarily limestone) by slightly acidic water has left a large residuum of chert gravel in Ozark soils, with floodplains generally consisting of coarse chert gravel overlain by a mantle (1 to 300 cm) of gravelly loam or silt loam. The process of alluvial sediment deposition is highly variable, and can cause gravel layers to outcrop on the soil surface at various locations within a floodplain. The objective of this research was to quantify heterogeneity in infiltration rates and phosphorus leaching at three floodplain sites in the Ozark ecoregion of Oklahoma and Arkansas. Innovative field studies, including plot scale (1 m^2 and 9 m^2) tracer injection experiments along with geophysical imaging,

were performed on both gravel outcrops and non-gravel outcrops. Plots maintained a constant head of 3 to 10 cm for up to 48 hours. Infiltration rates varied from 0.8 to 70 cm/h, and varied considerably even within a single floodplain. Electrical resistivity imaging was used to identify zones of preferential flow as well as characterize subsurface soil layering. Fluid samples from observation wells outside the plot (0.5 m from the boundary) indicated nonuniform subsurface flow and transport. Results indicated that flowpaths are sub-meter scale for detecting infiltrating solutions. Phosphorus was detected in the groundwater for 6 of the 12 plots and was positively correlated to the presence of gravel outcrops. Tension infiltrometers showed that macropore flow accounted for approximately 85% to 99% of the total infiltration. This research highlighted the difference between the conceptual model of uniform piston infiltration and actual infiltration in field conditions.

7.2. INTRODUCTION

In order to protect surface water, all transport mechanisms of nutrients, pesticides, and bacteria within a watershed need to be understood. Surface transport mechanisms are well understood, but subsurface transport mechanisms are not as well characterized (Fuchs et al., 2009). Considerable research has been performed on properties of point soil samples, and some research has been done on transport in undisturbed soil columns (Ulen, 1999; Maguire and Sims, 2002; Djodjic et al., 2004). However, relatively few studies on both infiltration and transport have been done at the plot scale where infiltration and transport may be controlled by heterogeneity present at various scales (Nelson et al., 2005).

For example, research is currently limited in understanding the potential significance of connectivity between phosphorus (P) in surface runoff and groundwater and nutrient movement from the soil to groundwater in watersheds with cherty and gravelly soils (Fox et al., 2011; Heeren et al., 2011; Mittelstet et al., 2011). While optimum crop growth requires a range of P

above 0.2 mg/L, preventing surface water enrichment generally requires P to be below 0.03 mg/L (Pierzynski et al., 2005). In fact, surface waters in the Ozark ecoregion in particular may have a threshold closer to 0.01 mg/L (D.E. Storm, 2012, personal communication). While surface runoff is considered to be the primary transport mechanism for P (Gburek et al., 2005), the potential for P leaching is commonly estimated based on point-measurements of soil test phosphorus (STP) or measurements of the sorption capability of disturbed soil samples representing the soil matrix. However, in many riparian floodplains, gravel outcrops and macropores are present (Heeren et al., 2011). These gravel outcrops can lead to extremely high infiltration rates, some of which are reported to be on the order of 10 cm/min (Sauer and Logsdon, 2002; Saur et al., 2005). In fact, infiltration of P-laden water during high flow discharges that exceed bankfull events can infiltrate in the floodplain subsoil and migrate back to the streams. Djodjic et al. (2004) performed experiments on P leaching through undisturbed soil columns, and stressed the need to consider larger-scale leaching processes due to soil heterogeneity. They stated that the "water transport mechanism through the soil and subsoil properties seemed to be more important for P leaching than soil test P value in the topsoil. In one soil, where preferential flow was the dominant water transport pathway, water and P bypassed the high sorption capacity of the subsoil, resulting in high losses."

A common best management practice in riparian floodplains is riparian buffers or vegetative filter strips (VFS), utilized to reduce sediment, nutrient, and pesticide loading to nearby surface water bodies (Popov et al., 2005; Reichenberger et al., 2007; Sabbagh et al., 2009). Reduced transport occurs through contact between dissolved phase solutes with vegetation in the filter strip, and/or by reducing flow velocities to the point where eroded sediment particles can settle out of the water. In floodplains with significant heterogeneity such as macroporosity and chert or gravel soils, the effectiveness in preventing loading to nearby streams and rivers may be less than originally anticipated if a significant transport pathway occurs into the shallow

groundwater and then bypasses the filtering capacity of the VFS. The impact of such heterogeneous infiltration and leaching is not known at this time.

Gravel outcrops and macropores can significantly affect infiltration and leaching in these floodplains. For water movement through soil, macropores have been shown to have a large impact on flow and solute transport (Thomas and Phillips, 1979; Fox et al., 2004; Djodjic et al., 2004; Akay and Fox, 2007; Gotovac et al., 2009). Infiltration is often assumed to be uniform (piston flow) at the field scale, but this neglects the high spatial variability common in anisotropic, heterogeneous alluvial-floodplain soils. Therefore, the objective of this research was to quantify infiltration and leaching at the plot scale and to evaluate the effects of gravel outcrops and macropores on these processes.

7.3. METHODS AND MATERIALS

7.3.1. Alluvial Floodplain Sites

The alluvial floodplain sites were located in the Ozark ecoregion of northeastern Oklahoma and northwestern Arkansas. The Ozark ecoregion of Missouri, Arkansas, and Oklahoma is approximately 62,000 km^2 (Figure 7.1) and is characterized by gravel bed streams and cherty soils in the riparian floodplains. The erosion of carbonate bedrock (primarily limestone) by slightly acidic water has left a large residuum of chert gravel in Ozark soils, with floodplains generally consisting of coarse, chert gravel overlain by a mantle (1 to 300 cm) of gravelly loam or silt loam. The alluvium is spatially heterogeneous, resulting in preferential flow pathways which are hypothesized to be ancient buried gravel bars (Heeren et al., 2010). Similar hydrogeologic conditions exist near gravel bed streams in their associated alluvial floodplains worldwide.

The Barren Fork Creek site (Figure 7.1, latitude: 35.90°, longitude: -94.85°) was immediately downstream of the Eldon Bridge U.S. Geological Survey (USGS) gage station

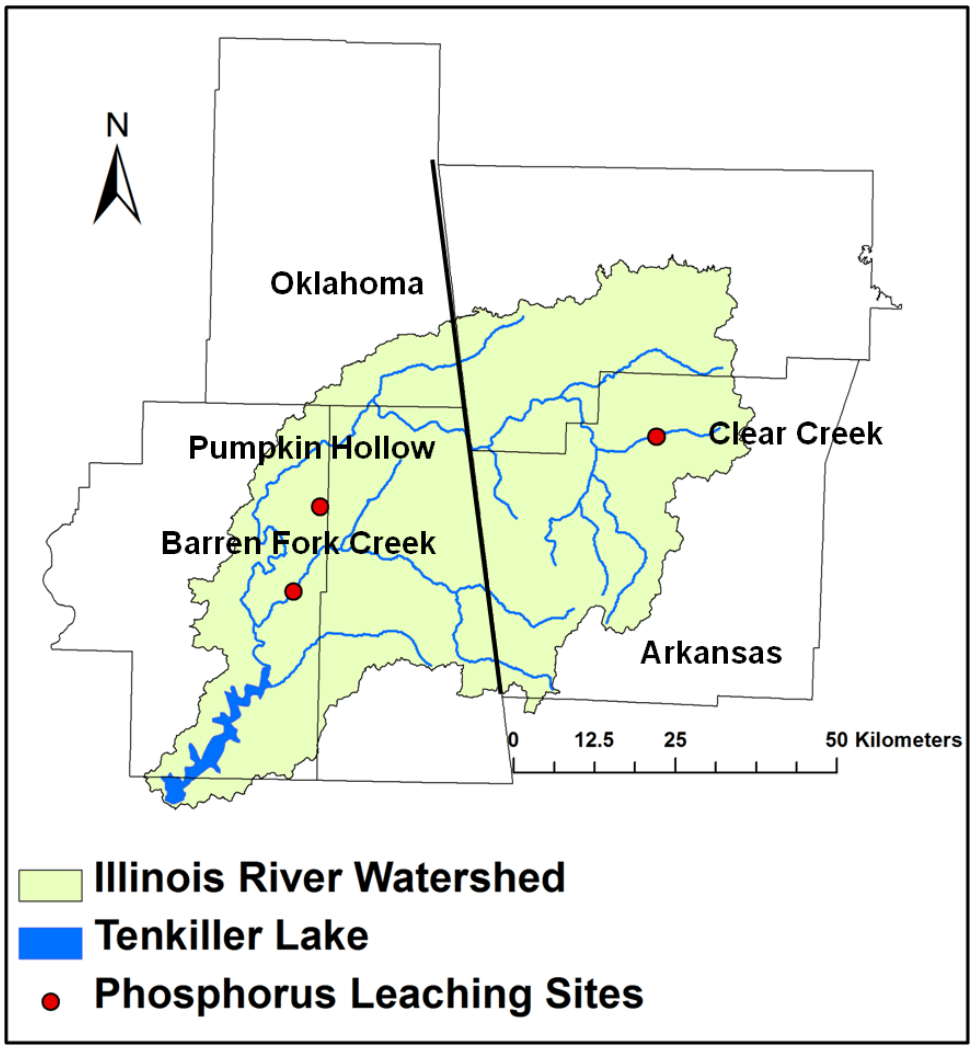

Figure 7.1. Selected alluvial floodplain sites in the Ozark ecoregion.

07197000. With a watershed size of 845 km2, the Barren Fork Creek site was a fourth order stream with a historical median discharge of 3.6 m3 s-1. The study area at the Barren Fork Creek was located on the outside of a meander bend which was being actively eroded by the stream (Midgley et al., 2012). The soils were classified as Razort gravelly loam underlain with alluvial gravel deposits. Thickness of the silt loam layer ranged from 0.5 to 1.0 m, with dry bulk densities ranging from 1.3 to 1.7 g cm^{-3}. Soil hydraulic studies on these soil types have shown that subtle morphological features can lead to considerable differences in soil water flow rates (Sauer and Logsdon, 2002). Fuchs et al. (2009) described some of the soil and hydraulic characteristics of the

Barren Fork Creek floodplain site, including estimates of hydraulic conductivity for the gravel subsoil between 140 and 230 m d^{-1} based on falling head trench tests. Heeren et al. (2010) performed a tracer injection into a PFP, identified as a buried gravel bar, at the Barren Fork Creek site. Local transient storage and physical nonequilibrium was observed as evidenced by the elongated tails of breakthrough curves in some observation wells due to physical heterogeneity in the aquifer materials. Background electrical resistivity data for the Barren Fork Creek site is presented in Miller (2012).

The Pumpkin Hollow floodplain site was also located in the Ozark ecoregion of northeastern Oklahoma (latitude: 36.02°, longitude: -94.81°). A small tributary of the Illinois River, Pumpkin Hollow Creek was a first order ephemeral stream in its upper reaches. The entire floodplain was 120 to 130 m across at the research site, with an estimated watershed area of 15 km^2. The land use at the site was pasture for cattle. The Pumpkin Hollow field site was a combination of Razort gravelly loam and Elsah very gravelly loam, although infiltration experiments were limited to the Razort gravelly loam soils. Topsoil thickness ranged from 0 to 3 cm, and bulk densities of the cohesive material were in the range of 1.3 to 1.5 g cm^{-3}. Background electrical resistivity data for the Pumpkin Hollow site is presented in Miller (2012).

The Clear Creek alluvial floodplain site was located just west of Fayetteville, AR in the Arkansas River Basin and flows into the Illinois River (Figure 7.1, latitude: 36.13°, longitude: 94.24°). The total drainage area was 199 km^2 for the entire watershed. Land use in the basin was 36% pasture, 34% forest, 27% urban and 3% other. Soils were loamy and silty, deep, moderately well drained to well drained (U.S. EPA, 2009), and generally contained less chert or gravel than the Barren Fork Creek or Pumpkin Hollow floodplain sites. Thickness of the top loam layer ranged from 0.3 to 2 m, with dry bulk densities ranging from 1.5 to 1.7 g cm^{-3}. A fourth order stream with a flow of approximately 0.5 m^3 s^{-1} at the study site, the area of the watershed above that point was 101 km^2. The land use in the study area was pasture and consisted of Razort

gravelly loam soils. Background electrical resistivity data for the Clear Creek site is presented in the appendix.

7.3.2 Berm Installation and Hydraulics

Measuring infiltration rates and/or leaching of solutes at a plot scale is difficult, especially for high hydraulic conductivity soils, without innovative field methods. In this research, a berm method (Heeren et al., 2012) was used to confine infiltration plots and maintain a constant head of water. Four infiltration experiments were performed at each site with plots selected to represent typical floodplain soils with and without gravel outcrops (Table 7.1). Plots were located on relatively level areas. Larger plots were required to have smaller slopes to ensure that the entire plot could be inundated without overflowing the berm.

Table 7.1. Infiltration experiments at three alluvial floodplain sites in the Ozark ecoregion.

Site	Date	Plot Size	Treatment	Duration (h)	Infiltration (cm/hr)
Clear Creek	4/12/11	1x1	control	41	5.6
Clear Creek	4/12/11	3x3	control	41	3.3
Clear Creek	7/27/11	1x1	outcrop	48	1.3
Clear Creek	7/27/11	3x3	outcrop	45	0.8
Pumpkin Hollow	5/4/11	1x1	outcrop	32	5.3
Pumpkin Hollow	5/5/11	3x3	outcrop	2.8	18
Pumpkin Hollow	6/1/11	1x1	outcrop	4.3	74
Pumpkin Hollow	6/2/11	3x3	control	24	6.3
Barren Fork	6/30/11	1x1	outcrop*	22	11
Barren Fork	6/30/11	3x3	outcrop*	22	13
Barren Fork	7/13/11	1x1	control	46	6.9
Barren Fork	7/13/11	3x3	control	48	3.8

*Gravel under 0.3 to 1 m of silt loam.

Each berm was constructed of four sections of 15 cm vinyl hose which were attached to 90° steel elbows and surrounded the infiltration gallery (Figure 7.2). A shallow trench (3 to 5 cm)

was cut through the thatch layer and liquid bentonite was used to create a seal between the berm and the soil.

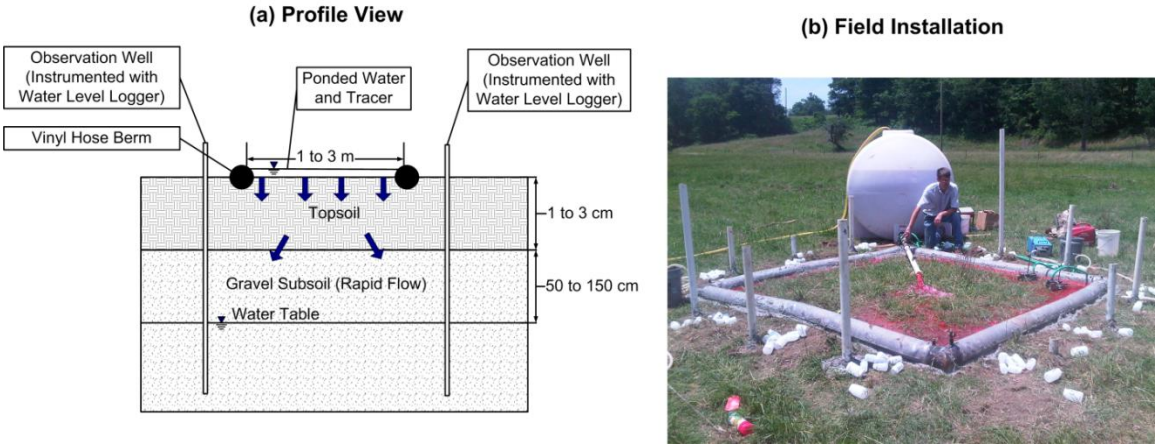

Figure 7.2. Berm infiltration method, including vinyl berms to contain water-solute solution and observation wells for collecting groundwater samples: (a) design and (b) implementation at the Pumpkin Hollow floodplain site.

High density polyethylene tanks (4.9 m^3 and 0.76 m^3) were used to mix stream water and solutes. A combination of 5.1-cm diameter PVC with manual valves and garden hoses with float valves were used to deliver water (gravity fed) from the tanks to the plots. When a tank was nearly empty, flow was temporarily stopped while the tank was refilled and solutes were added and mixed. Constant heads in the plots were maintained (Heeren et al., 2012) between 3 and 10 cm. Depth to the water table ranged from 50 to 150 cm.

Chloride (Cl^-) was used as a conservative (nonsorbing) tracer. Target tracer concentrations were 100 or 200 mg/L KCl (correlating to 48 to 95 mg/L Cl^-), depending on background EC levels. The RhWT was a slightly-sorbing dye and was introduced into the plots at concentrations of 10 to 100 mg/L. The RhWT was regarded as a slightly sorbing solute since the soils were expected to have organic matter contents of less than 2%, resulting in a minor amount of Rhodamine WT sorption. The RhWT served as a visual indicator of hydraulic connectivity in the observation wells.

Phosphorus (highly sorbing) concentrations of 3 to 10 mg/L (corresponding to 10 to 32 as phosphate) were used to represent poultry litter application rates (typically used as a fertilizer source in the Ozark ecoregion) in the range of 2 to 8 Mg/ha (1 to 3 ton/acre). Previous research (Kleinman et al., 2002; DeLaune et al., 2004; Schroeder et al., 2004) has observed dissolved reactive phosphorus in the range of 5 to 40 mg/L in runoff from recently applied poultry litter in the range of 2 to 14 Mg poultry litter per hectare.

Phosphorus concentrations were achieved by adding phosphoric acid (H_3PO_4), which deprotonated to $H_2PO_4^-$ and HPO_4^{2-} in the slightly acidic solution. The inflow water in the plot was sampled throughout the experiment to verify these concentrations. The source stream water was also sampled over time to quantify its P contribution. Redox conditions were not expected to be a concern for characterizing P fate and transport because of the lack of anaerobic conditions due to the high porosity and excessive drainage of both the soil and subsurface materials in Ozark floodplains. For example, dissolved oxygen (DO) of the groundwater at the Barren Fork Creek site (measured with a ProODO DO meter, YSI Inc., Yellow Springs, Ohio) ranged from approximately 8 mg/L near the creek to 4 mg/L up to 100 m from the creek.

In general, the P concentration in the groundwater samples were expected to decrease relative to input P concentration due to sorption as the water infiltrates down through the soil profile. Without considering macropore and/or gravel outcrop infiltration, P would be expected to only minimally, if at all, travel through the soil matrix. Comparisons in the breakthrough curves, peak concentrations, and the time to reach the peak concentration in the monitoring wells between the Cl^-, RhWT and P concentrations, which possess different sorption properties, were made to indicate differences in sorptive rates.

7.3.3. Monitoring with Electrical Resistivity

Vertical electrical resistivity profiles were collected at the floodplain sites during the infiltration/leaching experiments (Figure 7.3). Electrical resistivity was utilized to characterize the heterogeneity of the unconsolidated floodplain sediments, as well as locating the infiltrating plume of water and solutes by detecting changes in pore water. Electrical resistivity imaging (ERI) is based on measuring the electrical properties of near-surface earth materials (McNeill, 1980), which vary with grain size, pore-space saturation, pore water solute content, and electrical properties of the minerals. The electrical behavior of earth materials is controlled by Ohm's law, in which current is directly proportional to voltage and inversely proportional to resistance. Generally, electrical current travels readily in solute-rich pore water and poorly in air. In addition, cations adsorbed to soil particle surfaces reduce resistivity. Clay particles have a large surface area per volume and thus have generally lower resistivity (1 to 100 Ω-m) compared to sands or gravels (10 to 800 Ω-m), which are lower than limestone bedrock (McNeill, 1980).

ERI data were collected using a SuperSting R8/IP Earth Resistivity Meter (Advanced GeoSciences Inc., Austin, Tex.) with 28-electrode arrays. The first line ran through the center of the plots and lateral to the expected gradient, with the second line parallel and 3 m downgradient of the first line (Figure 7.3). The profiles employed electrode spacings of 0.5 m with an associated depth of investigation of approximately 3 m, which included the vadose zone as well as the top of the water table. The resistivity sampling with the SuperSting R8/IP, and subsequent inversion utilized a proprietary routine devised by Halihan et al. (2005), which produced higher resolution images than conventional techniques. The ERI resistivity data were interpolated into grids and contoured using Surfer 8 (Golden Software, Inc., Golden, CO). Inverted and interpolated resistivity data were termed “ERI profiles” as opposed to “ERI pseudosections”, which were the raw resistivity measurements as collected in the field. Differencing was used to

display the percent difference in resistivity between the background image and images collected during the infiltration experiments.

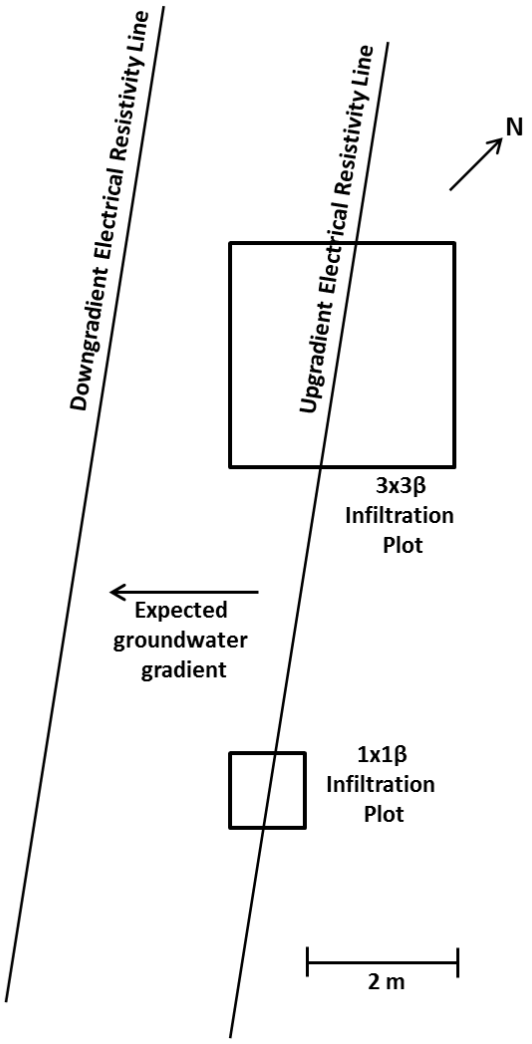

Figure 7.3. Electrical resistivity design for the control plots at the Barren Fork Creek site (July 13, 2011).

7.3.4. Observation Wells and Sample Analysis

Suction cup lysimeters were not used because of the difficulty of installation in gravelly soils, risk of creating preferential flow paths in vadose zone, and low likelihood of intercepting macropores. Since there are not currently any effective techniques for taking measurements from underneath a given plot in these gravelly soils, observation wells were installed every 0.5 to 2 m

around the perimeter of the plots to collect groundwater samples (Figure 7.2). When a confining layer was present (based on soil cores), shallow observation wells were installed with alternating wells designed specifically to sample from the vadose zone (where perched water was expected) and the remaining observation wells designed specifically to sample from the phreatic zone.

A Geoprobe Systems drilling machine (6200 TMP, Kejr, Inc., Salina, KS), which has been found to be effective in coarse gravel soils (Heeren et al., 2011; Miller et al., 2011), was used to install four to twelve observation wells around each plot. Boreholes were sealed with liquid bentonite to avoid water and solutes leaking down the borehole. Low flow sampling with a peristaltic pump was used to collect water samples from the top of the water table (Heeren et al., 2011). Sampling intervals were adjusted based on EC meter readings (to detect elevated levels of Cl^-) and visual observations of RhWT with the goal of having enough data points to characterize the breakthrough curve.

Well and plot water samples, as well as background stream and groundwater samples, were stored and transported on ice and were tested for both P and Cl^- at the AWRC Water Quality Laboratory on the University of Arkansas campus. The soluble reactive phosphorus (SRP) samples were filtered within 24 hours of sampling using 0.45 µm filters and acidified with sulfuric acid. The SRP was determined colorimetrically with the modified ascorbic acid method (EPA Method 365.2; Murphy and Riley, 1962) with a spectrophotometer (DU 720, Beckman Coulter, Indianapolis, IN, minimum detection limit of 0.002 mg/L). Autoclave per-sulfate digestions (APHA 4500 PJ) were performed on unfiltered total phosphorus (TP) samples in order to dissolve any particulate or organic P. The TP (minimum detection limit of 0.01 mg/L) was then determined colorimetrically with the modified ascorbic acid method. The Cl^- concentrations were determined with ion chromatography (minimum detection limit of 0.16 mg/L). The RhWT samples were analyzed at Oklahoma State University with a Trilogy laboratory fluorometer (Turner Designs, Inc., Sunnyvale, CA, minimum detection limit of 0.01 mg/L).

Automated water level loggers (HoboWare, Onset Computer Corp., Cape Cod, MA, water level accuracy of 0.5 cm) were used to monitor water level (one minute intervals) in the observation wells, plots, and tanks, from which flow rates were calculated. An additional logger was used to monitor atmospheric pressure. Logger data were processed with HoboWare Pro software, which accounted for changes in atmospheric pressure as well as changes in water density due to temperature.

7.3.5. Soil Cores and Particle Size Analysis

Soils samples were collected outside the berm before the leaching tests in order to keep the plot area undisturbed, and inside the plot after each experiment. Soil cores throughout the vadose zone were obtained at each site and were sliced into samples representing different soil horizons. The large particles that make up gravel-dominated soils make them problematic for soil sampling. Difficulties occur with all sampling methods and include large particles blocking tube sampler openings and the collapse of pits excavated in unconsolidated gravel. Furthermore, gravel soils are resistant to penetration and thus core sampling often requires mechanical assistance that may cause breakage of large particles. If the largest particle sizes present in the soil exceed the sampler diameter, the collected sample may not truly represent the actual size distribution.

With a realization of these limitations, direct push cores were recovered from one to four wells per plot. Core samples were collected at known depths with a Geoprobe Systems (Salina, KS) 6200 TMP (Trailer-mounted Probe) direct-push drilling machine using a dual-tube core sampler with a 4.45 cm opening. The sampler opening (size) limited the particle size that could be sampled and large cobbles occasionally clogged the sampler resulting in incomplete cores for that depth interval.

A subset of the soil core samples were dry sieved with a sieve stack ranging from 2 to 12.5 mm for a particle size analysis. Samples preparation included disaggregation with a rubber-tipped pestle when necessary. If particles were retained on the 12.5 mm sieve, a measurement of the "b" axis (longest intermediate axis perpendicular to the long "a" axis) of the largest particle was utilized as the sieve size that 100% of the sample would pass through because that dimension largely controls whether a particle will pass a particular sieve (Bunte and Abt, 2001).

7.3.6. Tension Infiltrometers

After the plot infiltration experiments, mini-disk infiltrometers (Decagon Devices, Pullman, WA) were used inside the plots (after the soil profile had dried) to measure soil matrix infiltration. Tension infiltrometers are designed to measure unsaturated soil infiltration rates by exposing water that is under tension (negative pressure) to the soil surface. Water must flow from a higher potential to a lower potential. Therefore, water under tension infiltrated into the soil matrix, which had a more negative capillary pressure. However, the water did not infiltrate into the macropores, which had a less negative capillary pressure. Since the macropores remained dry, flow was restricted to the soil matrix with the infiltration rate equivalent to matrix infiltration. Saturated infiltration from the plot scale experiments represented total infiltration from both matrix and macropores. Macropore infiltration was estimated by subtracting the matrix infiltration from the total infiltration.

Suction levels of 1, 3, and 6 cm, spanning the ability of the infiltrometer, were used. Equivalent radii were calculated for each suction level with the capillary rise equation (Scott, 2000):

$$h = \frac{2\sigma \cos\theta}{r\rho_w g} = \frac{0.15}{r} \tag{7.1}$$

where h is the capillary rise or suction (L), σ is the surface tension of water (F/L), θ is the contact angle, r is the equivalent radius (L), ρ_w is the density of water (M/L^3), and g is the acceleration

due to gravity (L/T^2). The θ was assumed to be zero and σ was assumed to be 72.8 mN/m (for water at 20^0C). The unit conversion coefficient of 0.15 arises for *h* and *r* in cm.

In order to enable the comparison between suction level and pore geometry, the following conceptual model was used. The soil pore space was conceptualized as circular tubes (not necessarily vertical) with a distribution of radii. Each pore was considered either activated (saturated) or dry. For a given suction level, the infiltration is limited to pores with radii less than or equal to the radius corresponding to the suction level. A comparison between plot infiltration data (all pores activated) and tension infiltrometer was used to differentiate between matrix and macropore flow. The simplification in this conceptualization is that it neglects flow in a thin film along a pore wall when that pore is unsaturated. Accounting for thin film flow in macropores would increase their contribution; therefore, this approach gives a conservative estimate of the impact of macropores.

Soils pores have been classified as macropores (greater than 75 μm), mesopores (30 to 75 μm), and micropores (5 to 30 μm) (SSSA, 2008). In this research, macropores were defined as pore spaces with equivalent diameters of 500 μm (i.e. 6 cm capillary pressure) or more due to limitations of the infiltrometer.

The unsaturated hydraulic conductivity (*k(h)*) was calculated from the tension infiltrometer results using the method of Zhang (1997). Readings were taken until the infiltrometer reservoir was depleted (14 to 121 minutes), which was sufficient to fit the two parameters hydraulic conductivity and sorptivity to the cumulative infiltration versus time data.

7.4. RESULTS AND DISCUSSION

7.4.1. Soil Infiltration Rates and Heterogeneity

Soils were heterogeneous, even within a small area of a given floodplain (Figure 7.4). Not surprisingly, infiltration rates also varied greatly, ranging over two orders of magnitude (Figure 7.5, Table 7.1). Pumpkin Hollow generally had the highest infiltration rates, while Clear Creek had the lowest infiltration rates.

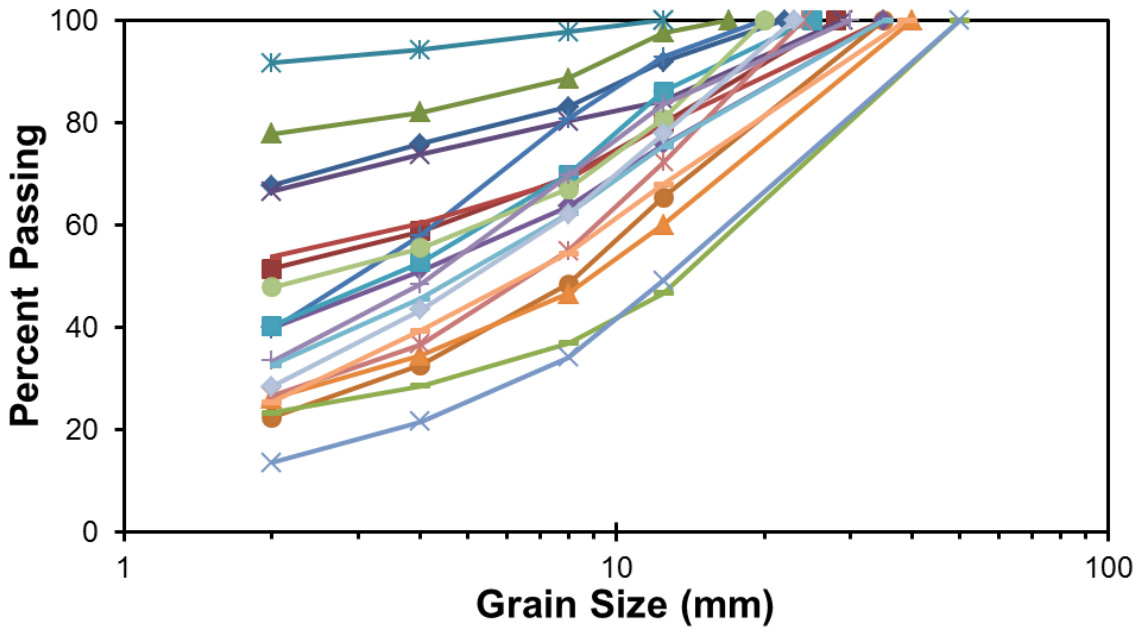

Figure 7.4. Particle size distributions of Pumpkin Hollow soil core samples.

Though not strong, there was a positive correlation between infiltration rate and the presence of gravel outcrops (Figure 7.5). The geometric mean infiltration rate for gravel outcrops (7.2 cm/hr) was higher than the infiltration rate for control plots (5.0 cm/hr). In fact, the two lowest infiltration rates were on gravel outcrops at the Clear Creek site. In that particular location, there was significant gravel, but the fines (which were the limiting factor for water flow) had higher clay content than any of the other plots.

Measured infiltration rates were greater than the estimated permeability of the limiting layer reported by the U.S. Natural Resources Conservation Service (NRCS) for Cherokee County, Oklahoma (NRCS, 2012), which ranged from 1.5 to 5 cm/hr for the Razort gravelly loam soil (Figure 7.5). This difference indicates the need for larger scale field measurements of infiltration rate. For example, soil survey measurements may represent a typical soil pedon but miss gravel outcrops or large macropores which may be infrequent but have a disproportionate impact on infiltration.

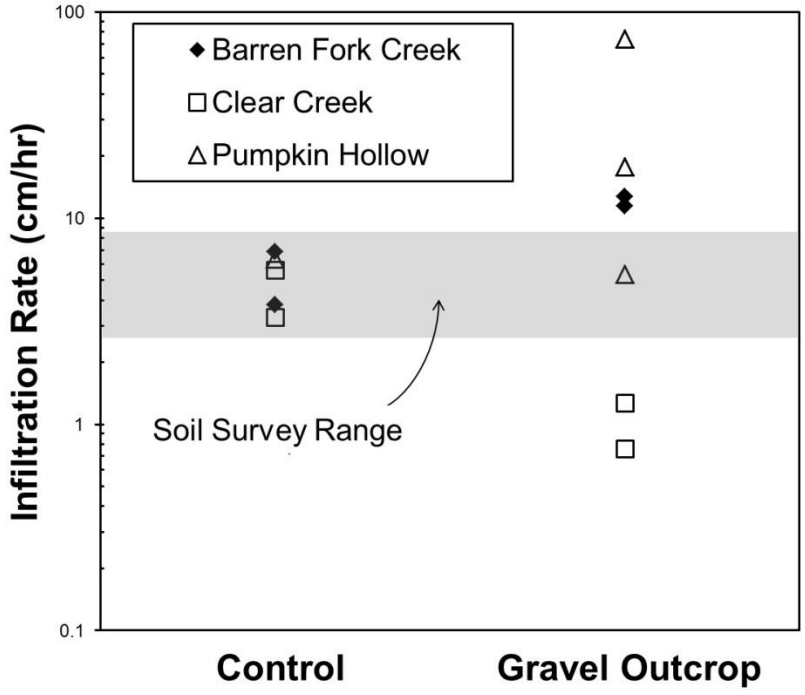

Figure 7.5. Infiltration rates from plot scale experiments for both control and gravel outcrop locations. The expected range of infiltration rates based on the permeability of the limiting layer reported in the Natural Resources Conservation Service Soil Survey (NRCS, 2012) is shown in gray.

Infiltrating water either reached the water table before moving laterally or lateral movement in the vadose zone was induced by a confining layer. Water table elevations in phreatic zone wells were used to discern the presence of a groundwater mound (Figure 6). Sharp

decreases indicate the times when fluid samples were collected and the rate of recovery of the piezometric surface gives a qualitative indication of hydraulic conductivity.

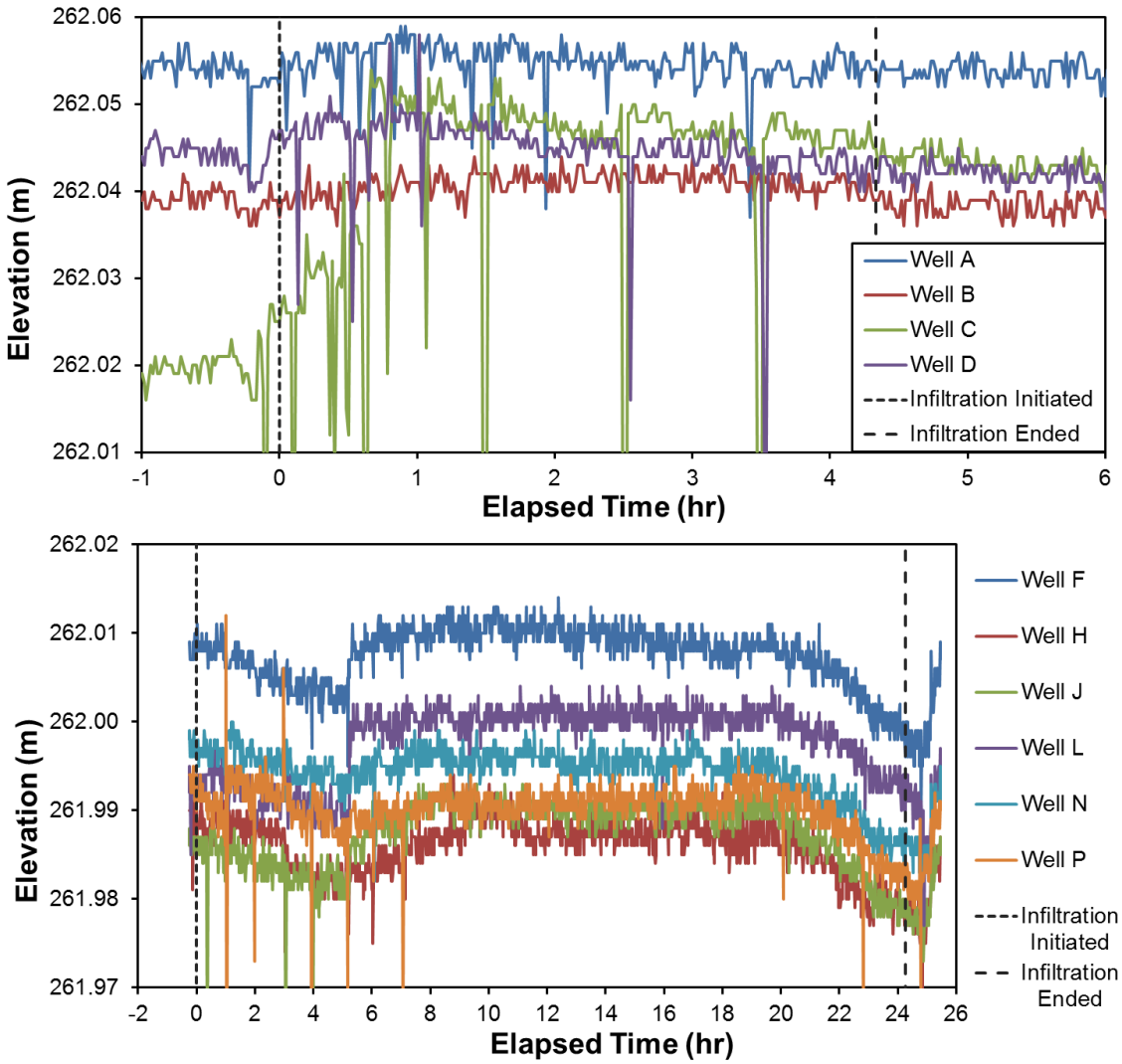

Figure 7.6. Water levels in phreatic zone observation wells of the 1 by 1 m gravel outcrop infiltration plot (top, June 1, 2011) and of the 3 by 3 m control infiltration plot (bottom, June 2, 2011) at the Pumpkin Hollow floodplain site.

7.4.2. Transport

Rhodamine WT and Cl^- were observed in no wells in some plots to all wells in other plots, while detection of P ranged from no wells to nearly half of the wells for a given plot (Table

7.1). Response times ranged from 18 min to greater than 48 hr. Infiltration and leaching appear to correlate weakly to topsoil thickness and stream order.

For each solute, the concentration ratio (C_r=C/C_o) between the concentration in the well (C) and the concentration injected into the plot (C_0) was used to examine break through curves (BTC's) (Figure 7.7). Concentration ratios began at background levels (near zero) and generally increased with time, approaching unity for Cl^- in some cases. Within a well, the Cl^- (conservative) BTC generally began first, followed by RhWT (slightly sorbing), and finally P (highly sorbing) (Figure 7.7, Table 7.2).

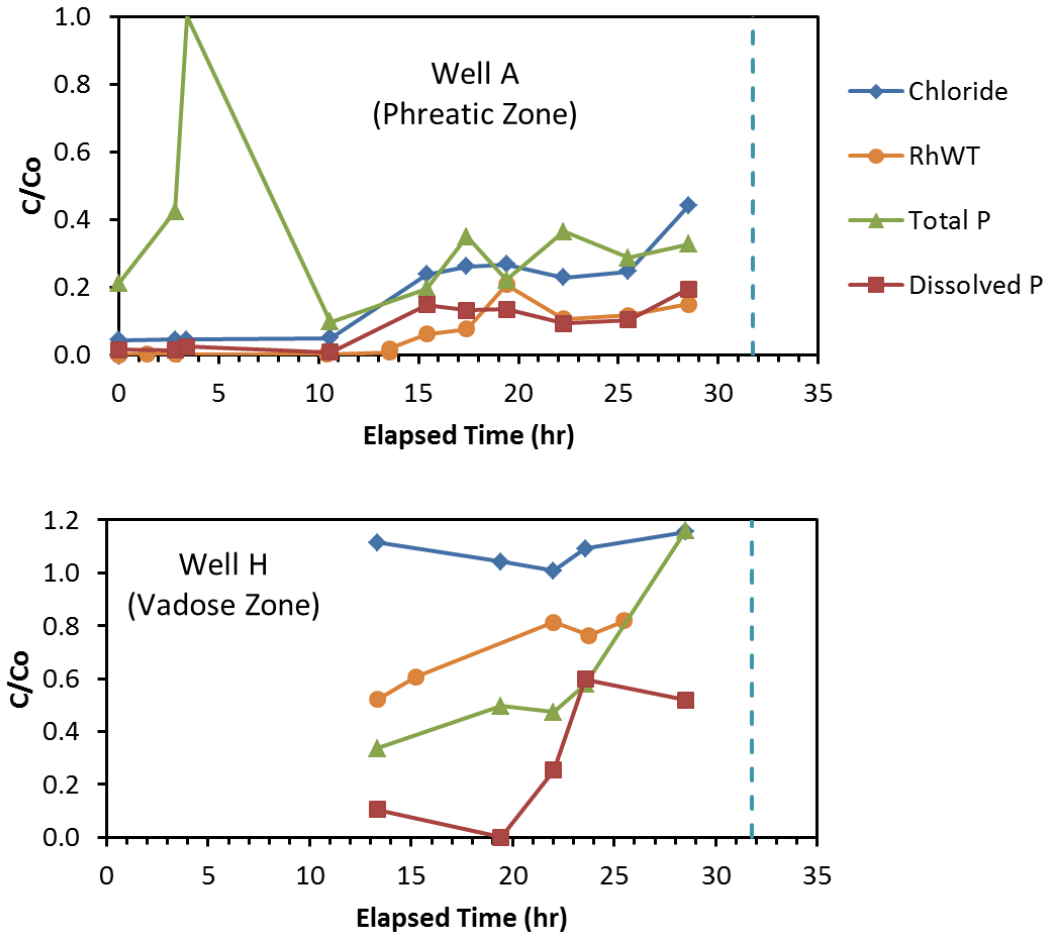

Figure 7.7. Concentration ratio (C/C_o) data for two of the observation wells for the Pumpkin Hollow gravel outcrop 1 by 1 m (top, May 4, 2011) and 3 by 3 m (bottom, May 5, 2011) infiltration experiments.

Table 7.2. Transport data by well for the 1 m by 1 m (May 4, 2011, gravel outcrop, 32 hr duration, 5.3 cm/hr infiltration) and 3 m by 3 m (May 5, 2011, gravel outcrop, 2.8 hr duration, 18 cm/hr infiltration) plots at the Pumpkin Hollow floodplain site.

			Time to detection (hr)			Time to peak (hr)			Peak concentration ratio		
Plot	Well	Zone	Cl	RhWT	DP	Cl	RhWT	DP	Cl	RhWT	DP
1x1α	A	Phreatic	15	14	15	>29	19	>29	0.44	0.21	0.19
	B	Vadose	--	14	--	29	>29	>29	1.04	0.35	0.21
	C	Phreatic	>29	>29	>29	>29	>29	>29	--	--	--
	D	Vadose	remained dry								
	E	Phreatic	>29	>29	>29	>29	>29	>29	--	--	--
	F	Vadose	remained dry								
	G	Phreatic	>29	26	>29	>29	26	>29	--	0.001	--
	H	Vadose	13	13	13	29	>26	24	1.16	0.82	0.60
3x3α	I	Vadose	0.7	0.5	0.8	1.4	0.8	0.8	0.51	0.49	0.03
	J	Phreatic	>3.1	0.7	>3.1	>3.1	0.8	>3.1	--	0.0003	--
	K	Vadose	remained dry								
	L	Phreatic	>3	0.7	>3	>3	1.1	>3	--	0.004	--
	M	Vadose	remained dry								
	N	Phreatic	0.6	0.6	0.6	1.5	0.8	0.8	0.58	0.28	0.06
	O	Vadose	--	0.7	--	1.0	1.0	>1.0	0.67	0.36	0.14
	P	Phreatic	>2.9	0.7	>2.9	>2.9	2.9	>2.9	--	0.01	--
	Q	Vadose	1.1	0.6	1.1	2.2	>1.8	>3.0	0.75	0.32	0.30
	R	Phreatic	>2.9	>2.9	>2.9	>2.9	>2.9	>2.9	--	--	--
	S	Vadose	0.8	--	0.8	0.8	1.1	1.6	0.80	0.40	0.13
	T	Phreatic	>2.9	>2.9	>2.9	>2.9	>2.9	>2.9	--	--	--
	Seep	Stream	--	--	>2.9	2.3	2.3	>2.9	0.08	0.02	--

For observation wells in the vadose zone, sample collection was not possible until a sufficient level of water had perched, at which point concentrations were usually high (Figure 7.7, Table 7.2). In vadose zone wells, dilution was expected to be limited to displaced water from the unsaturated zone, so the C_r of a conservative tracer should be near 100%.

For the Barren Fork Creek gravel outcrop plots (June 30, 2011), the RhWT and Cl^- concentrations increased by the second sample after the start of the experiment, which was approximately two hours after initiating the leaching. In fact, slight increases in concentrations of both RhWT and Cl^- were observed after the first sample in some wells, which was taken approximately thirty minutes to one hour after the start of the experiment. Groundwater

concentrations reached approximately 50% of the injected Cl^- concentration at a breakthrough time of less than two hours after the initiation of infiltration. Samples were collected from the water table approximately 300 cm below the surface, meaning the Cl^- had an advective transport rate, or pore velocity, up to 150 cm/hr. Combining measured infiltration rates of 11 to 13 cm/hr with an estimated porosity of 0.5 results in a pore velocity of only 24 cm/hr assuming uniform matrix flow. This indicates the importance of macropore flow, transporting water and solutes an order of magnitude faster than the average soil infiltration rate at the Barren Fork Creek site.

During the May 5, 2011, infiltration experiment at Pumpkin Hollow (3x3), RhWT was observed in the stream approximately 15 m from infiltration plot in less than 1.7 hr after initiation infiltration. The C_r of RhWT in the stream near the seep face reached 0.02 (Table 7.2).

Spatial variability in flow and transport data was significant. Advection along the regional groundwater gradient generally resulted in higher concentrations on the down-gradient side of the plots (Figure 7.8). The soils in the alluvial floodplain were extremely heterogeneous, which corroborates previous research (Miller, 2012; Heeren et al., 2011). Even wells only 1 m apart showed significant variation in Cl^- (Figure 7.8).

At the Pumpkin Hollow 3 m by 3 m control plot (June 2, 2011), 1.5 m of infiltration occurred over 24 hr. With a shallow water table (0.9 to 1.0 m below ground surface), the infiltrating water must have moved laterally beyond the wells (0.5 m from the edge of the plot), especially when considering porosity. Yet, RhWT was never observed in any of the 12 observation wells, with observation wells in the phreatic zone spaced from 2 to 3 m apart. Either the flow must have been occurring at a small enough scale to flow between the well spacing, or RhWT sorption to organic matter was sufficient to reduce concentrations to below the minimum detection limit (over three orders of magnitude less than the plot RhWT concentration).

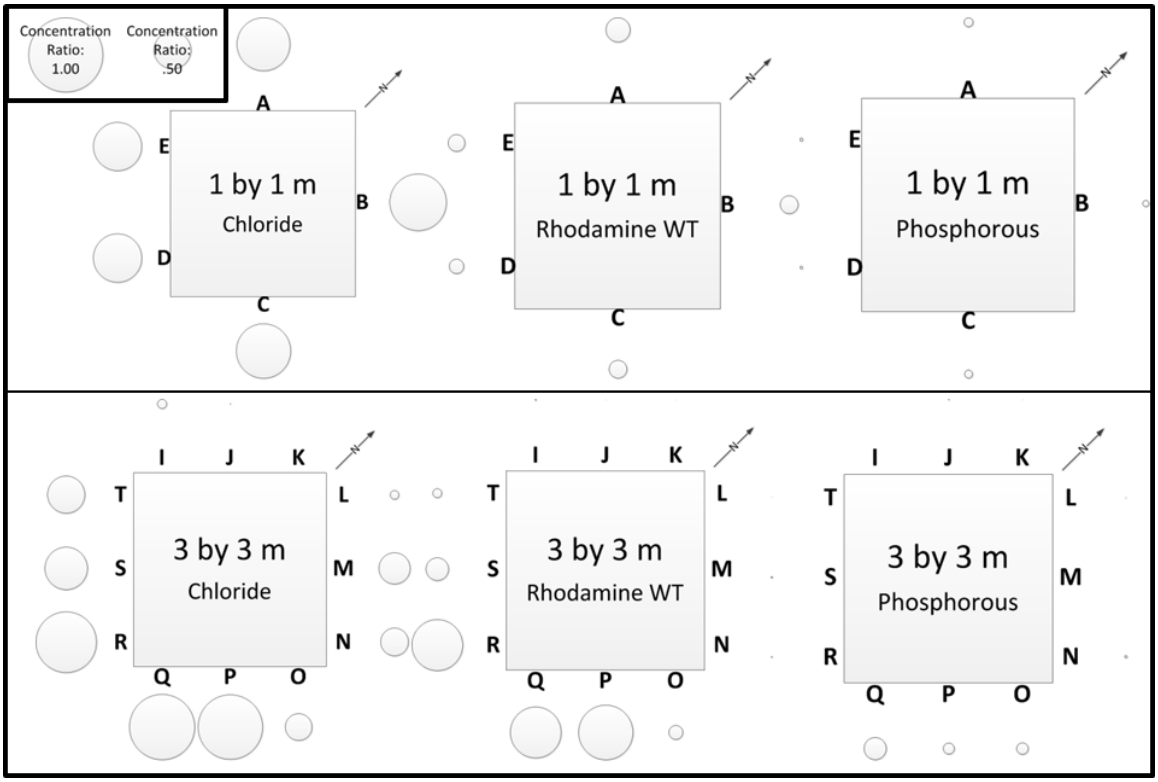

Figure 7.8. Maximum concentrations of samples from each well for the Barren Fork Creek gravel outcrop plots. Note that the plots are not drawn to scale. Size of the circle around each given well represents the concentration.

7.4.3. Electrical Resistivity of Infiltration Plume

Transient electrical resistivity results showed downward (Figure 7.9) and lateral (Figure 7.10) migration of the water and Cl^- plume. For the Barren Fork Creek control plots, Cl^- was detected in the water table (3 m below ground surface) only 7 hr after the initiation of infiltration for both the 1 m by 1 m and 3 by 3 m plots. Yet the ERI data shows only 1 to 2 m of infiltration after 19 hr. This indicates that rapid flow and transport may be occurring in macropores which only represent a small volume of the soil column, possible escaping detection by the electrical resistivity equipment. It is also possible that the gravel may have remained mostly unsaturated (except for fingering) while transporting all of the water delivered to it by the silt loam (top 1 m of soil profile). The limited downward movement may also indicate some lateral migration,

which would be consistent with the plume observed in the lateral line located 1.5 to 2.5 m downgradient from the edge of the plots (Figures 7.3 and 7.10).

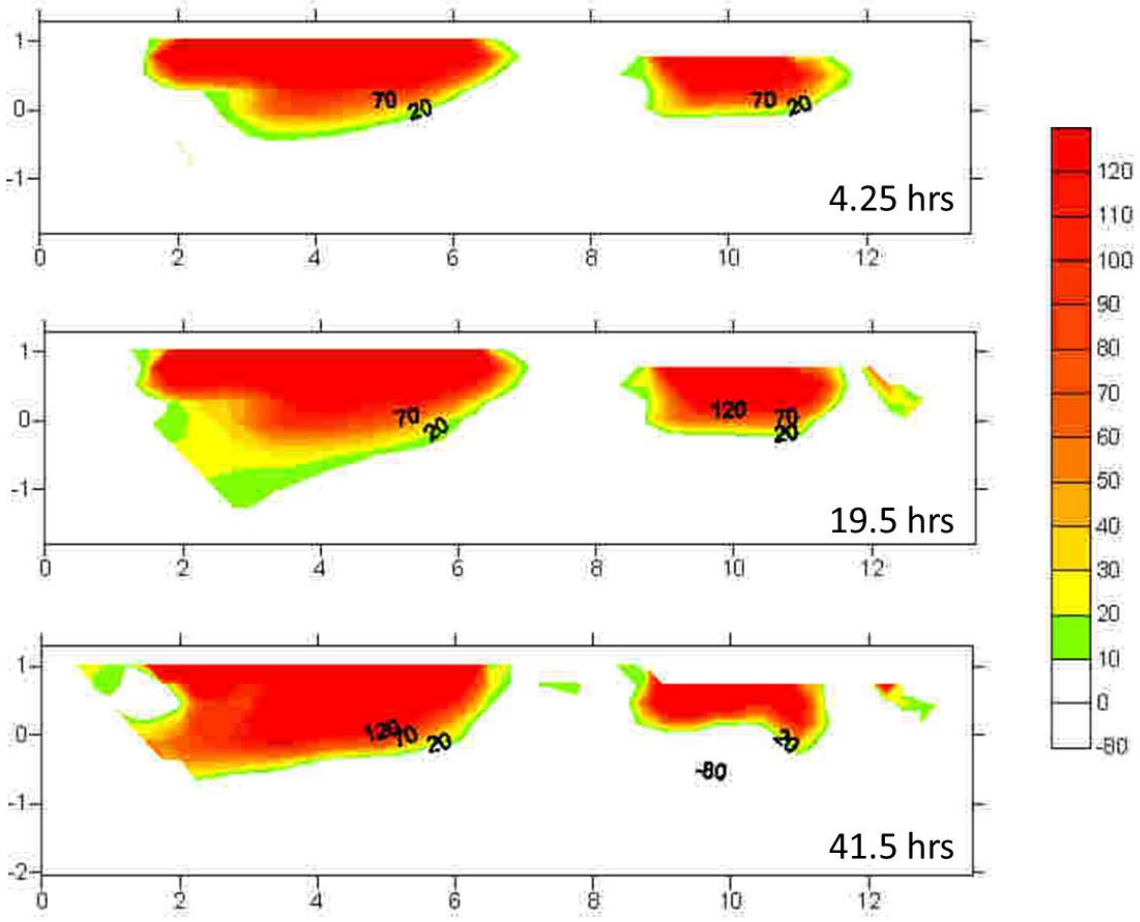

Figure 7.9. Vertical profile (y-axis is elevation in m) of percent difference in electrical resistivity of the upgradient lateral line (Figure 7.3) through the center of the 3 m by 3 m plot (left) and the 1 m by 1 m plot (right) of control area at the Barren Fork Creek site, July 13, 2011. Horizontal axis is distance along the electrical resistivity line in m. Time is the elapsed time from the onset of infiltration. The water table is located approximately at the bottom of each plot (-2 m).

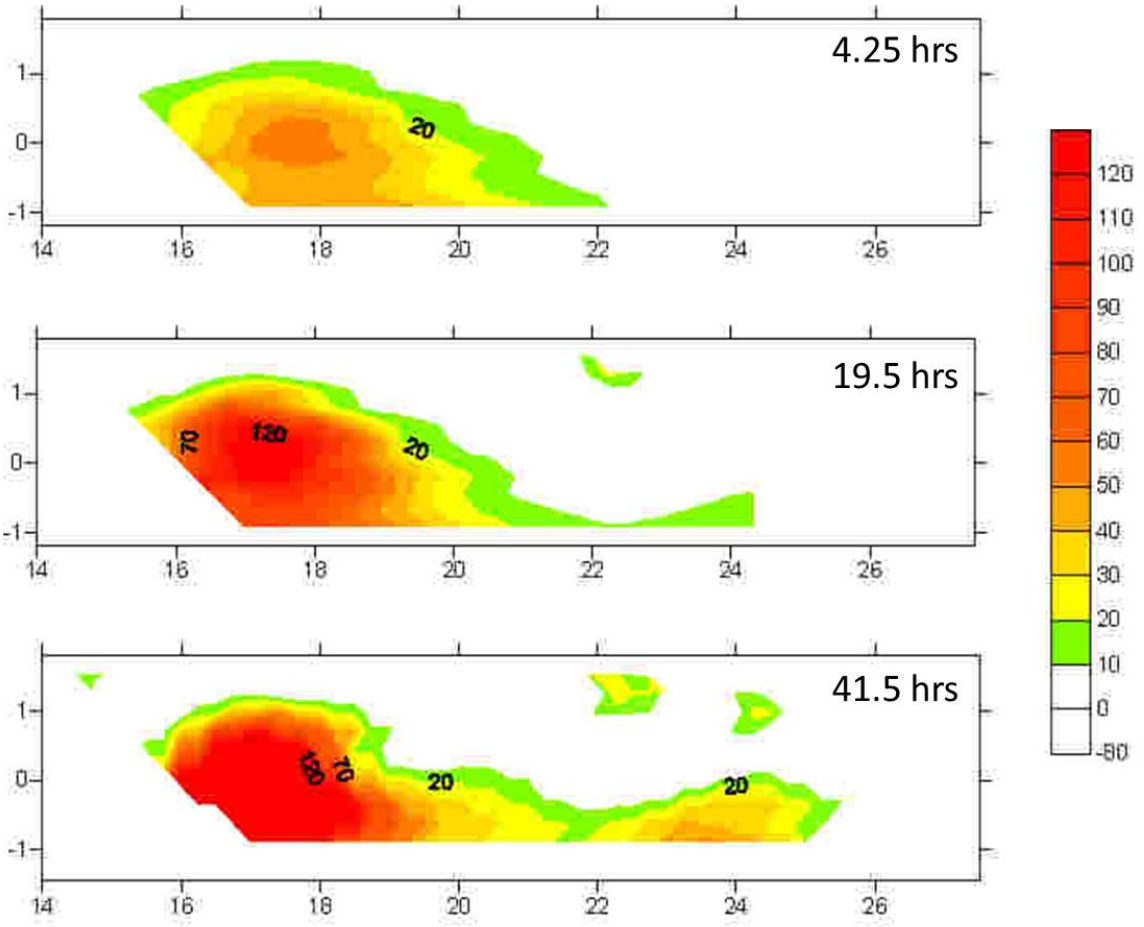

Figure 7.10. Vertical profile (y-axis is elevation in m) of percent difference in electrical resistivity of the downgradient lateral line (Figure 7.3) 3 m downgradient of the center of the 3 m by 3 m plot (left) and the 1 m by 1 m plot (right) of control area at the Barren Fork Creek site, July 13, 2011. Horizontal axis is distance along the electrical resistivity line in m. Time is the elapsed time from the onset of infiltration. The water table is located approximately at the bottom of each plot (-1 m).

7.4.4. Tension Infiltrometers

Tension infiltrometers confirmed the importance of macropore flow (Figure 7.11). Matrix (pore space less than or equal to 500 μm) infiltration was quantified with a tension of 6 cm and was one to two orders of magnitude lower than saturated infiltration rates (Figure 7.11). Macropore flow accounted for approximately 99% of the total infiltration at the Barren Fork Creek site, 85% to 87% at the Clear Creek site, and 97% to 99% at the Pumpkin Hollow site.

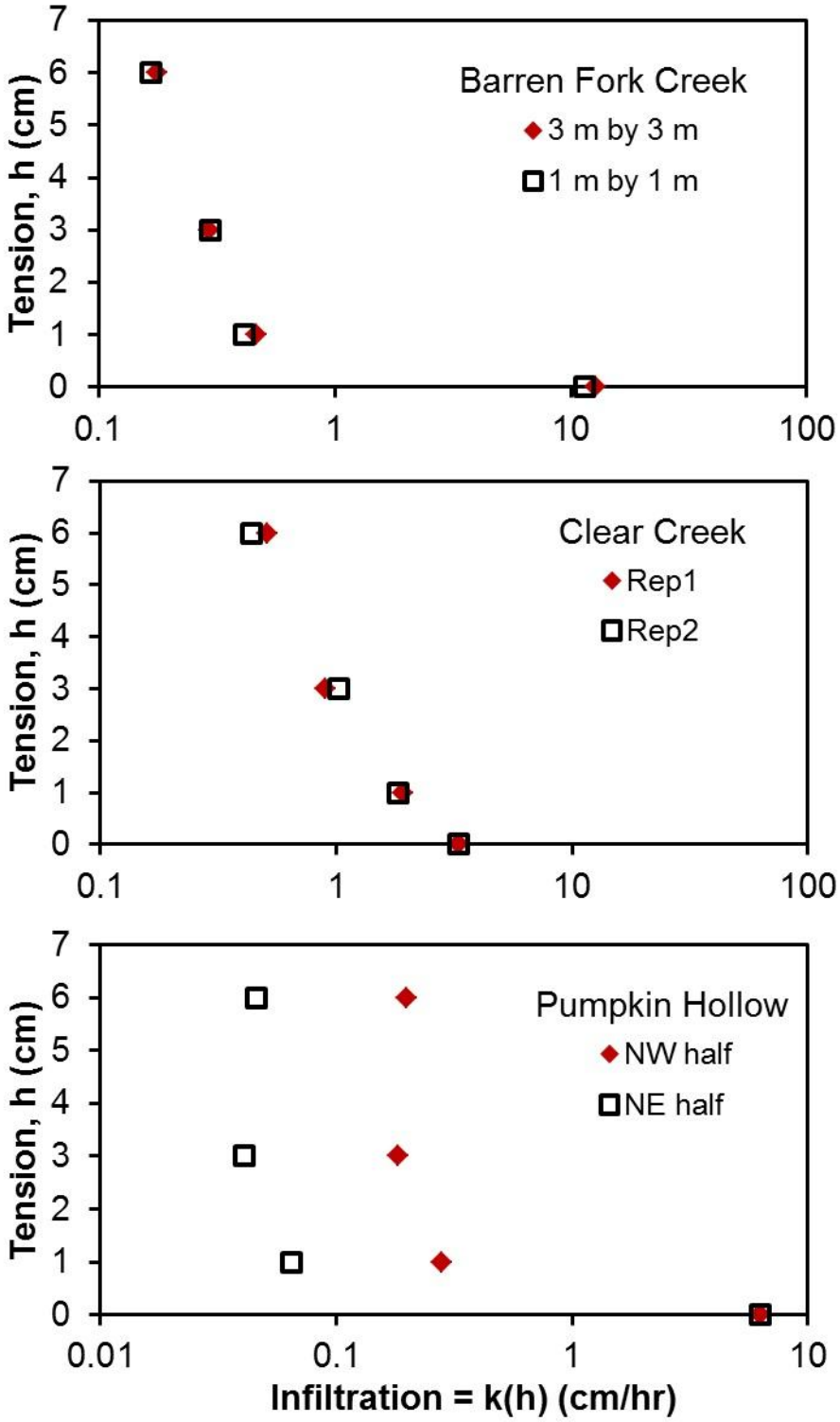

Figure 7.11. Infiltration rates based on infiltration plots for saturated infiltration (h = 0 cm) and unsaturated hydraulic conductivity (*k*) calculated from tension infiltrometer data. Locations included gravel outcrop plots at the Barren Fork Creek site, the 3 m by 3 m control plot at the Clear Creek site, and the 3 m by 3 m control plot at the Pumpkin Hollow site.

7.4.5. Macropore Excavation

The importance of macropore flow was observed visually (Figure 7.12a) at the Barren Fork Creek site during a 10 m by 10 m infiltration experiment (Heeren, 2012, unpublished data). The macropore was first detected audibly as water flowed into the hole, which was approximately 4 to 5 cm in diameter. After completion of the plot scale infiltration experiment, infiltration into that single macropore was quantified as 20 to 30 L/min under a constant head of 4 cm (the maximum head on the macropore during plot scale infiltration). After the soil profile had drained, the macropore was filled with two cans of expandable foam and allowed to harden. Excavation revealed that the macropore descended vertically to a depth of 1.0 m before proceeding laterally 15 cm (Figure 7.12b). The soil profile transitioned from silt loam to gravel at a depth of 0.7 m. Few animals would burrow into gravel, but the taproot of a large tree would be expected to proceed into the gravel layer. One hypothesis is that the macropore is an abandoned fence post hole, although fence posts aren't typically installed to that depth. The diameter of the excavated macropore was up to 14 cm. It is unknown how much erosion occurred on the sidewalls of the macropore during infiltration experiments, although silt was observed to have been recently deposited at the bottom of the macropore. Another indicator of macropore flow was that the soil profile matrix was not as wet as expected after infiltration experiments (Figure 7.12b).

7.5. CONCLUSIONS

Plot scale experiments simulated field conditions more realistically compared to smaller infiltrometers and laboratory testing. Highly heterogeneous flow and transport indicated that the soils in floodplains of the Ozark ecoregion are highly complex and not homogeneous. Elevated chloride, RhWT, and P concentrations were observed in specific groundwater samples. Phosphorus concentrations reached 1.3 mg/L, showing that even a highly sorbing contaminant can be transported through the silt loam topsoil and the gravelly subsoils. This research

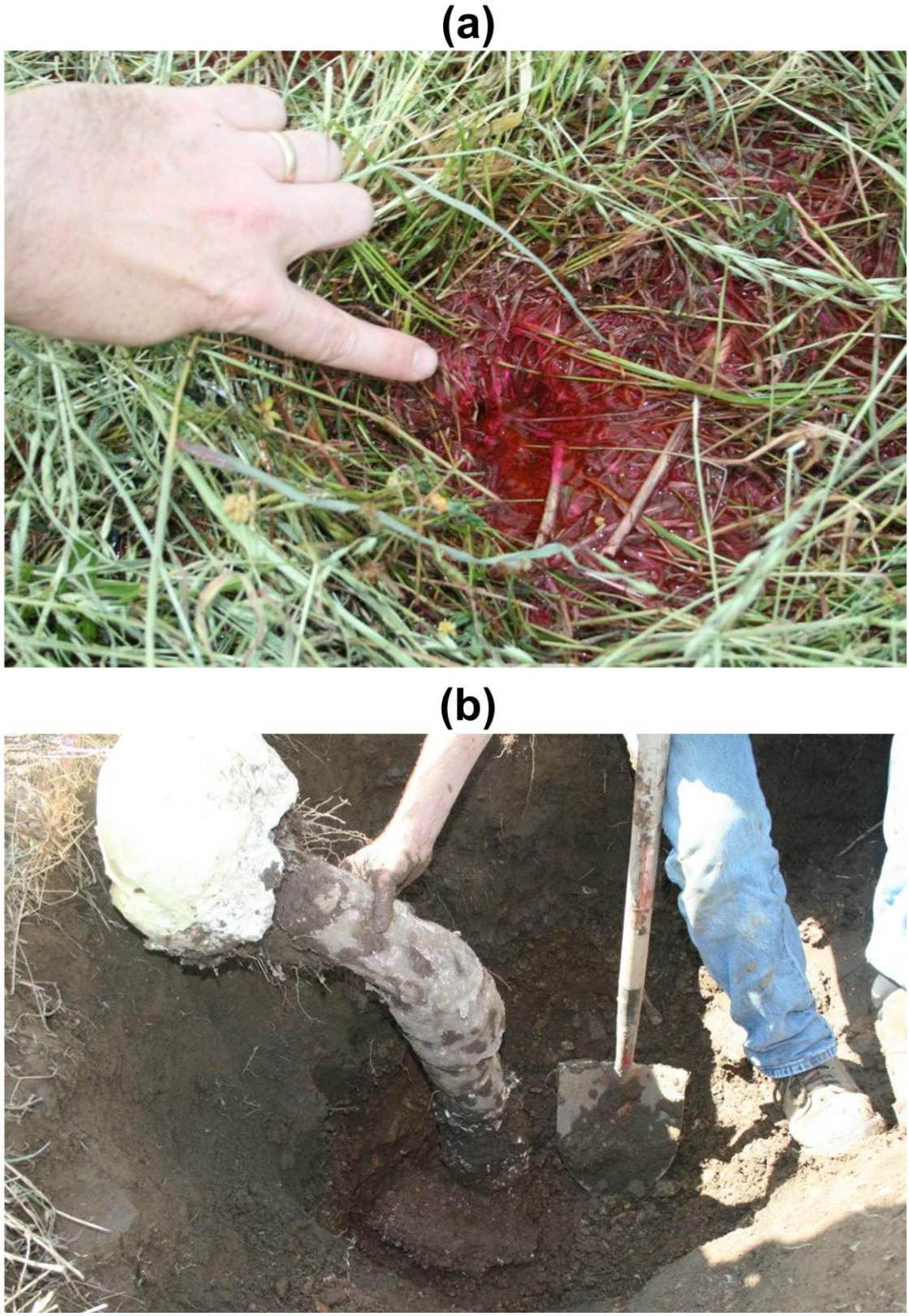

Figure 7.12. Large macropore at the Barren Fork Creek site observed during plot scale infiltration experiment (a) and subsequently filled with expandable foam and excavated (b).

highlighted the difference between the conceptual model of uniform piston infiltration and actual infiltration in field conditions. Since floodplains are well-connected to alluvial aquifers and streams in gravelly watersheds, a higher level of agricultural stewardship may be required for floodplains than upland areas. This has implications for the development of best management practices specifically for floodplains in the Ozark ecoregion due to their close proximately and connectedness to streams. Future research should include a more quantitative and rigorous analysis of the heterogeneity and scale effects in these data. Also, numerical modeling of the field experiments should be performed in order to estimate long term P loads to the alluvial aquifers.

7.6. ACKNOWLEDGEMENTS

The project described in this publication was supported by Grant/Cooperative Agreement Number G10AP00137 from the United States Geological Survey. Its contents are solely the responsibility of the authors and do not necessarily represent the official views of the USGS. This material was also developed under STAR Fellowship Assistance Agreement no. FP-917333 awarded by the U.S. Environmental Protection Agency (EPA). It has not been formally reviewed by EPA. The views expressed in this paper are solely those of the author, and EPA does not endorse any products or commercial services mentioned in this paper. Drs. Garey A. Fox, Daniel E. Storm, Todd Halihan, Chad J. Penn, Oklahoma State University, and Brian Haggard, University of Arkansas, contributed significantly to the project as PI and co-PI's. Peter Q. Storm, Oklahoma State University, contributed significantly to this work as a Freshman Research Scholar. The author also acknowledges Mr. Dan Butler, Mrs. Shannon Robertson, Dr. Bill Huff, and Mrs. Sara Boelkins for providing access to their alluvial floodplain properties. Finally, David A. Correll, Ronald B. Miller, Qualla J. Parman, and David T. Criswell, Oklahoma State Univeristy, are acknowledged for their assistance with field and lab work. Dr. Halihan has a managed conflict of interest with Oklahoma State University regarding the use of ERI developments.

REFERENCES

Addiscott, T. M., D. Brockie, J. A. Catt, D. G. Christian, G. L. Harris, K. R. Howse, N. A. Mirza, and T. J. Pepper. 2000. Phosphate losses through field drains in a heavy cultivated soil. *J. Environ. Qual.* 29: 522–532, doi: 10.2134/jeq2000.00472425002900020021x.

Akay, O., G. A. Fox, and J. Šimůnek. 2008. Numerical simulation of flow dynamics during macropore-subsurface drain interaction using HYDRUS. *Vad. Zone J.* 7(3): 909-918, doi: 10.2136/vzj2007.0148.

Akay, O., and G. A. Fox. 2007. Experimental investigation of direct connectivity between macropores and subsurface drains during infiltration. *Soil Sci. Soc. Am. J.* 71(5): 1600-1606.

Amoros, C., and G. Bornette. 2002. Connectivity and biocomplexity in waterbodies of riverine floodplains. *Freshwater Biology* 47(4): 761-776.

Andrews, W. J., M. F. Becker, S. J. Smith, and R. L. Tortorelli. 2009. Summary of Surface-Water Quality Data from the Illinois River Basin in Northeast Oklahoma, 1970-2007. Scientific Investigations Report 2009-5182. U.S. Geological Survey: Reston, Va.

Arnold, J. G., R. Srinivasan, R. S. Muttiah, and J. R. Williams. 1998. Large area hydrologic model development and assessment part 1: model development. *J. Am. Water Resourc. As.* 34: 73-89.

Bastian, M. 2011. Water quality credit trading: Does it make sense for the upper Illinois River Watershed? Arkansas Water Resources Center (AWRC) Annual Watershed and Research Conference, Fayetteville, Ark.

Bencala, K. E., and R. A. Walters. 1983. Simulation of solute transport in a mountain pool-and-riffile stream: A transient storage zone model. *Water Resour. Res* 19: 718-724.

Blackstock, R. B. 2003. Using computer models in court: Challenges for expert witnesses. ASAE Publication Number 701P1503. St. Joseph, Mich.: American Society of Agricultural and Biological Engineers.

Broberg, O., and G. Persson. 1988. Particulate and dissolved phosphorus forms in freshwater: Composition and analysis. *Hydrobiologia* 170: 61-90.

Brown, G. O., H. T. Hsieh, and D. A. Lucero. 2000. Evaluation of laboratory dolomite core sample size using representative elementary volume concepts. *Water Resour. Res.* 36(5): 1199-1207.

Brusseau, M. L. 1998. Multiprocess nonequilibrium and nonideal transport of solutes in porous media. In *Physical Nonequilibrium in Soils: Modeling and Application*, 63-82. H. M. Selim and L. Ma, eds. Chelsea, Mich.: Ann Arbor Press.

Bunte, K., and S. Abt. 2001. Sampling Surface and Subsurface Particle-Size Distributions in Wadable Gravel- and Cobble-Bed Streams for Analyses in Sediment Transport, Hydraulics, and Streambed Monitoring. USFS General Technical Report 74, USDA. Rocky Mtn. Res. Sta. Fort Collins, Colo.

Cardenas, M. B. 2009. Stream-aquifer interactions and hyporheic exchange in gaining and losing sinuous streams. *Water Resour. Res.* 45: W06429, doi: 10.1029/2008WR0007651.

Carlyle, G. C., and A. R. Hill. 2001. Groundwater phosphate dynamics in a river riparian zone: Effects of hydrologic flow paths, lithology, and redox chemistry. *J. Hydrol.* 247(3-4): 151-168.

Carsel, R. F., and R. S. Parrish. 1988. Developing joint probability distributions of soil water retention characteristics. *Water Resour. Res.* 24: 755-769.

Clark, G., D. K. Meuller, and M. A. Mast. 2000. Nutrient concentrations and yields in undeveloped stream basins of the United States. *J. Am. Water Res. Assoc.* 36(4): 849-860.

Cooper, A. B., C. M. Smith, and M. J. Smith. 1995. Effects of riparian set-aside on soil characteristics in an agricultural landscape: Implications for nutrient transport and retention. *Agric. Ecosyst. Environ.* 55(1): 61-67.

Cressie N. 1991. *Statistics for Spatial Data*. John Wiley and Sons: New York, N.Y.; 900.

Crowder, B., C. E. Young. 1988. Managing Farm Nutrients: Tradeoffs for Surface and Ground Water Quality. Agricultural Economic Report no. 583. USDA, Washington, D.C.

D'Angelo, D. J., J. R. Webster, S. V. Gregory, and J. L. Meyer. 1993. Transient storage in Appalachian and Cascade mountain streams as related to hydraulic characteristics. *J. N. Am. Benthol. Soc.* 12: 223-235.

Daniel, T. C., A. N. Sharpley, and J. L. Lemunyon. 1998. Agricultural phosphorus and eutrophication: A symposium overview. *J. Environ. Qual.* 27: 251-257, doi: 10.2134/jeq1998.00472425002700020002x.

Davis, R. K., S. Hamilton, and J. Van Brahana. 2005. *Escherichia coli* survival in mantled karst springs and streams, Northwest Arkansas Ozarks, USA. *J. Am. Water Res. Assoc.* 41: 1279-1287, doi: 10.1111/j.1752-1688.2005.tb03800.x.

de Jonge, L. W, D. Kjaergaard, and P. Moldrup. 2004. Colloids and colloid-facilitated transport of contaminants in soils: An introduction. *Vad. Zone J.* 3: 321-325, doi: 10.2136/vzj2004.0321.

DeLaune, P. B., P. A. Moore, Jr., D. K. Carman, A. N. Sharpley, B. E. Haggard, and T. C. Daniel. 2004. Development of a phosphorus index for pastures fertilized with poultry litter: Factors affecting phosphorus runoff. *J. Environ. Qual.* 33(6): 2183-2191.

DeLaune, P. B., B. E. Haggard, T. C. Daniel, I. Chaubey, and M. J. Cochran. 2006. The Eucha/Spavinaw phosphorus index: A court mandated index for litter management. *J. Soil Water Cons.* 61(2): 96-105.

Djodjic, F., B. Katarina, and L. Bergstrom. 2004. Phosphorus leaching in relation to soil type and soil phosphorus content. *J. Environ. Qual.* 33: 678–684, doi: 10.2134/jeq2004.0678, doi: 10.2134/jeq2004.0678.

Engle, B. 2003. Poultry Waste Generation and Land Application in the Illinois River Watershed and Phosphorus Loads to the Illinois River Watershed Streams and Rivers and Lake Tenkiller. Expert Report for *State of Oklahoma v. Tyson Foods, et al*.

EPA. 2003. Final Water Quality Trading Policy. Washington, D.C.: U.S. Environmental Protection Agency.

Fiedler, F. R., G. W. Frasier, J. A. Ramirez, and R. L. Ahuja. 2002. Hydrologic response of grasslands: Effects of grazing, interactive infiltration, and scale. *J. Hydrol. Eng.* 7(4): 293-301.

Fox, G. A., R. Malone, G. J. Sabbagh, and K. Rojas. 2004. Interrelationship of macropores and subsurface drainage for conservative tracer and pesticide transport. *J. Environ. Qual.* 33(6): 2281-2289.

Fox, G. A., R. Munoz-Carpena, and G. J. Sabbagh. 2010. Influence of flow concentration on parameter importance and prediction uncertainty of pesticide trapping by vegetative filter strips. *J. Hydrol.* 384: 164-173.

Fox, G. A., D. M. Heeren, R. B. Miller, A. R. Mittelstet, and D. E. Storm. 2011. Flow and transport experiments for a streambank seep originating from a preferential flow pathway. *J. Hydrol.* 403(3-4): 360-366.

Fuchs, J. W., G. A. Fox, D. E. Storm, C. J. Penn, and G. O. Brown. 2009. Subsurface transport of phosphorus in riparian floodplains: Influence of preferential flow paths. *J. Environ. Qual.* 38(2): 473-484.

Gachter, R., J. M. Ngatiah, and C. Stamm. 1998. Transport of phosphate from soil to surface waters by preferential flow. *Environ. Sci. Technol.* 32: 1865-1869, doi: 10.1021/es9707825.

Gotovac, H., Cvetkovic, V., and R. Andricevic. 2009. Flow and travel time statistics in highly heterogeneous porous media. *Water Resour. Res.* 45: W07402, doi: 1029/2008WR007168.

Gburek, W. J., E. Barberis, P. M. Haygarth, B. Kronvang, and C. Stamm. 2005. Phosphorus mobility in the landscape. In *Phosphorus: Agriculture and the Environment*, Agronomy Monograph No. 46. J. T. Sims and A. N. Sharpley, eds. Madison, Wis.: American Society of Agronomy.

Haggard, B. E. 2010. Phosphorus concentrations, loads, and sources within the Illinois River drainage area, Northwest Arkansas, 1997-2008. *J. Environ. Qual.* 39(6): 2113-2120.

Halihan, T., S. Paxton, I. Graham, T. Fenstemaker, and M. Riley. 2005. Post-remediation evaluation of a LNAPL site using electrical resistivity imaging. *J. Environ. Monit.* 7(4): 283-287.

Hart, D. R., Mulholland, P.J., Marzolf, E.R., Deangelis, D.L., and S. P. Hendricks. 1999. Relationships between hydraulic parameters in a small stream under varying flow and seasonal conditions. *Hydrol. Process.* 13: 1497-1510.

Harvey, J. W., B. J. Wagner, and K. E. Bencala. 1996. Evaluating the reliability of the stream tracer approach to characterize stream-subsurface water exchange. *Water Resour. Res.* 32: 2441-2451.

Haygarth, P. M., M. S. Warwick, and W. A. House. 1997. Size distribution of colloidal molybdate reactive phosphorus in river waters and soil solution. *Water Res.* 31: 439-448, doi: 10.1016/S0043-1354(96)00270-9.

Heathwaite, A. L., and R. M. Dil. 2000. Characterizing phosphorus loss in surface and subsurface hydrological pathways. *Sci. Total Environ.* 251-252: 523-538.

Heeren, D. M, R. B. Miller, G. A. Fox, D. E. Storm, T. Halihan, and C. J. Penn. 2010. Preferential flow effects on subsurface contaminant transport in alluvial floodplains. *T. ASABE* 53 (1): 127-136.

Heeren, D. M., G. A. Fox, R. B. Miller, D. E. Storm, A. R. Mittelstet, A. K. Fox, C. J. Penn, C.J., and T. Halihan. 2011. Stage-dependent transient storage of phosphorus in alluvial floodplains. *Hydrol. Process.*, 25(20): 3230-3243, doi: 10.1002/hyp.8054.

Heeren, D. M., G. A. Fox, and D. E. Storm. 2012. Berm method for quantification of infiltration and leaching at the plot scale in high conductivity soils. *J. Hydrol. Eng.* (in review).

Hively, W. D., P. Gerard-Marchant, and T. S. Steenhuis. 2006. Distributed hydrological modeling of total dissolved phosphorus transport in an agricultural landscape, part II: Dissolved phosphorus transport. *Hydrol. Earth Syst. Sci.* 10: 263-276, doi: 10.5194/hess-10-263-2006.

Hunt, B. W. 1995. *Fluid mechanics for Civil Engineers*. Christchurch, New Zealand: Dept. of Civil Engineering, University of Canterbury.

Kavvas, M. L., Karakas, A., 1995. On the stochastic theory of solute transport by unsteady and steady groundwater flow in heterogeneous aquifers. *J. Hydrol.* 179: 321-351.

Kleinman, P. J. A., A. N. Sharpley, A. M. Wolf, D. B. Beegle, and P. A. Moore, Jr. 2002. Measuring water-extractable phosphorus in manure as an indicator of phosphorus in runoff. *Soil Sci. Soc. Am. J.* 66(6): 1009-2015.

Kleinman, P. J. A., B. A. Needelman, A. N. Sharpley, and R. W. McDowell. 2004. Using soil phosphorus profile data to assess phosphorus leaching potential in manured soils. *Soil Sci. Soc. Am. J.* 67: 215-224, doi: 10.2136/sssaj2003.0215.

Kumar, M., C. J. Duffy, and K. M. Salvage. 2009. A second-order accurate, finite volume-based, integrated hydrologic modeling (FIHM) framework for simulation of surface and subsurface flow. *Vad. Zone J.* 8: 873-890.

Lacas, J.-G., M. Voltz, V. Gouy, N. Carluer, and J.-J. Gril. 2005. Using grassed strips to limit pesticide transfer to surface water: A review. *Agron. Sustain. Dev.* 25(2): 253-266.

Lai, J., and L. Ren. 2007. Assessing the size dependency of measured hydraulic conductivity using double-ring infiltrometers and numerical simulation. *Soil Sci. Soc. Am. J.*, 71(6): 1667-1675.

Lee, M., and K. R. Douglas-Mankin. 2011. An environmental trading ratio for water quality trading. *T. ASABE* 54(5): 1599-1614.

Maguire, R. O., and J. T. Sims. 2002. Soil testing to predict phosphorus leaching. *J. Environ. Qual.* 31: 1601-1609.

Malard, F., K. Tockner, M. J. Dole-Oliver, and J. V. Ward. 2002. A landscape perspective of surface-subsurface hydrological exchanges in river corridors. *Freshwater Biol.* 47: 621-640, doi: 10.1046/j.1365-2427.2002.00906.x.

Massman, J. W. 2003. Implementation of infiltration ponds research. Final Research Report. Olympia, Wash.: Washington State Transportation Commission.

McBride, C. 2011. Oklahoma v. Tyson: Playing chicken with environmental cleanup. *Ecol. Law Quarterly* 38: 603-609.

McCarty, G., and J. Angier. 2001. Impact of preferential flow pathways on ability of riparian wetlands to mitigate agricultural pollution. In *Proc. 2nd Intl. Symp. on Preferential Flow: Water Movement and Chemical Transport in the Environment*, 53-56. D. Bosch and K. King, eds. St. Joseph, Mich.: ASABE.

McCorley, J., M. McPhail, T. Halihan, and S. Paxton. 2003. Direct push electrical resistivity tomography for evaluation of an LNAPL plume. In *GSA Abstracts with Programs*. Boulder, Colo.: Geological Society of America.

McKay, M. D., 1995. Evaluating prediction uncertainty. NUREG/CR-6311. Los Alamos, N.M.: U.S. Nuclear Regulatory Commission and Los Alamos National Laboratory.

McNeill, J. D. 1980. Electrical conductivity of soils and rocks. Technical Note TN-5. Mississauga, Ontario, Canada: Geonics, Ltd.

Midgley, T. L., G. A. Fox, and D. M. Heeren. 2012. Evaluation of the Bank Stability and Toe Erosion Model (BSTEM) for predicting lateral retreat on composite streambanks. *Geomorphology* 145-146: 107-114, doi: 10.1016/j.geomorph.2011.12.044.

Miller, R. B., D. M. Heeren, G. A. Fox, D. E. Storm, T. Halihan, and A.R. Mittelstet. 2010. Geophysical mapping of preferential flow paths across multiple floodplains. ASABE Paper No. 1008730. St. Joseph, Mich.: ASABE.

Miller, R. B., D. M. Heeren, G. A. Fox, D. E. Storm, and T. Halihan. 2011. Design and application of a direct-push vadose zone gravel permeameter. *Ground Water* 49(6): 920-925.

Miller, R. B. 2012. Hydrogeophysics of gravel-dominated alluvial floodplains in eastern Oklahoma. PhD diss. Stillwater, Okla.: Oklahoma State University, Department of Biosystems and Agricultural Engineering.

Mittelstet, A. R., D. M. Heeren, D. E. Storm, G. A. Fox, M. J. White, and R. B. Miller. 2011. Comparison of subsurface and surface runoff phosphorus transport rates in alluvial floodplains. *Agric. Ecosyst. Environ.* 141: 417-425.

Morrice, J. A., H. M. Valett, C. N. Dahm, and M. E. Campana. 1997. Alluvial characteristics, groundwater-surface water echange and hydrologic retention in headwater streams. *Hydrol. Process.* 11: 253-267.

Murphy J., and J. P. Riley. 1962. A modified single solution method for the determination of phosphate in natural waters. *Anal. Chim. Acta* 27: 31-36.

Naiman, R. J., H. Decamps, and M. E. McClain. 2005. Catchments and the physical template. In *Riparia: Ecology, Conservation, and Management of Streamside Communities*, 19-48. Boston, Mass.: Elsevier Academic Press.

National Research Council (NRC), Committee on Hydrologic Science (COHS). 2004. Groundwater Fluxes across Interfaces. Washington, D.C.: The National Academies Press.

Natural Resources Conservation Service. 2012. Web Soil Survey (WSS). Washington, D.C.: USDA-NRCS. Available at: http://websoilsurvey.nrcs.usda.gov/. Accessed February, 2012.

Neill H., M. Gutierrez, and T. Aley. 2003. Influences of agricultural practices on water quality of Tumbling Creek cave stream in Taney County, Missouri. *Environ. Geol.* 45: 550-559, doi: 10.1007/s00254-003-0910-2.

Nelson, N. O., J. E. Parsons, and R. L. Mikkelson. 2005. Field-scale evaluation of phosphorus leaching in acid sandy soils receiving swine waste. *J. Environ. Qual.* 34: 2024-2035, doi: 10.2134/jeq2004.0445.

Oklahoma Water Resources Board (OWRB). 2010. Oklahoma's Water Quality Standards 785:45. Available at: http://www.owrb.ok.gov/util/rules/pdf_rul/RulesCurrent2010/Ch45.pdf.

Packman, A. I., and K. E. Bencala. 2000. Modeling surface-subsurface hydrological interactions. In *Streams and Ground Waters*, 46-77. J. B. Jones and P. J. Mulholland, eds. San Diego, Calif.: Academic Press.

Pellerin, L. 2002. Applications of electrical and electromagnetic methods for environmental and geotechnical investigations. *Surv. Geophys.* 23(2-3): 101-132.

Pierzynski, G. M., R. W. McDowell, and J. T. Sims. 2005. Chemistry, cycling, and potential movement of inorganic phosphorus in soils. In *Phosphorus: Agriculture and the Environment*, Agronomy Monograph No. 46. J. T. Sims and A. N. Sharpley, eds. Madison, Wis.: American Society of Agronomy.

Pittman, H. M. 2011. A legal perspective: Agriculture, water quality, and the Illinois River. In *Proceedings of the Annual Watershed and Research Conference*. Fayetteville, Ark.: Arkansas Water Resources Center (AWRC).

Poletika, N. N., P. N. Coody, G. A. Fox, G. J. Sabbagh, S. C. Dolder, and J. White. 2009. Chlorpyrifos and atrazine removal from runoff by vegetated filter strips: Experiments and predictive modeling. *J. Environ. Qual.* 38(3): 1042-1052.

Polyakov, V., A. Fares, and M. H. Ryder. 2005. Precision riparian buffers for the control of nonpoint-source pollutant loading into surface water: A review. *Environ. Rev.* 13(3): 129-144.

Poole, G. C., R. J. Naiman, J. Pastor, and J. A. Stanford. 1997. Uses and limitations of ground penetrating RADAR in two riparian systems. In *Groundwater/Surface Water Ecotones: Biological and Hydrological Interactions and Management Options*, 140-148. J. Gibert, J. Mathieu, and F. Fournier, eds. Cambridge, U.K.: Cambridge University Press.

Poole, G. C., J. A. Stanford, C. A. Frissell, and S. W. Running. 2002. Three-dimensional mapping of geomorphic controls on flood-plain hydrology and connectivity from aerial photos. *Geomorphology* 48(4): 329-347.

Poole, G. C., J. A. Standford, S. W. Running, and C. A. Frissell. 2006. Multiscale geomorphic drivers of groundwater flow paths: subsurface hydrologic dynamics and hyporheic habitat diversity. *J. N. Am. Benthol. Soc.* 25(2): 288-303.

Popov, V. H., P. S. Cornish, and H. Sun. 2005. Vegetated biofilters: The relative importance of infiltration and adsorption in reducing loads of water-soluble herbicides in agricultural runoff. *Agric. Ecosyst. Environ.* 114(2-4): 351-359.

Pote, D.H., T. C. Daniel, and P. B. DeLaune. 2009. Total phosphorus and total dissolved phosphorus in water samples. In *Methods of Phosphorus Analysis for Soils, Sediments, Residuals, and Waters*, 113-114. J. L. Kovar and G. M. Pierzynski, eds. Blacksburg, Va.: SERA-IEG 17, Virginia Tech University,

Pryor, M., J. Inhofe, T. Coburn, J. Boozman, D. Boren, and S. Womack. 2011. Letter to EPA Administrator Lisa Jackson regarding modeling for TMDL development in the Illinois River Watershed, dated December 9, 2001.

Reichenberger, S., M. Bach, A. Skitschak, and H.-G. Frede. 2007. Mitigation strategies to reduce pesticide inputs into ground- and surface water and their effectiveness: A review. *Sci. Total Environ.* 384: 1-35.

Ribaudo, M. 2008. Creating markets for environmental stewardship: Potential benefits and problems. *Amber Waves* 6(4): 24-31.

Robinson, D. A., A. Binley, N. Crook, F. D. Day-Lewis, T. P. A. Ferré, V. J. S. Grauch, R. Knight, M. Knoll, V. Lakshmi, R. Miller, J. Nyquist, L. Pellerin, K. Singha, and L. Slater. 2008. Advancing process-based watershed hydrological research using near-surface geophysics: A vision for, and review of, electrical and magnetic geophysical methods. *Hydrol. Proc.* 22(18): 3604-3635.

Romeis, J. J., C. R. Jackson, L. M. Risse, A. N. Sharpley, and D. E. Radcliffe. 2011. Hydrologic and phosphorus export behavior of small streams in commercial poultry-pasture watersheds. *J. Am. Water Res. Assoc.* 47(2): 367-385, doi: 10.1111/j.1752-1688.2011.00521.x.

Rooij, G. H., and F. Stagnitti. 2000. Spatial variability of solute leaching: Experimental validation of a quantitative parameterization. *Soil Sci. Soc. Am. J.* 64: 499-504.

Sabbagh, G. J., G. A. Fox, A. Kamanzi, B. Roepke, and J. Z. Tang. 2009. Effectiveness of vegetative filter strips in reducing pesticide loading: Quantifying pesticide trapping efficiency. *J. Environ. Qual.* 38(2): 762-771.

Sarker, R., S. Dutta, and S. Panigrahy. 2008. Effect of scale on infiltration in a macropore-dominated hillslope. *Curr. Sci. India* 94(4): 490-494.

Sauer, T. J., and S. D. Logsdon. 2002. Hydraulic and physical properties of stony soils in a small watershed. *Soil Sci. Soc. Am. J.* 66(6): 1947-1956.

Sauer, T. J., S. D. Logsdon, J. Van Brahana, and J. F. Murdoch. 2005. Variation in infiltration with landscape position: Implications for forest productivity and surface water quality. *Forest Ecol. Manag.* 220: 118-127.

Schroeder, P. D., D. E. Radcliffe, and M. L. Cabrera. 2004. Rainfall timing and poultry litter application rate effects on phosphorus loss in surface runoff. *J. Environ. Qual.* 33(6): 2201-2209.

Scott, H.D. 2000. *Soil Physics: Agricultural and Environmental Applications*. Ames, Iowa: Iowa State University Press.

Sharpley, A. N., T. Daniel, T. Sims, J. Lemunyon, R. Stevens, and R. Parry. 2003. *Agricultural Phosphorus and Eutrophication*. 3rd ed. ARS-149. Washington, D.C.: USDA Agricultural Research Service.

Sims, J.T., R. R. Simard, and B. C. Joern. 1998. Phosphorus loss in agricultural drainage: Historical perspective and current research. *J. Environ. Qual.* 27: 277-293.

Sims, J. T., and A. N. Sharpley. 2005. *Phosphorus: Agriculture and the Environment*. Agronomy Monograph No. 46. Madison, Wis.: ASA-CSSA-SSSA.

Šimůnek, J., M. Th. van Genuchten, and M. Šejna. 2006. The HYDRUS software package for simulating two- and three-dimensional movement of water, heat, and multiple solutes in variably-saturated media, 241. Technical Manual, Version 1.0. Prague, Czech Republic: PC Progress.

Sisson, J. B., and P. J. Wierenga. 1981. Spatial variability of steady-state infiltration rates as a stochastic process. *Soil Sci. Soc. Am. J.* 45: 699-704.

Soerens, T. S., E. H. Fite, III, and J. Hipp. 2003. Water quality in the Illinois River: Conflict and cooperation between Oklahoma and Arkansas. Diffuse Pollution Conference Paper. Dublin, Ireland: University College Dublin.

Soil Science Society of America. 2008. Glossary of soil science terms. Madison, Wis.: SSSA.

Stamm C., H. Flühler, R. Gächter, J. Leuenberger, and H. Wunderli. 1998. Preferential transport of phosphorus in drained grassland soils. *J. Environ. Qual.* 27: 515-522.

Stanford, J. A., and J. V. Ward. 1992. Management of aquatic resources in large catchments: Recognizing interaction between ecosystem connectivity and environmental disturbance. In *Watershed Management*, 91-124. R. J. Naiman, ed. New York, N.Y.: Springer-Verlag.

Stofleth, J. M., F. D. Shields, Jr., and G. A. Fox. 2008. Hyporheic and total storage exchange in small sand-bed streams. *Hydrol. Proc.* 22: 1885-1894.

Storm, D. E., M. White, M. D. Smolen, and H. Zhang. 2001. Modeling Phosphorus Loading for the Lake Eucha Basin. Final report. Stillwater, Okla.: Oklahoma State University, Department of Biosystems and Agricultural Engineering.

Storm, D. E., M. J. White, and M. D. Smolen. 2006. Illinois River upland and in-stream phosphorus modeling. Final report. Stillwater, Okla.: Oklahoma State University, Department of Biosystems and Agricultural Engineering.

Storm, D. E., M. J. White, M. D. Smolen, H. Zhang, and T. Gibson. 2007. Monitoring Edge of Field P Loss to Validate P Loss Index for the Spavinaw Creek Watershed. Final report submitted to the Oklahoma Conservation Commission. Stillwater, Okla.: Oklahoma State University, Department of Biosystems and Agricultural Engineering.

Storm, D. E., P. R. Busteed, A. R. Mittlestet, and M. J. White. 2010. Hydrologic modeling of the Oklahoma/Arkansas Illinois River basin using SWAT 2005. Final report. Stillwater, Okla.: Oklahoma State University, Department of Biosystems and Agricultural Engineering.

Tellam, J. H., and D. N. Lerner. 2009. Management tools for the river-aquifer interface. *Hydrol. Proc.* 23(15): 2267-2274.

Thomas, G. W., and R. E. Phillips. 1979. Consequences of water movement in macropores. *J. Environ. Qual.* 8(2): 149-152.

Thompson, C. A., and A. M. S. McFarland. 2010. Effects of surface and groundwater interactions on phosphorus transport within streambank sediments. *J. Environ. Qual.* 39: 548-557, doi: 10.2134/jeq2009.0313.

Tortorelli, R. L., and B. E. Pickup. 2006. Phosphorus concentrations, loads, and yields in the Illinois River basin, Arkansas and Oklahoma, 2000-2004. USGS Scientific Investigations Report 2006-5175. Reston, Va.: U.S. Geological Survey.

Turner, B. L., and P. M. Haygarth. 2000. Phosphorus forms and concentrations in leachate under four grassland soil types. *Soil Sci. Soc. Am. J.* 64(3): 1090-1099.

Ulen, B. 1999. Leaching balances of phosphorus and other nutrients in lysimeters after application of organic manures or fertilizers. *Soil Use Manage.* 15: 56-61.

U.S. EPA (Environmental Protection Agency). 2009. Pathogen TMDLs for Clear Creek in Arkansas Planning Segment 3J. Dallas, Tex.: U.S. EPA Region 6, Water Quality Protection Division.

USDA. 1970. Soil Survey: Cherokee and Delaware Counties, Oklahoma. Washington, D.C.: USDA Soil Conservation Service.

USDA. 2008. USDA-NRCS geospatial data gateway. Salt Lake City, Utah: USDA Farm Service Agency (FSA), Aerial Photography Field Office (APFO). Available at: http://datagateway.nrcs.usda.gov. Accessed 28 July 2009.

Vadas, P. A., M. S. Srinivasan, P. J. A. Kleinman, J. P. Schmidt, and A. L. Allen. 2007. Hydrology and groundwater nutrient concentrations in a ditch-drained agro-ecosystem. *J. Soil Water Conserv.* 62: 178-188.

van Genuchten, M. Th. 1980. A closed-form equation for predicting the hydraulic conductivity of unsaturated soils. *Soil Sci. Soc. Am. J.* 44: 892–898.

Vanek, V. 1993. Transport of groundwater-borne phosphorus to Lake Bysjon, South Sweden. *Hydrobiologia* 251: 211-216.

Warren, D. M. 2003. City of Tulsa v. Tyson Foods: CERCLA comes to the Farm—but did arranger liability come with it? *Arkansas Law Review* 59(1): 169-197.

Wentworth, C. K. 1922. A scale of grade and class terms for classic sediments. *J. Geol.* 30(5): 377-392.

White, M. J., D. E. Storm, M. D. Smolen, and H. Zhang. 2009. Development of a quantitative pasture phosphorus management tool using the SWAT model. *J. Am. Water Resourc. As.* 45: 397-406.

White, M. J., D. E. Storm, P. R. Busteed, M. D. Smolen, H. Zhang, and G. A. Fox. 2010. A quantitative phosphorus loss assessment tool for agricultural fields. *Environ. Model. Softw.* 25: 1121-1129.

Wilson, G. V., F. E. Rhoton, and H. M. Selim. 2004. Modeling the impact of ferrihydrite on adsorption-desorption of soil phosphorus. *Soil Sci.* 169(4): 271-281.

Worman, A., A. I. Packman, H. Johansson, and K. Jonsson. 2002. Effect of flow-induced exchange in hyporheic zones on longitudinal transport of solutes in streams and rivers. *Water Resour. Res.* 38(1): 1001, doi:10.1029/2001WR000769.

Wroblicky, G. W., M. E. Campana, H. M. Valett, and C. N. Dahm. 1998. Seasonal variation in surface-subsurface water exchange and lateral hyporheic area of two stream-aquifer systems. *Water Resour. Res.* 34: 317-328.

Yandle, B. 2008. Markets for water quality. *Property and Environment Research Center (PERC) Reports* 26(3): 14-17.

Zhang, R. 1997. Determination of soil sorptivity and hydraulic conductivity from the disk infiltrometer. *Soil Sci. Soc. Am. J.* 61: 1024-1030.

Zarnetske, J. P., M. N. Gooseff, T. R. Brosten, J. H. Bradford, J. P. McNamara, and W. B. Bowden. 2007. Transient storage as a function of geomorphology, discharge, and permafrost active layer conditions in Arctic tundra streams. *Water Resour. Res.* 43: W07410, doi:10.1029/2005WR004816.

APPENDIX

BACKGROUND ELECTRICAL RESISTIVITY MAPPING OF THE CLEAR CREEK FLOODPLAIN SITE

The Clear Creek alluvial floodplain site was located just west of Fayetteville, AR in the Arkansas River Basin and flows into the Illinois River (Figure 7.1, latitude: 36.13°, longitude: 94.24°). The total drainage area was 199 km^2 for the entire watershed. Land use in the basin was 36% pasture, 34% forest, 27% urban and 3% other. Soils were loamy and silty, deep, moderately well drained to well drained (U.S. EPA, 2009), and generally contained less chert or gravel than the Barren Fork Creek or Pumpkin Hollow floodplain sites. Thickness of the top loam layer ranged from 0.3 to 2 m, with dry bulk densities ranging from 1.5 to 1.7 g cm^{-3}. A fourth order stream with a flow of approximately 0.5 m^3 s^{-1} at the study site, the area of the watershed above that point was 101 km^2. The land use in the study area was pasture and consisted of Razort gravelly loam soils.

Vertical electrical resistivity profiles were collected at the floodplain site to characterize the heterogeneity of the unconsolidated floodplain sediments. Electrical resistivity imaging (ERI) is based on measuring the electrical properties of near-surface earth materials (McNeill, 1980), which vary with grain size, pore-space saturation, pore water solute content, and electrical properties of the minerals. The electrical behavior of earth materials is controlled by Ohm's law,

in which current is directly proportional to voltage and inversely proportional to resistance. Generally, electrical current travels readily in solute-rich pore water and poorly in air. In addition, cations adsorbed to soil particle surfaces reduce resistivity. Clay particles have a large surface area per volume and thus have generally lower resistivity (1 to 100 Ω-m) compared to sands or gravels (10 to 800 Ω-m), which are lower than limestone bedrock (McNeill, 1980).

ERI data were collected using a SuperSting R8/IP Earth Resistivity Meter (Advanced GeoSciences Inc., Austin, Tex.) with 56-electrode arrays (Figure A.1). The profiles employed electrode spacings of 1 to 1.5 m with an associated depth of investigation of approximately 13 m, which included the vadose zone, alluvial aquifer, and bedrock. The resistivity sampling with the SuperSting R8/IP, and subsequent inversion utilized a proprietary routine devised by Halihan et al. (2005), which produced higher resolution images than conventional techniques. The ERI resistivity data were interpolated into grids and contoured using Surfer 8 (Golden Software, Inc., Golden, CO). Inverted and interpolated resistivity data were termed "ERI profiles" (Figures A.2 to Appendix.13) as opposed to "ERI pseudosections", which were the raw resistivity measurements as collected in the field.

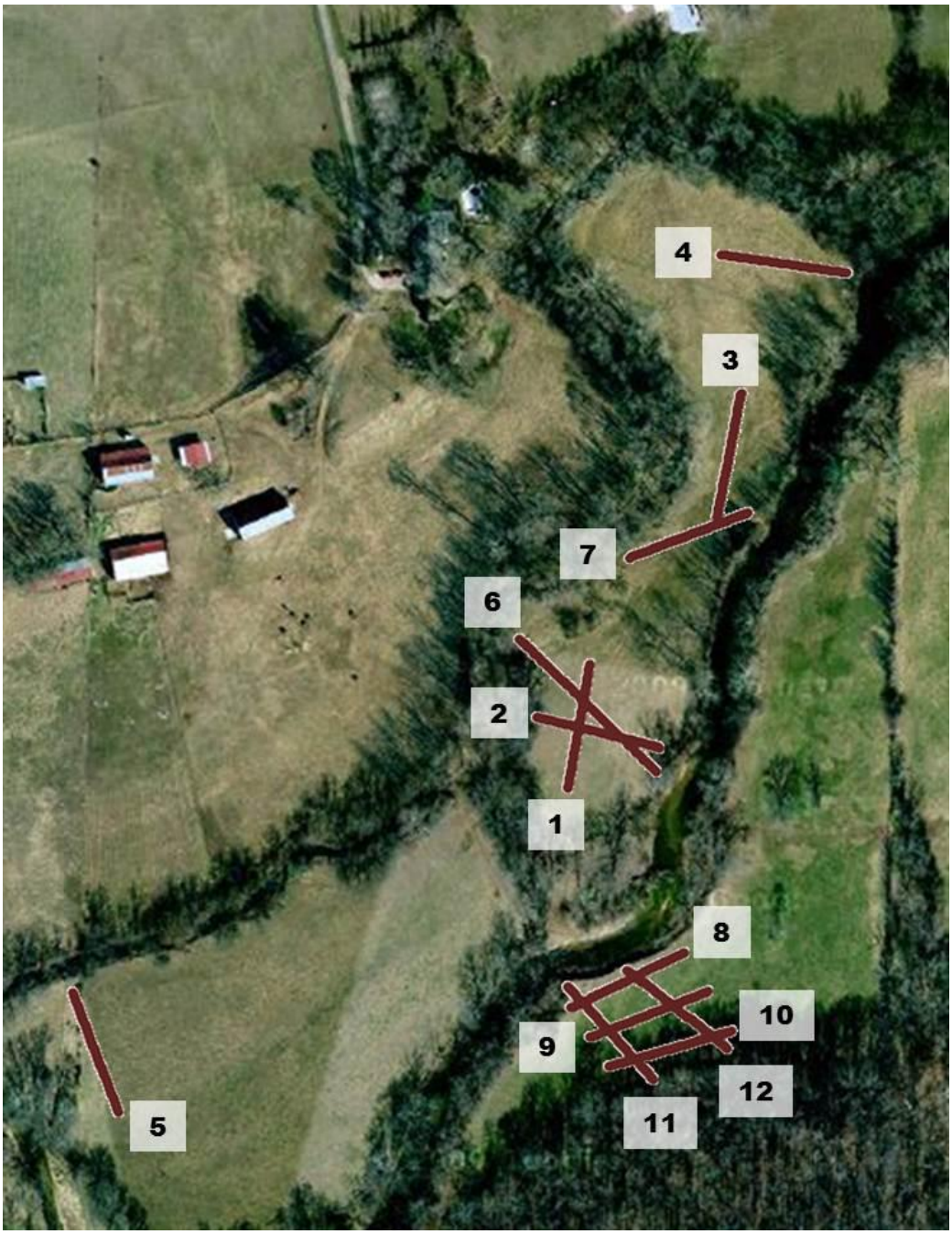

Figure A.1. Locations of vertical electrical resistivity profiles at the Clear Creek alluvial floodplain site.

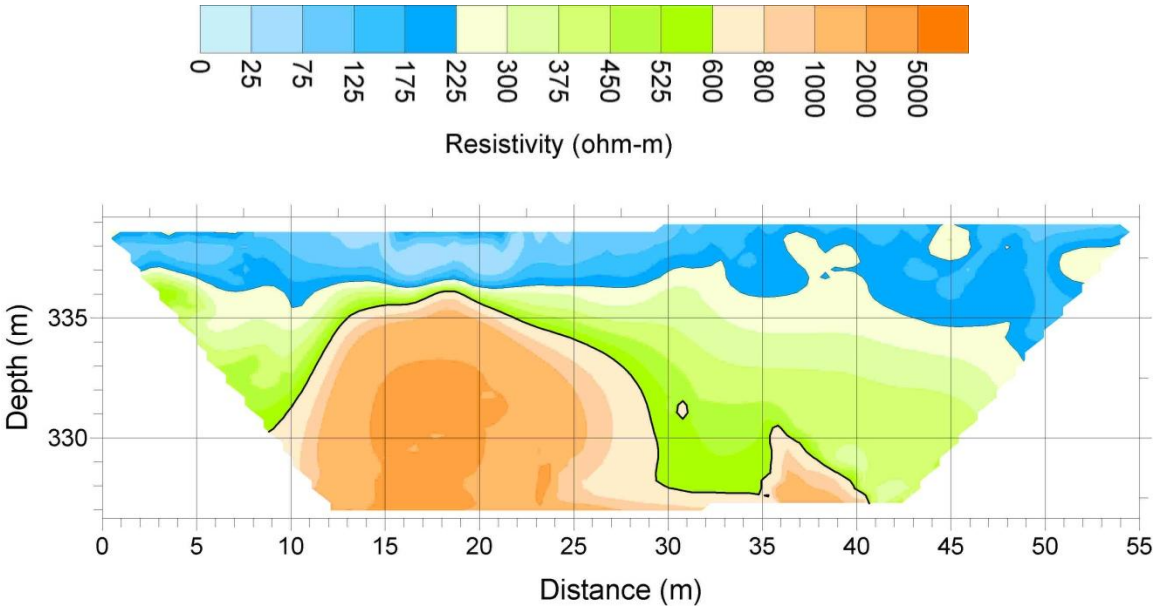

Figure A.2. Electrical resistivity profile 1 at the Clear Creek alluvial floodplain site, which runs from south (left) to north (right). See Figure A.1 for location of the profile.

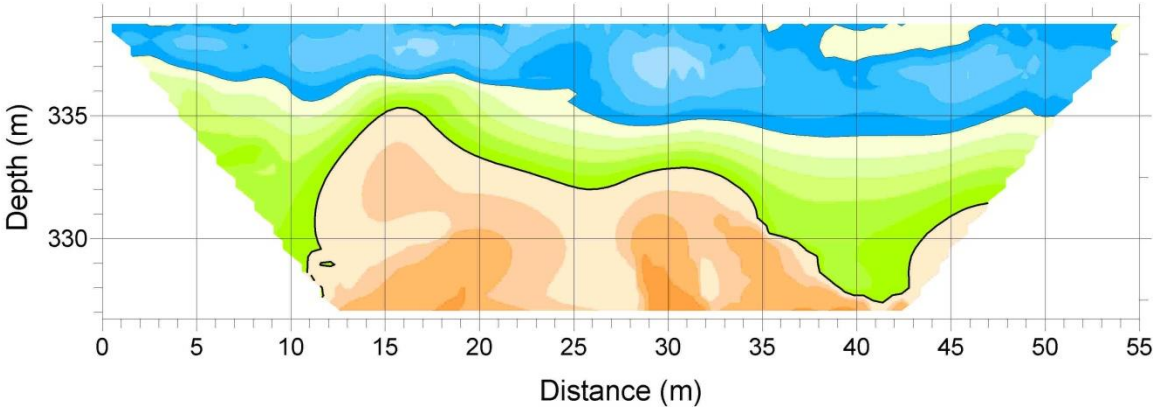

Figure A.3. Electrical resistivity profile 2 at the Clear Creek alluvial floodplain site, which runs from west (left) to east (right). See Figure A.1 for location of the profile.

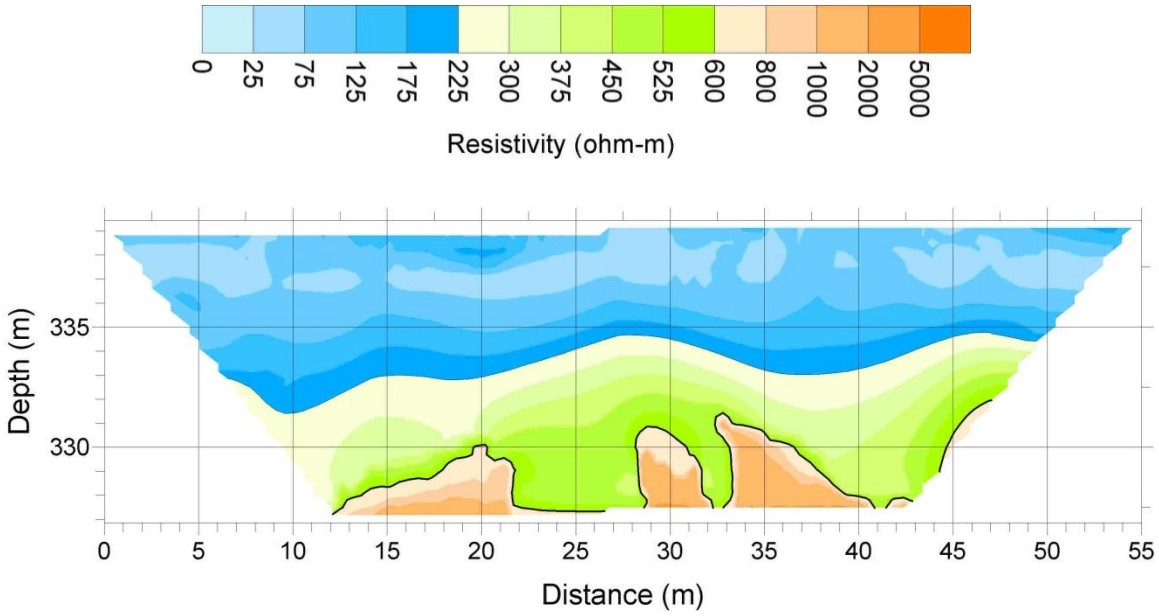

Figure A.4. Electrical resistivity profile 3 at the Clear Creek alluvial floodplain site, which runs from south (left) to north (right). See Figure A.1 for location of the profile.

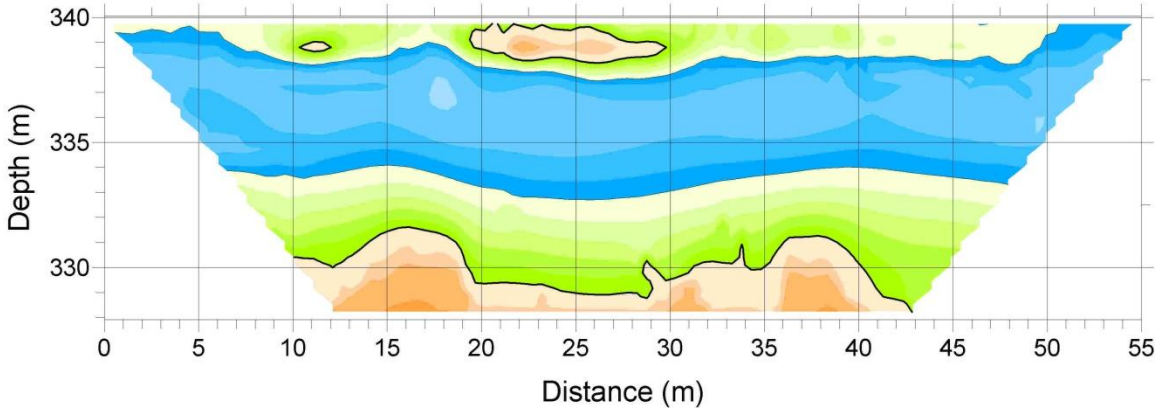

Figure A.5. Electrical resistivity profile 4 at the Clear Creek alluvial floodplain site, which runs from west (left) to east (right). See Figure A.1 for location of the profile.

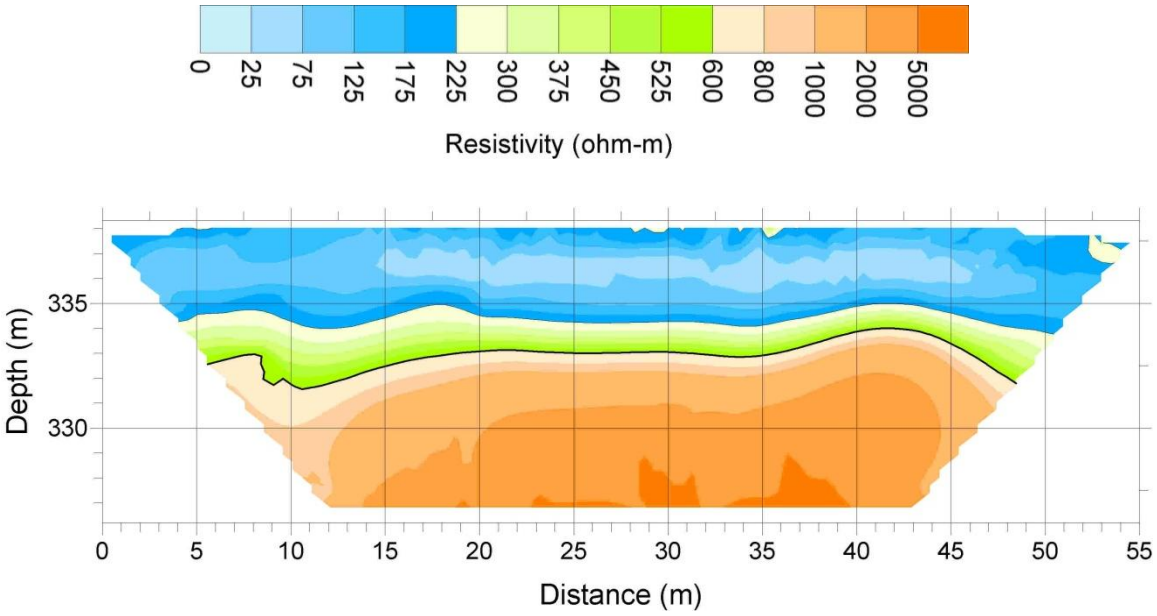

Figure A.6. Electrical resistivity profile 5 at the Clear Creek alluvial floodplain site, which runs from south (left) to north (right). See Figure A.1 for location of the profile.

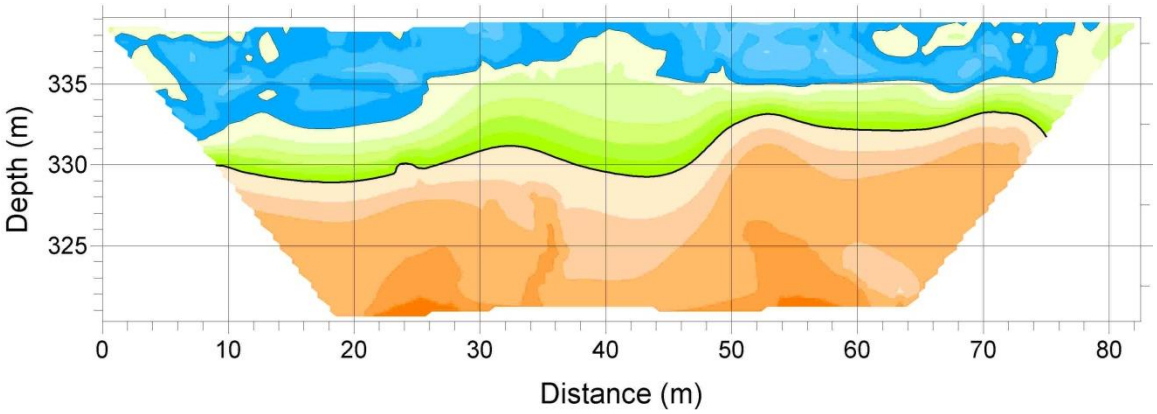

Figure A.7. Electrical resistivity profile 6 at the Clear Creek alluvial floodplain site, which runs from northwest (left) to southeast (right). See Figure A.1 for location of the profile. Profile 6 was the only one to use an electrode spacing of 1.5 m instead of 1 m.

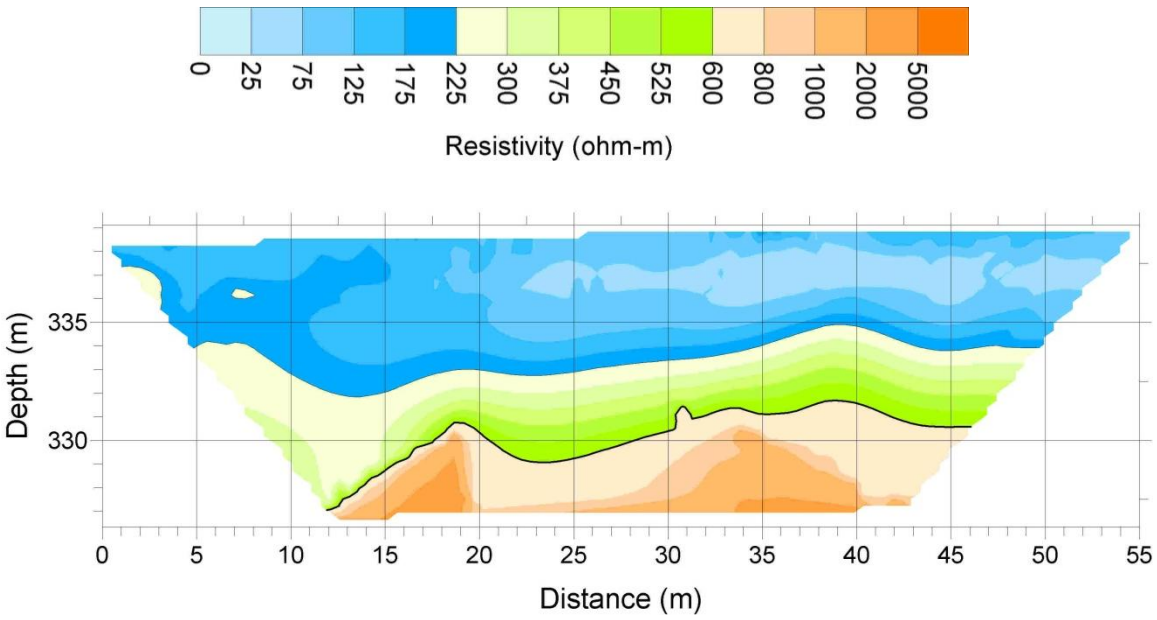

Figure A.8. Electrical resistivity profile 7 at the Clear Creek alluvial floodplain site, which runs from west (left) to east (right). See Figure A.1 for location of the profile.

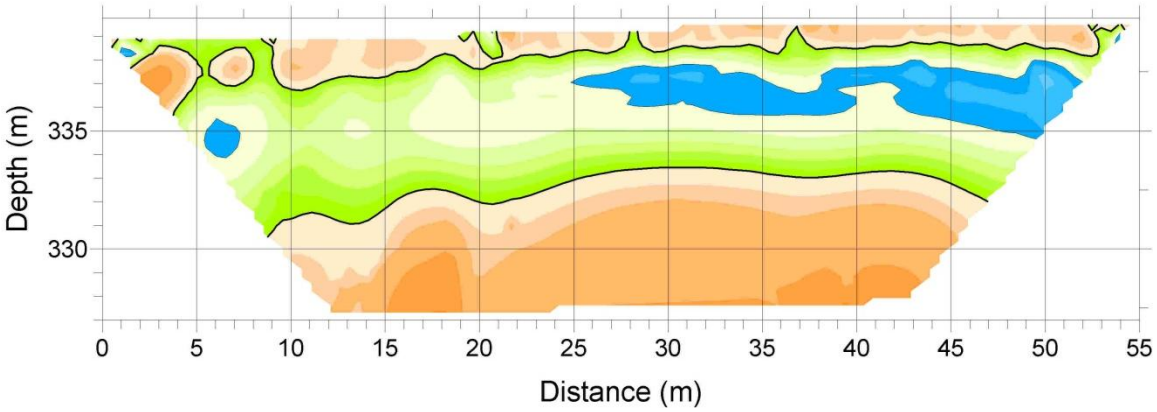

Figure A.9. Electrical resistivity profile 8 at the Clear Creek alluvial floodplain site, which runs from southwest (left) to northeast (right). See Figure A.1 for location of the profile.

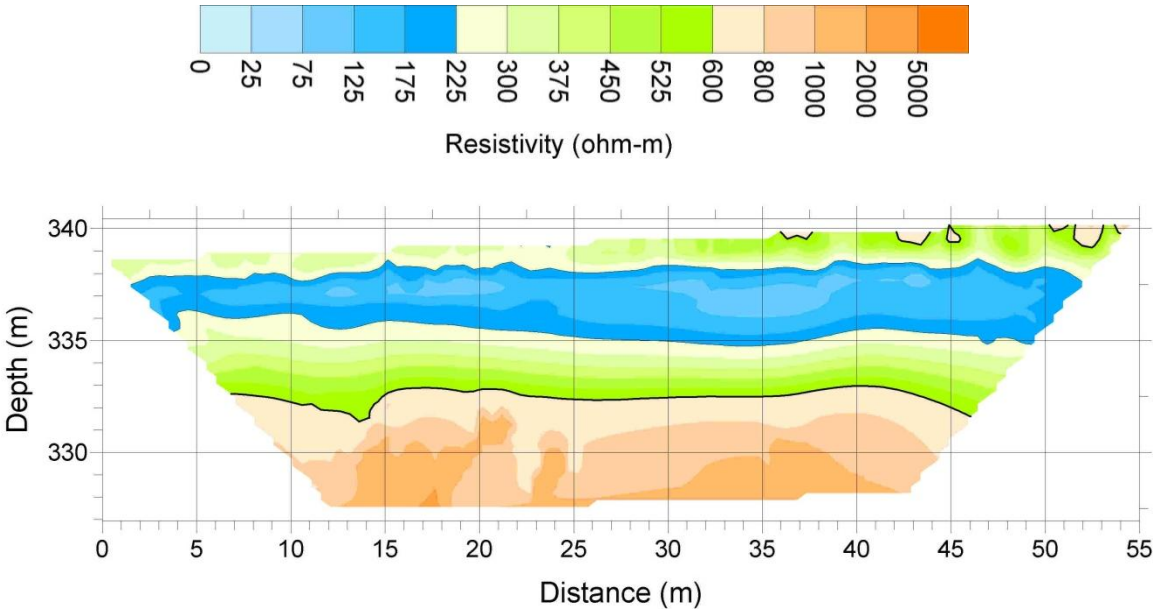

Figure A.10. Electrical resistivity profile 9 at the Clear Creek alluvial floodplain site, which runs from southwest (left) to northeast (right). See Figure A.1 for location of the profile.

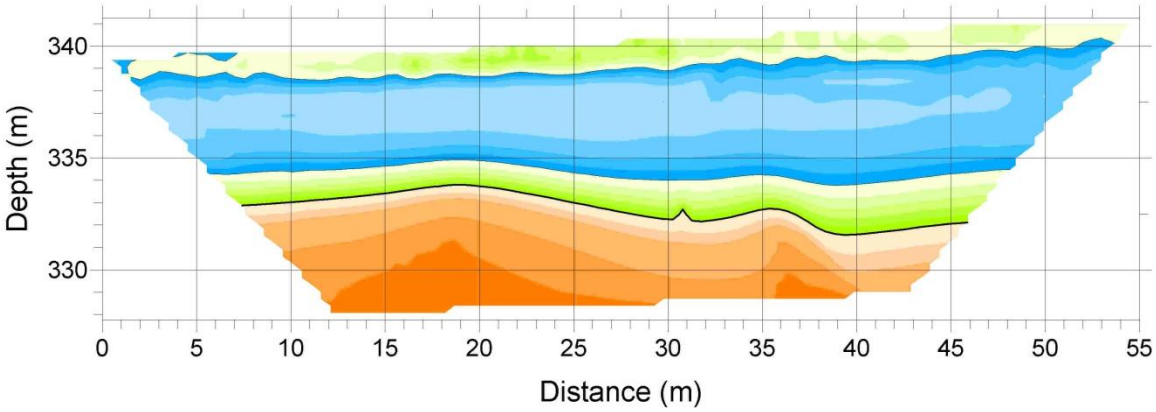

Figure A.11. Electrical resistivity profile 10 at the Clear Creek alluvial floodplain site, which runs from southwest (left) to northeast (right). See Figure A.1 for location of the profile.

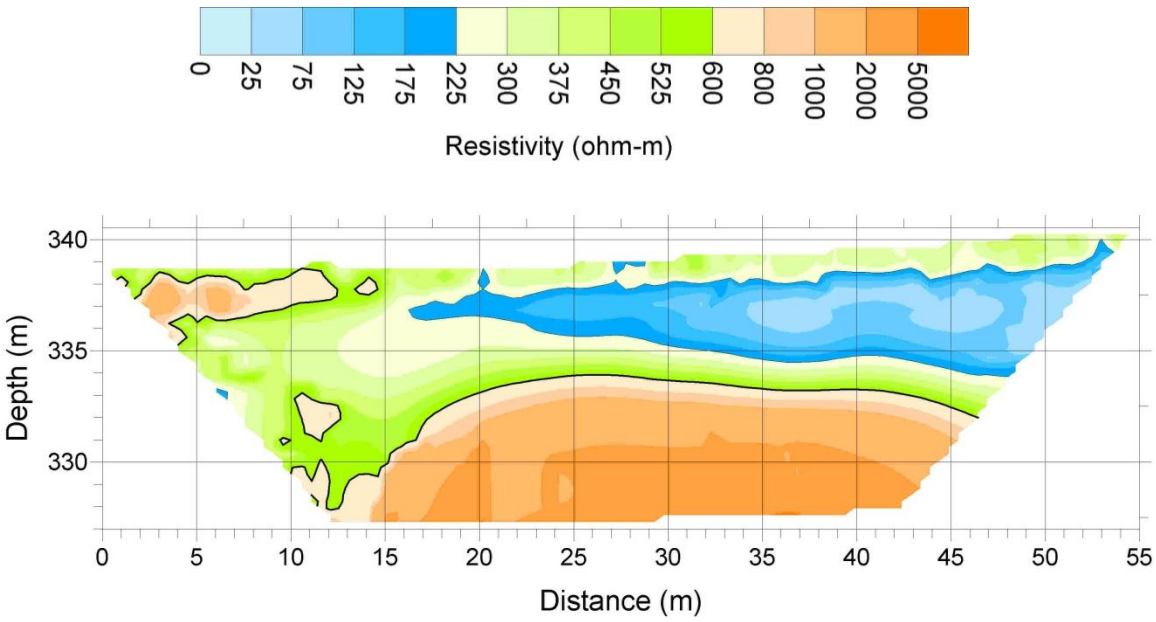

Figure A.12. Electrical resistivity profile 11 at the Clear Creek alluvial floodplain site, which runs from northwest (left) to southeast (right). See Figure A.1 for location of the profile.

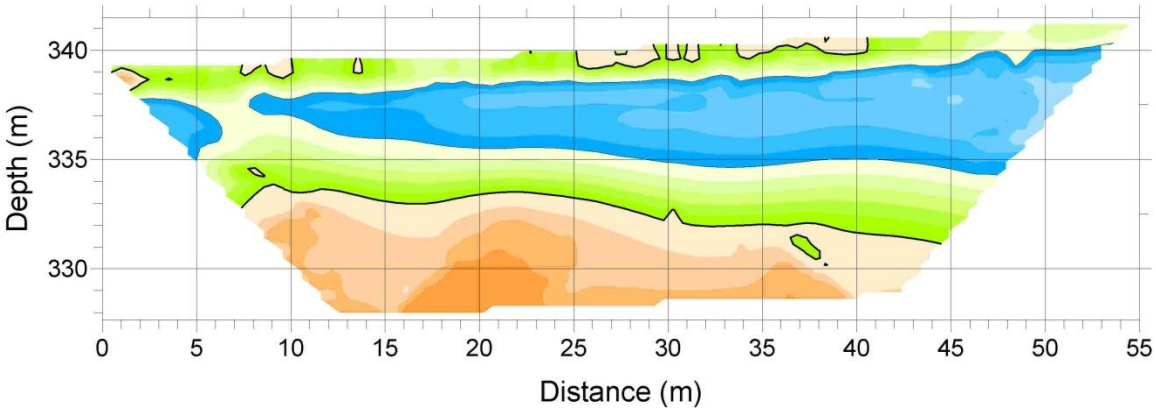

Figure A.13. Electrical resistivity profile 12 at the Clear Creek alluvial floodplain site, which runs from northwest (left) to southeast (right). See Figure A.1 for location of the profile.

VITA

Derek Michael Heeren

Candidate for the Degree of

Doctor of Philosophy

Thesis: SUBSURFACE PHOSPHORUS TRANSPORT AND SCALE DEPENDENT PHOSPHORUS LEACHING IN ALLUVIAL FLOODPLAINS

Major Field: Biosystems Engineering

Biographical:

Education:

Completed the requirements for the Doctor of Philosophy in Biosystems Engineering at Oklahoma State University, Stillwater, Oklahoma in July, 2012.

Completed the requirements for the Master of Science in Agricultural Engineering at South Dakota State University, Brookings, South Dakota in 2008.

Completed the requirements for the Bachelor of Science in Agricultural and Biosystems Engineering at South Dakota State University, Brookings, South Dakota in 2004.

Experience:

2008 – 2012: Research Engineer, Oklahoma State University
2011 – 2012: U.S. EPA STAR Fellow, Oklahoma State University
2010: Instructor, Fluvial Hydraulics, Oklahoma State University
2006 – 2008: Graduate Research Assistant, South Dakota State University
2007: Instructor, Mechanics of Materials, South Dakota State University
2004 – 2006: Laboratory Supervisor, SCI Engineering, Inc., St. Louis, Mo.

Professional Memberships:

American Society of Agricultural and Biological Engineers
American Society of Civil Engineers
Soil Science Society of America
Registered Professional Engineer in State of Oklahoma (PE No.: 25541)

Name: Derek Michael Heeren Date of Degree: July, 2012

Institution: Oklahoma State University Location: Stillwater, Oklahoma

Title of Study: SUBSURFACE PHOSPHORUS TRANSPORT AND SCALE DEPENDENT PHOSPHORUS LEACHING IN ALLUVIAL FLOODPLAINS

Pages in Study: 160 Candidate for the Degree of Doctor of Philosophy

Major Field: Biosystems Engineering

Scope and Method of Study:

Scientists and engineers need to identify critical nutrient source areas and transport mechanisms within a catchment in order to cost effectively protect and enhance drinking water systems, recreation activities, and aquatic ecosystems. The objective of this research was to characterize phosphorus (P) leaching through the vadose zone and subsurface transport through coarse gravel subsoils to streams. An aquifer injection test, long term monitoring of water table elevation and P, and infiltration experiments were performed in the Ozark ecoregion of Oklahoma and Arkansas. A berm method was developed in order to quantify infiltration and P leaching at the plot scale.

Findings and Conclusions:

The injection test showed preferential flow paths and physical non-equilibrium in the coarse gravel vadose and phreatic zones. Preferential flow paths were interpreted to be buried gravel bars. Long-term flow and transport monitoring of alluvial aquifers showed aquifer heterogeneity and large scale bank storage of stream water, as well as large scale, stage-dependent transient storage of P in the alluvial aquifer. Subsurface P transport rates in the alluvial aquifers were quantified and found to be significant compared to surface runoff P transport rates on well managed pastures. The surface soil type (ranging from silt loam to clean gravel) and macroporosity were found to have a significant impact on P leaching through the vadose zone. This research highlighted the difference between the conceptual model of uniform piston infiltration and actual infiltration in field conditions.

Since floodplains are well-connected to alluvial aquifers and streams in gravelly watersheds, a higher level of agricultural stewardship may be required for floodplains than upland areas. This has implications for the development of best management practices specifically for floodplains in the Ozark ecoregion due to their close proximately and connectedness to streams.

ADVISER'S APPROVAL: Dr. Garey A. Fox